AD-A142 291 A UNIFIED THEORY FOR THIN WIRE ANTENNAS OF ARBITRARY LENGTH(U) COLORADO UNIV AT BOULDER ELECTROMAGNETICS LAB L RISPIN ET AL. FEB 80 SCIENTIFIC-38 N00014-76-C-0318 1/2

UNCLASSIFIED F/G 9/1 NL

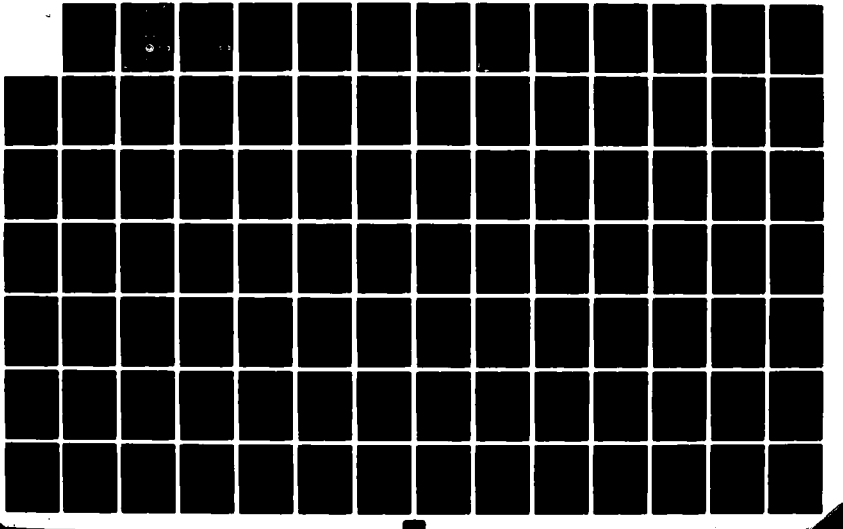

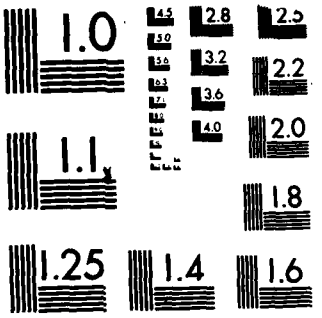

MICROCOPY RESOLUTION TEST CHART
NATIONAL BUREAU OF STANDARDS-1963-A

AD-A142 291

Electromagnetics Laboratory
Department of Electrical Engineering

Scientific Report No. 58

A UNIFIED THEORY FOR THIN WIRE ANTENNAS OF ARBITRARY LENGTH

by

Larry Rispin and David C. Chang

UNIVERSITY OF COLORADO

BOULDER, COLORADO

DTIC FILE COPY

DTIC ELECTE JUN 21 1984 S D B

DISTRIBUTION STATEMENT A
Approved for public release;
Distribution Unlimited

84 03 13 081

Scientific ~~Report No~~. 38

A UNIFIED THEORY FOR THIN WIRE ANTENNAS OF ARBITRARY LENGTH

by

Larry Rispin and David C. Chang

Electromagnetics Laboratory
Department of Electrical Engineering
University of Colorado
Boulder, Colorado 80309

February 1980

DTIC
ELECTE
JUN 21 1984
S D
B

Prepared for

US Office of Naval Research
Arlington, Virginia 22217

This project is monitored by Dr. H. Mullaney of the Office of Naval Research under contract no. ~~N0014~~-76-C-0318.
N00014

DISTRIBUTION STATEMENT A
Approved for public release;
Distribution Unlimited

ABSTRACT

A simple theory based upon traveling wave concepts and the Wiener-Hopf technique is developed which describes the current distributions on tubular cylindrical receiving and transmitting antennas. A close examination of the conditions necessary to obtain sufficiently accurate asymptotic solutions for reflected current distributions is given along with several numerical examples for cooboration. This along with corresponding modifications to other relevant terms in the traveling wave solution for a finite length cylindrical antenna allow for the consideration of a much wider range of cylindrical antennas than normally possible under the traditional thin-wire approximations, $ka \ll 1$ and $kh \geq 1$. Specific examples discussed include electrically short, ($kh = 0.4$ and $\Omega(h) = 2\ln(2h/a) = 10$), practical half-wave, ($kh = \pi/2$ and $\Omega(h) = 2\ln(2h/a) = 10$), and electrical thick, ($ka = 1$ and $kh = 3\pi$), receiving and transmitting antennas. Comparisons with existing theories in these cases and others yield very acceptable agreements. Further, the receiving antenna formulation allows for an arbitrary angle of incidence, $0 \leq \theta_i \leq \pi$, of the uniform plane wave and the transmitting antenna formulation gives excellent input conductance data over an extremely wide range of antenna parameters. Discussions are given for such related topics as the current distributions on the internal wall of a cylindrical antenna, loaded cylindrical antennas and the far field radiation pattern of a cylindrical transmitting antenna.

Table of Contents

Accession For
NTIS GRA&I ☑
DTIC TAB ☐
Unannounced ☐
Justification
PER LETTER
By
Distribution/
Availability Codes
Dist | Avail and/or Special
A-1

DTIC COPY INSPECTED

1. Introduction

As is well known, thin-wire conductors are commonly used as radiators in the design of antenna systems. The radius, a, of each wire is typically much smaller than its half length, h, which for most applications is of the order of a wavelength, λ. Only in limited situations, such as the case of probing an unknown field, will the length be much smaller than a free-space wavelength, (i.e., $2h << \lambda$), or as in the case of a trailing antenna behind an aircraft, will the length be much greater than a free space wavelength, (i.e., $2h >> \lambda$). Consequently most linear antenna theories, both analytical and numerical, are developed with an explicit or implicit assumption that $a << \lambda$ and $2h \gtrsim \lambda/2$, which is commonly referred to as the thin wire assumption. On the other hand, theories not in this general category, usually have a much more limited range of application, such as for the very short antenna and the very long antenna.

More recently, the time-transient response, as well as the broadband frequency response of a thin-wire structure has become a problem of considerable importance. For instance, in order to access the susceptibility of a long thin cylindrical metallic enclosure, one must obtain statistical information concerning the performance of the cylinder as a receiving antenna, over an extremely wide frequency range as well as an arbitrary angle of incidence (referring to illumination by an incident plane wave). Computations not only become excessive when conventional theories are utilized because virtually thousands of responses are needed, but also very awkward since different methods have to be used in different frequency ranges. A similar statement, of course, can also be made for studying the impulse response of an antenna.

Beginning with Hallén's [1] integral equation formulation for the current on a cylindrical antenna and including the work of many others [2] - [10], the thin-wire approximations mentioned above have nearly always been employed. Weinstein [2] did, however, observe that his final approximate solutions, which were derived under the thin wire assumptions, could be applied to cylinders having larger values of ka if the electrical length, kz, were very much larger. In contrast, the theory of King and Middleton [11, Chap. II], however, which involves the iterative solution of an integral equation for the current on a finite length cylinder, requires explicitly that the parameter, $\Omega = 2\,\ell n(2h/a)$, to be large, h being the half-length of the cylinder. Although the parameter, Ω, relates only to the physical length and radius of the antenna, this approach still requires the electrical radius, ka , to be small compared to unity and the electrical length, kh, cannot be very small nor very large. King also developed a receiving theory [11, Chap. IV] for antennas having a large Ω. A large Ω was also the basis for two electrically short ($kh \lesssim 1$) antenna theories developed by King [11, Sec.II.31 and IV.8] and [12, Sec. 3.7] which were developed by making approximations relevant to the short antenna situation in the integral equation formulation of the problem.

Another means of analysis for the cylindrical antenna problem is the numerical method of moments technique [13], which has the capability of computing antenna characteristics without invoking the thin wire approximations. Realistically, however, the computation time is considerable if the antenna is not thin or the length is more than a few free space wavelengths.

In this paper, our aim is to develop a simple unified theory for computing the broadband characteristics of a transmitting and/or receiving antenna when the parameter, $\Omega = 2\ \ell n(2h/a)$ is large. For a typical thin-wire antenna where $\Omega = 2\ \ell n(2h/a) = 10$, our theory is applicable for antenna lengths as short as $2h \approx 0.12\lambda$ and as long as $2h \approx 23\lambda$ (where for $\Omega = 10$, ka is almost equal to 1), which in terms of frequency covers well over two orders of magnitude and is more than adequate even for transient computations. We also show that our formulation may be applied to an electrically thick (up to $ka = 1$) cylindrical transmitting antenna or the electrically thick receiving antenna (for the angularly independent current) and obtain favorable agreement with existing theories even when the parameter $\Omega = 2\ \ell n(2h/a)$ is not large.

We begin with a re-examination of the conditions necessary to obtain simple approximate solutions to cylindrical antenna problems via the Wiener-Hopf technique. Section 2 discusses a pair of canonical integrals which characterize cylindrical antenna problems. Approximate expressions for these canonical integrals are derived subject to the condition, $\Omega(z) = 2\ \ell n(2z/a) >> |\ell n[2kz \sin^2(\theta_i/2)]|$. The angle, θ_i, refers to the incident angle of the incoming wave and is more fully described later. In Section 3 the various currents on both infinite and semi-infinite cylindrical receiving and transmitting antennas are given and their relationships to the canonical integrals established. Data obtained from the approximate expressions is then compared with numerically evaluated "exact" data in Section 4. A most important observation in this section is that the parameter, $\Omega(z) = 2\ \ell n(2z/a)$, in the basic condition of our analysis, need not be very much larger than $|\ell n[2kz \sin^2(\theta_i/z)]|$, especially when thicker antennas ($ka \gtrsim 0.1$)

are involved. Utilizing the process of summing multiple reflections, approximate expressions for the receiving and transmitting currents and the input admittance for finite length cylindrical antennas are formulated in Section 5. Expressions for the currents flowing on the internal walls of receiving and transmitting tubular antennas are given in Section 6. In Section 7, numerical results from our theory for specific antennas are compared with the results of other authors using different approaches, with acceptable agreement in all the cases considered. The special case of the electrically short antenna is discussed in Section 8. General conclusions as well as extensions of our theory to loaded antennas and the determination of the far field radiation from a transmitting antenna are given in Section 9.

The exact integral expressions appearing in Section 4 are for the most part, based upon the Wiener-Hopf technique (see for example Nobel [14], Weinstein [2] and Mittra and Lee [15]). The assumed time variation is $e^{-i\omega t}$ and the implied Fourier transform pair is given by,

$$\tilde{F}(\alpha) = \int_{-\infty}^{\infty} F(z) e^{i\alpha z}\, dz \tag{1}$$

and

$$F(z) = \frac{1}{2\pi} \int_{-\infty}^{\infty} \tilde{F}(\alpha) e^{-i\alpha z}\, d\alpha \,. \tag{2}$$

2. The canonical integral in cylindrical antenna problems

As will be shown later, the external current distributions on both the receiving and transmitting cylindrical antennas can be written in terms of the canonical integral,

$$U(\theta_i;z) = -i\frac{k}{\eta}(1 - \cos\theta_i)\int_{\Gamma_0}\frac{e^{-i\alpha z}}{(k+\alpha)(k\cos\theta_i+\alpha)K(\alpha)}\,d\alpha$$

$$; \ 0 \le z < \infty, \ 0 \le \theta_i \le \pi \qquad (3)$$

The contour, Γ_0, is shown in Figure 1 and,

$$K(\alpha) = i\pi J_0(\xi a)\, H_0^{(1)}(\xi a) \qquad (4)$$

where

$$\xi = \sqrt{k^2 - \alpha^2} = i\sqrt{\alpha^2 - k^2}$$

θ_i is the incident angle of the incoming current wave when (3) is used to describe a particular current distribution reflected from an end of a cylinder and z is a numerical distance along the axis of the antenna. $k = 2\pi/\lambda$ and η are the plane wave wavenumber and the intrinsic impedance, respectively, of the medium surrounding the antenna. The antenna to be considered is assumed to have an infinitely-thin, perfectly-conducting wall concentric about the z-axis at a radius, a. The suppressed time factor is $\exp(-i\omega t)$, where ω is the operating frequency in radians/sec.

We shall also find it useful to define the auxiliary canonical integral, $W(\theta_i;z)$, which is similar to $U(\theta_i;z)$ in (3) except for the appearance in the integrand of the additional function, $K_+(\alpha)$, defined as the factor of $K(\alpha)$ in (4) which is analytic and free of zeroes in the upper half complex α-plane,

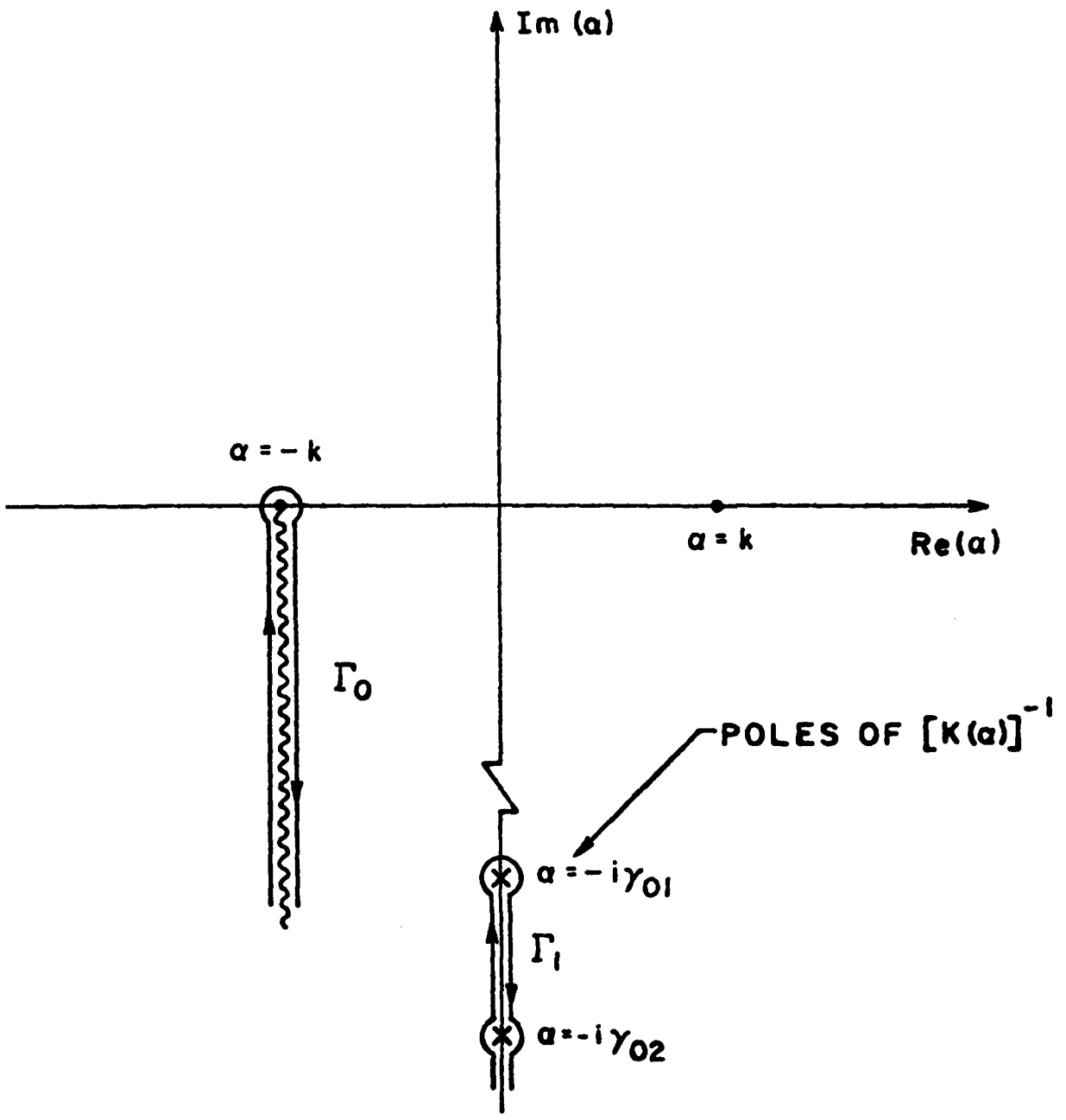

Figure 1. The complex α-plane

$$W(\theta_i;z) = -i\,\frac{k}{\eta}\,(1-\cos\theta_i)\int_{\Gamma_0}\frac{K_+(-\alpha)e^{-i\alpha z}}{(k+\alpha)(k\cos\theta_i+\alpha)\,K(\alpha)}\,d\alpha$$

$$; \ 0 \le z \le \infty, \ 0 \le \theta_i \le \pi \tag{6}$$

Properties of $K_+(\alpha)$ are discussed in Appendix C. We note that the integral $W(\theta_i;z)$ usually occurs in problems concerning the currents reflected from the ends of cylindrical antennas. As shown in (A8) of Appendix A, when $z >> a$, we may approximate (6) by

$$W(\theta_i;z) \approx K_+(k)U(\theta_i;z) \tag{7}$$

where $U(\theta_i;z)$ is our original canonical integral given in (3). Thus with $W(\theta_i;z)$ given in terms of $U(\theta_i;z)$, our particular use of the form of $W(\theta_i;z)$ in (6) will be limited to providing exact date (from the numerical integration of (6)) to compare with the approximate solutions to follow.

Subject to the condition,

$$\Omega(z) = 2\,\ell n\left(\frac{2z}{a}\right) >> \left|\ell n\left[2kz\,\sin^2\left(\frac{\theta_i}{2}\right)\right]\right| \tag{8}$$

an approximate solution to the canonical integral, $U(\theta_i;z)$, is obtained to order $[\Omega(z)]^{-2}$ in Appendix A. From (A17) of Appendix A, this approximate solution may be stated as

$$U(\theta_i;z) = \frac{i}{\eta}\,e^{ikz}\{\ell n[f(\theta_i;z) - i\pi] - \ell n[f(\theta_i;z) + i\pi]\} \tag{9}$$

where

$$f(\theta_i;z) = 2C_w + \gamma + i\pi/2 + \ell n(2kz) + e^{-iv_0}\,E_1(-iv_0) \tag{10}$$

is a slowly varying function of z. C_w is defined as

$$C_w = - \ell n(ka) - \gamma \quad ; \gamma = 0.57721..... \tag{11}$$

which is usually taken as a large parameter in the typical thin wire application and,

$$v_0 = v_0(\theta_i, z) = 2\, kz\, \sin^2\left(\frac{\theta_i}{2}\right) \tag{12}$$

The function, E_1, appearing in (10) is the exponential integral of the first kind defined in Equation 5.1.1 of [16]. We note that the antenna parameter, $\Omega(z)$, is defined in the same way as in [11] where it has been used as a large parameter for the iterative solution of the antenna problem.

Another approximate form of the canonical integral, $U(\theta_i;z)$, which stems from a Taylor series expansion of (9) subject to the basic restriction stated in (8) is given in (A18) of Appendix A and repeated here,

$$U(\theta_i;z) = \frac{2\pi}{\eta}\, \frac{e^{ikz}}{f(\theta_i;z)} \tag{13}$$

Even though (9) and (13) are equivalent with respect to the order of approximation (i.e., $[\Omega(z)]^{-2}$), we shall find (13) to have a more desirable behavior in the near-grazing, $\theta_i \sim 0$, and near the end, $z \sim 0$, situations. Otherwise, (9) will appear to be a more accurate result than is (13) for $U(\theta_i;z)$.

It is interesting to compare our approximate forms of $U(\theta_i;z)$ to similar expressions derived by other authors. For the current on an infinitely long transmitting antenna ($\theta_i = \pi$), Shen, Wu and King [6] by a semi-

analytical, semi-curve fitting technique found a result similar to our $U(\theta;z)$ in (9), except that the term, $\ell n[kz + \sqrt{(kz)^2 + \exp(-2\gamma)}$, replaces our terms, $\ell n(2kz) + \exp(-i2kz)E_1(-i2kz)$. Thus for large kz, our approximate solution for $U(\pi;z)$ in (9) and that of Shen, et al. [6, Eq. 6] are quite similar. Weinstein [2] found an approximate solution to an integral similar to (3), (he called it the "key" integral), but having a different coefficient outside the integral. Apart from this coefficient (our approach introduces this term at a later time), Weinstein obtained, through a complicated variational approach, an approximate result equivalent to our second approximate form of $U(\theta_i;z)$ in (13). Also, in a more recent work by Chang, Lee and Rispin [17], a further approximation of (13) was obtained and used in a receiving antenna analysis. However, the analyses of Shen,et al., Weinstein and Chang, et al., mentioned above, all assumed the conventional thin wire restrictions,

$$ka << 1 \quad (\text{and} \quad kz > 1) \tag{14}$$

Although in [2], Weinstein did observe, a posteriori,that the approximate form of his "key" integral (similar to (13)) could be used for larger values of ka if at the same time, kz was very much larger. Thus, the importance of our work is not so much contained in the approximate formulas for $U(\theta_i;z)$ in (9) and (13), but rather in the realization of a less restrictive condition (given in (8)) for the validity of these approximate formulas. In fact, it will be shown in Section 4 that the approximate formulas for $U(\theta_i;z)$ in (9) and (13) yield remarkably good agreement with numerically obtained "exact" results even when $\Omega(z)$ is of the same order as $|\ell n(v_0)|$. Hence, even the "much greater" restriction appearing in (8) can be significantly relaxed.

3. Currents on cylindrical antennas

In this section, the currents on infinite and semi-infinite cylindrical receiving and transmitting antennas, given in terms of the canonical integral, $U(\theta_i;z)$ in (3) of Section 2, are described.

3.1 Primary receiving current

The longitudinal current averaged over the circumference on an infinitely long cylindrical antenna due to a plane wave polarized in the same plane as the antenna and incident at an angle, θ_i, with respect to the cylinder axis (which is also the z-axis as shown in Figure 2a), may be written as [8, eq. 10],

$$I_\infty^R(\theta_i,z) = E_\theta^i \, V(\theta_i;z) \tag{15}$$

where,

$$V(\theta_i;z) = -i \frac{4\pi}{k\eta} \frac{J_0(ka \sin\theta_i)}{\sin\theta_i \, K(k\cos\theta_i)} e^{ikz\cos\theta_i} ; -\infty < z < \infty ,$$

$$0 \le \theta_i \le \pi \tag{16}$$

J_0 is the zero order Bessel function and $K(\alpha)$ is given in (4). $k = 2\pi/\lambda$ and η are the plane wave propagation constant and intrinsic impedance, respectively, of the surrounding medium. Higher order variations of the z-directed current with respect to the azimuthal angle, ϕ, and the ϕ-directed currents on the cylinder are not treated in this report. Thus, while $V(\theta_i;z)$ represents the total longitudinal current on an infinitely long electrically thin ($ka << 1$) antenna very well, it corresponds only to the azimuthally uniform longitudinally directed current on an infinite cylindrical antenna in general.

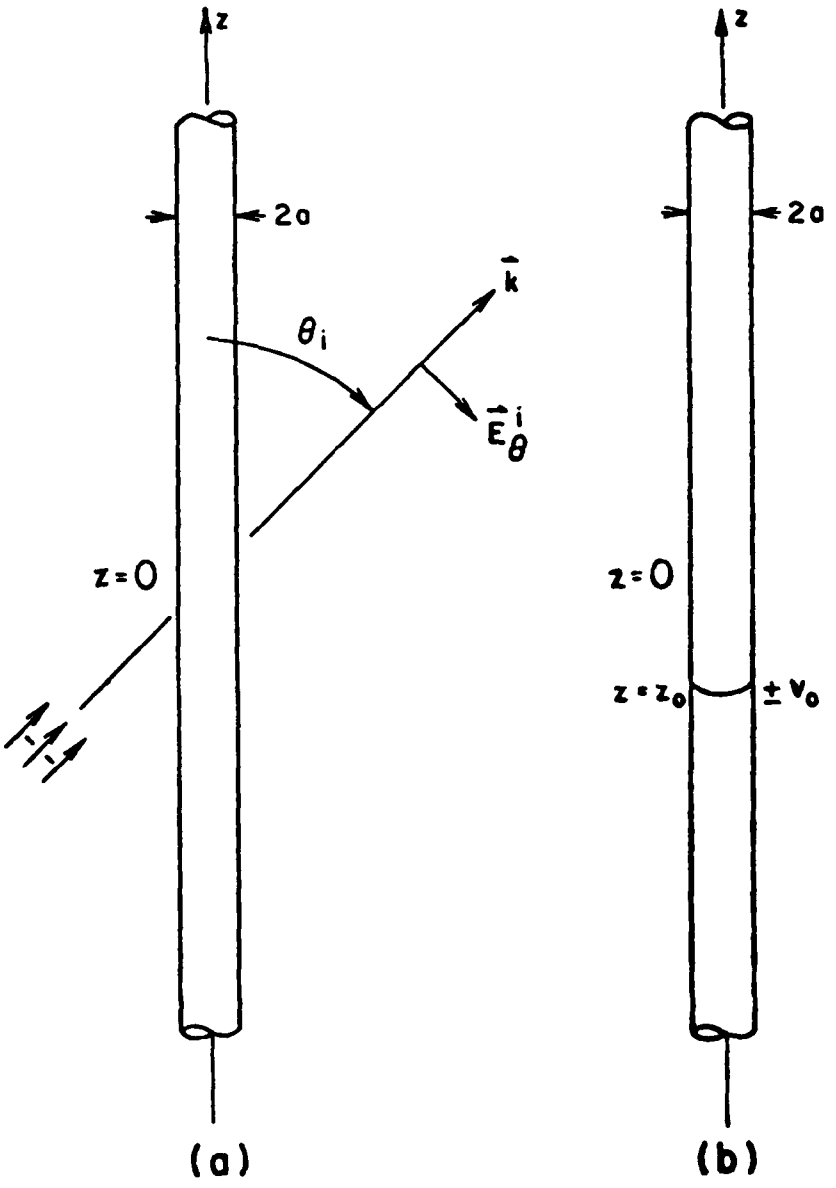

Figure 2. Infinitely long tubular cylindrical antennas

a. receiving; uniform plane wave incident at an angle, θ_i, with respect to the z (antenna) axis.

b. transmitting; delta function voltage source of strength, V_0 volts, located at $z = z_0$.

In the special case of a thin cylinder, i.e., ka << 1, the Bessel function and kernel, $K(\alpha)$ in (4), may be approximated by the leading terms in their respective small argument expressions to yield,

$$V(\theta_i;z) = -i\,\frac{4\pi}{k\eta}\,\frac{e^{ikz\cos\theta_i}}{\sin\theta_i\left[2C_w + i\pi - 2\,\ell n\left(\frac{\sin\theta_i}{2}\right)\right]}\;;\; ka << 1 \qquad (17)$$

where C_w is given in (11).

3.2 Primary transmitting current

The longitudinal current on an infinitely long hollow cylinder due to a uniform (with respect to the azimuthal angle, ϕ) delta function voltage source of strength, V_0, at $z = z_0$ (see Figure 2b), may be written as [6, Eq. 1],

$$I^T_\infty(z_0;z) = i\,\frac{2k}{\eta}\;V_0\int_{\Gamma_0}\frac{e^{-i\alpha|z-z_0|}}{(k^2-\alpha^2)K(\alpha)}\,d\alpha\;;\quad -\infty < z < \infty \qquad (18)$$

where the contour, Γ_0, is shown in Figure 1 and $K(\alpha)$ is given in (4). Comparing (18) with the canonical integral definition in (3), we may write the driven infinite cylinder current as

$$I_\infty(z_0;z) = V_0 U(\pi;|z-z_0|)\;;\; -\infty < z < \infty \qquad (19)$$

and use either approximate form of $U(\pi,z)$ in (9) or (13) to determine this current provided the restriction in (8) is satisfied. This procedure, however, does not yield a good result at the source since the condition on $\Omega(z)$ is violated. In particular, the real part of the current at the source needs to be evaluated very accurately, since physically it

corresponds to the input conductance and hence the power that can be radiated from the antenna. To this end, it is shown in Appendix B, how an approximate expression for primary transmitting current similar to that of Shen, et al. [6] may be constructed. This current expression denoted as $U_s(|z-z_0|)$ replaces the term $U(\pi;|z-z_0|)$ in (19) and is given by

$$U_s(|z-z_0|) = \frac{i}{\eta} e^{ik|z-z_0|} \{\ell n[f_s(|z-z_0|) - i\pi] - \ell n[f_s(|z-z_0|) + i\pi]\} \quad (20)$$

where

$$f_s(|z-z_0|) = 2C_w + \gamma + i\pi/2 + \ell n[(k|z-z_0|) + \sqrt{(k|z-z_0|)^2 + \exp(-2\gamma - 2g)}] \quad (21)$$

C_w and γ are given in (11) and,

$$g = 33.88\ (ka)^2 \exp\left(-\frac{3.26}{ka}\right) \quad (22)$$

From (18) and (20), the input conductance of an infinitely long cylinder is then given by

$$G_\infty(ka) \approx \text{Re}\{U_s(0)\} = \text{Re}\{[\frac{i}{\eta} \ell n(2C_w - g - i\pi/2) - \ell n(2C_w - g + i3\pi/2)]\} \quad (23)$$

It will be shown later in Section 4 that (23) yields a very good input conductance for an infinitely long cylinder as thick as $ka = 1.0$. Also, we note that $U_s(z)$ in (20) is asymptotic to both forms of $U(\pi;z)$ in (9) and (13) for large kz and differs only in the vicinity of the source, $kz \approx 0$.

3.3 Secondary current on a semi-infinite receiving antenna

The secondary current on the external wall of a semi-infinite receiving cylinder (see Figure 3a), arises from the reflection of the current

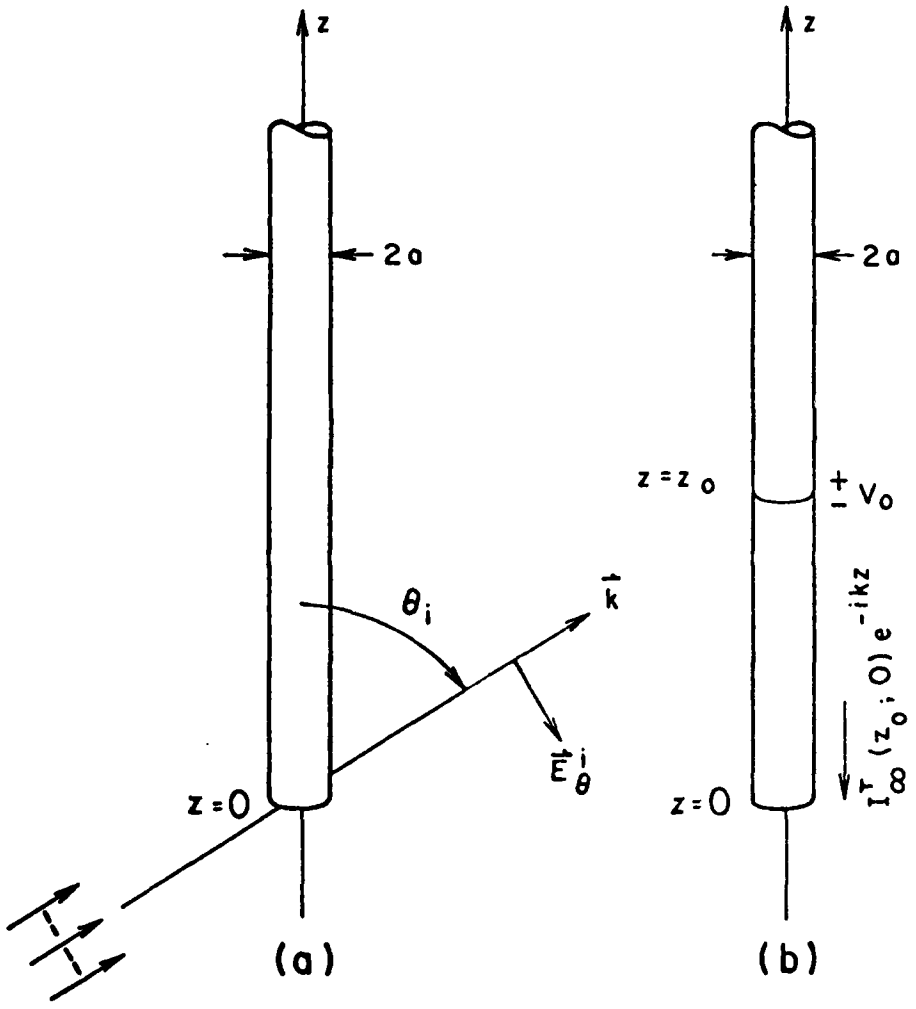

Figure 3. **Semi-infinite tubular** cylindrical antennas

a. **receiving; uniform** plane wave incident at an angle, θ_i, **with respect to the** z (antenna) axis.

b. **transmitting, delta** function voltage source of strength, V_0 **volts, located at** $z = z_0$.

$I_{\infty}^{R}(\theta_i,z)$ in (15) from the end of the cylinder. From a Wiener-Hopf analysis this reflected current may be expressed as [17, Eq. 27],

$$I_{refl}^{R}(\theta_i,z) = E_{\theta}^{i}\, V(\theta_i;0)\ \frac{ik}{2\pi}(1-\cos\theta_i)K_{+}(-k\cos\theta_i)$$

$$\int_{\Gamma_0} \frac{K_{+}(-\alpha)\, e^{-i\alpha z}}{(k+\alpha)(k\cos\theta_i+\alpha)K(\alpha)}\, d\alpha\ ;\quad 0 \le z < \infty \qquad (24)$$

$$0 \le \theta_i \le \pi$$

The contour Γ_0 is shown in Figure 1, and as previously noted, $K_{+}(\alpha)$ comes from the factorization of $K(\alpha)$ in (4) into functions analytic in the upper and lower halves of the complex α plane, i.e., $K(\alpha) = K_{+}(\alpha)K_{-}(\alpha)$. This factorization is more fully discussed in Appendix C. The superscript R in (24) signifies the receiving situation. We may write (24) in terms of the auxiliary canonical integral $W(\theta_i;z)$ in (6), and by virtue of (7), we have the approximate expression,

$$I_{refl}^{R}(\theta_i,z) \simeq -E_{\theta}^{i}\, V(\theta_i;0)R(\theta_i)U(\theta_i;z);\quad 0 < z < \infty\ ,$$

$$0 \le \theta_i \le \pi \qquad (25)$$

where we have defined the "reflection coefficient",

$$R(\theta_i) = \frac{\eta}{2\pi} K_{+}(k)K_{+}(-k\cos\theta_i) \qquad (26)$$

The approximate expression for the reflected current in (25) is valid if the basic condition in (8) is satisfied. We note that the reflected current distribution considered here is, as in the primary receiving current distribution in Section 3.1, the total z-directed current averaged over the circumference of the cylinder.

One of the obstacles, which in the past has prevented the practical

application of the Wiener-Hopf technique to thicker antennas, has been the absence of a tractable expression for $K_+(\alpha)$ in the range $-k \le \alpha \le k$ which appears in (26). It is shown in Appendix C, that a curve fitting procedure involving the factor, $K_+(\alpha)$, with compensation for its dominant irregularity, yields the approximate formula,

$$K_+(\alpha) = \begin{cases} \dfrac{K_+^0(\alpha)}{|A|[1 + B_r(\frac{\alpha}{k})]} & ; \ 0 \le \alpha \le k \\ \dfrac{K_+^0(\alpha)}{|A|[1 + B_r(\frac{\alpha}{k}) + C(\frac{\alpha}{k})^2]} & ; \ -k \le \alpha \le 0 \end{cases} \tag{27}$$

where $K_+^0(\alpha)$ is the small argument form of $K_+(\alpha)$ based upon the assumptions that $ka << 1$ and $\alpha a << 1$ [1, Sec. 38] given by

$$K_+^0(\alpha) = \sqrt{2C_w + i\pi}\,\left[1 - \frac{1}{2C_w + i\pi}\,\ell n(\frac{k+\alpha}{2k})\right] . \tag{28}$$

$|A|$ is the magnitude of A given by,

$$A = K_+^0(0)[i\pi J_0(ka)H_0^{(1)}(ka)]^{-1/2} . \tag{29}$$

B_r is given by

$$B_r = \frac{\eta}{2\pi}\,G_\infty(ka) - \mathrm{Re}\{[2C_w + i\pi + \ell n(2)]^{-1}\} \tag{30}$$

and is the real part of a more complicated function, B, given in (C19) in Appendix C. Here $G_\infty(ka)$ is the input conductance of an infinite cylindrical antenna having an electrical radius, ka, for which we have the approximate formula given in (23). Appendix B gives a detailed discussion

of the exact and approximate forms of $G_\infty(ka)$. And finally, the coefficient C is given in terms of $|A|$ and B_r by,

$$C = \frac{1 - |A|^2(1 - B_r^2)}{|A|^2 (1 + B_r)} \tag{31}$$

Although (27) is basically a curve-fit solution for $K_+(\alpha)$ in the range, $-k < \alpha \leq k$, the coefficients $|A|$ and B_r were obtained in much the same manner as those in a two-term Taylor series expanion of $K_+^0(\alpha)/K_+(\alpha)$ in the upper-half of the complex α-plane. The coefficient, C, was obtained by requiring that the approximate constructed quantity $K(\alpha) = K_+(\alpha)K_-(\alpha)$ (see (C5) and (C6) of Appendix C) using (27) have the same limiting form as the exact $K(\alpha)$ in (4) as $\alpha \to \pm k$.

3.4 Secondary current on a semi-infinite transmitting antenna

The secondary current eminating from the end at $z = 0$ of a semi-infinite, $0 \leq z < \infty$, cylinder having a delta function voltage source of strength V_0 at $z = z_0$ is usually approximated by the reflection of a wave incident at $\theta_i = \pi$ [6], as illustrated in Figure 3b. Hence, from (24) we may write,

$$I^T_{refl}(z_0;z) = -I^T_\infty(z_0;0)R(\pi)U(\pi;z) \qquad , 0 < z < \infty \tag{32}$$

where we have replaced the receiving incident current, $E^i_\theta V(\theta_i;0)$ by the transmitting incident current, $I^T_\infty(z_0;0)$.

4. Numerical comparisons: infinite and semi-infinite antennas

4.1 Primary transmitting current

As discussed in Section 3.1, we shall use the modified Shen, et al. [6] formula denoted as $U_s(z)$ in (20) for the primary current on a cylindrical transmitting antenna. And since Shen has already compared his approximate expression with numerically "exact" data in [6] for values of ka up to 0.08 with good agreements, we shall only consider cases in which $0.1 \leq ka \leq 1.0$ to justify the extension of the theory to this range. In Figure 4, we show the real and imaginary components of the current distribution on an infinitely long cylinder as predicted by the modified Shen formula in (20) with $V_0 = 1$ volt, for the particular values of the electrical radii, ka = 0.1, 0.5, and 1.0. "Exact" data for these cases obtained from the numerical integration of (18) is also shown in Figure 4 (as circles). And it may be observed that the real component of the current distribution predicted by (20) compares very favorably with the exact numerical data over the entire range of kz shown especially for the smaller values of ka. The imaginary component of the current distribution predicted by (20) compares favorably with the exact data only when the ratio, 2z/a, somewhat exceeds unity.

As mentioned earlier, the purpose of Shen's and our curve-fitting procedures leading to (20) for the primary transmitting current was to obtain a good value for the real part of the current at the source, i.e., the input conductance of an infinitely long cylindrical antenna. To demonstrate the level of success attained in this respect we offer Figure 5, which shows the input conductance of an infinitely long cylinder as obtained from the real part of $U_s(0)$ in (23) and the "exact" numerically evaluated input conductance from the exact integral expression stated in (B1) of Appendix

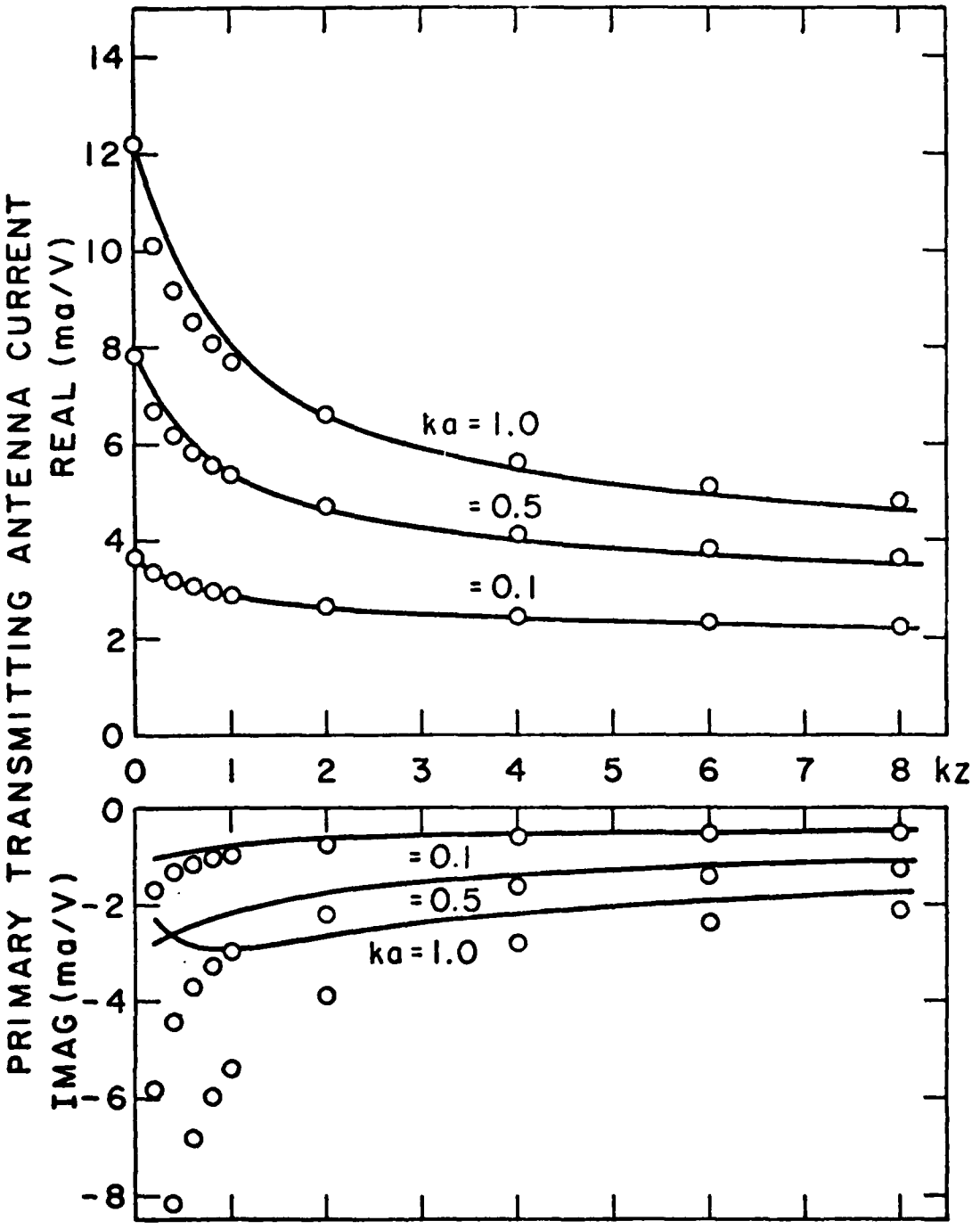

Figure 4. Current distribution on an infinitely long cylindrical transmitting antenna with a delta function voltage source at $z = z_0 = 0$.

———— Approximate distribution from the modified Shen [6] formula denoted by $U_s(|z - z_0|)$ in eq. (20).

o "Exact" numerically evaluated data from eq. (18).

Note: The traveling wave factor, e^{ikz}, has been suppressed.

B as functions of ka over the range $10^{-4} \leq ka \leq 1$. Obviously, excellent agreement is obtained. In fact, the error, which is also shown in Figure 5, never exceeds 2% over the entire range.

4.2 Reflection coefficient $R(\theta_i)$

The behavior of the "exact" numerically evaluated (using the formula of Mittra and Lee [15, Sec. 5-2.(3)]) $K_+(\alpha)$ is shown in Figure 6 as a function of α in the range $-k < \alpha < k$ for the specific cases ka = 0.01, 0.05, 0.1, 0.5, and 1.0. This variation in α when $\alpha = -k \cos \theta_i$ corresponds to the range $0 < \theta_i < \pi$. The behavior of our approximate form of $K_+(\alpha)$ in (27) is so close to the exact we have not included this data in Figure 6 but have elected to show, in Figure 7, the error between the approximate and "exact" values of $K_+(\alpha)$ for the same range and set of parameters as those in Figure 6. The magnitude and phase error illustrated in Figure 7 is seen to be quite small, typically below 1% and ±5°, respectively. And it should be noted, that this magnitude error is many times smaller than the magnitude error of the normally accepted small argument approximation, $K_+^0(\alpha)$ in (28). For example, at ka = 0.01 $K_+^0(k)$ differs from the exact value of $K_+(k)$ by about 1.5%, while our approximate form of $K_+(k)$ from (27) possesses an error of less than 0.1%. And as the value of ka increases, the error in $K_+^0(k)$ increases quite rapidly, reaching over 200% at ka = 1.

Obviously, the quantity of more crucial importance is the so-called "reflection coefficient", $R(\theta_i)$ in (26). Figure 8 shows the magnitude and phase of $R(\theta_i)$ as calculated using the "exact" numerically determined values of $K_+(k)$ and $K_+(-k \cos \theta_i)$ (again from the formula of Mittra and Lee [15, Sec. 5-2.(3)]) as a function of ka over the range $10^{-4} \leq ka \leq 1$ for the incident angles $\theta_i = \pi/36, \pi/4, \pi/2, 3\pi/4$ and π.

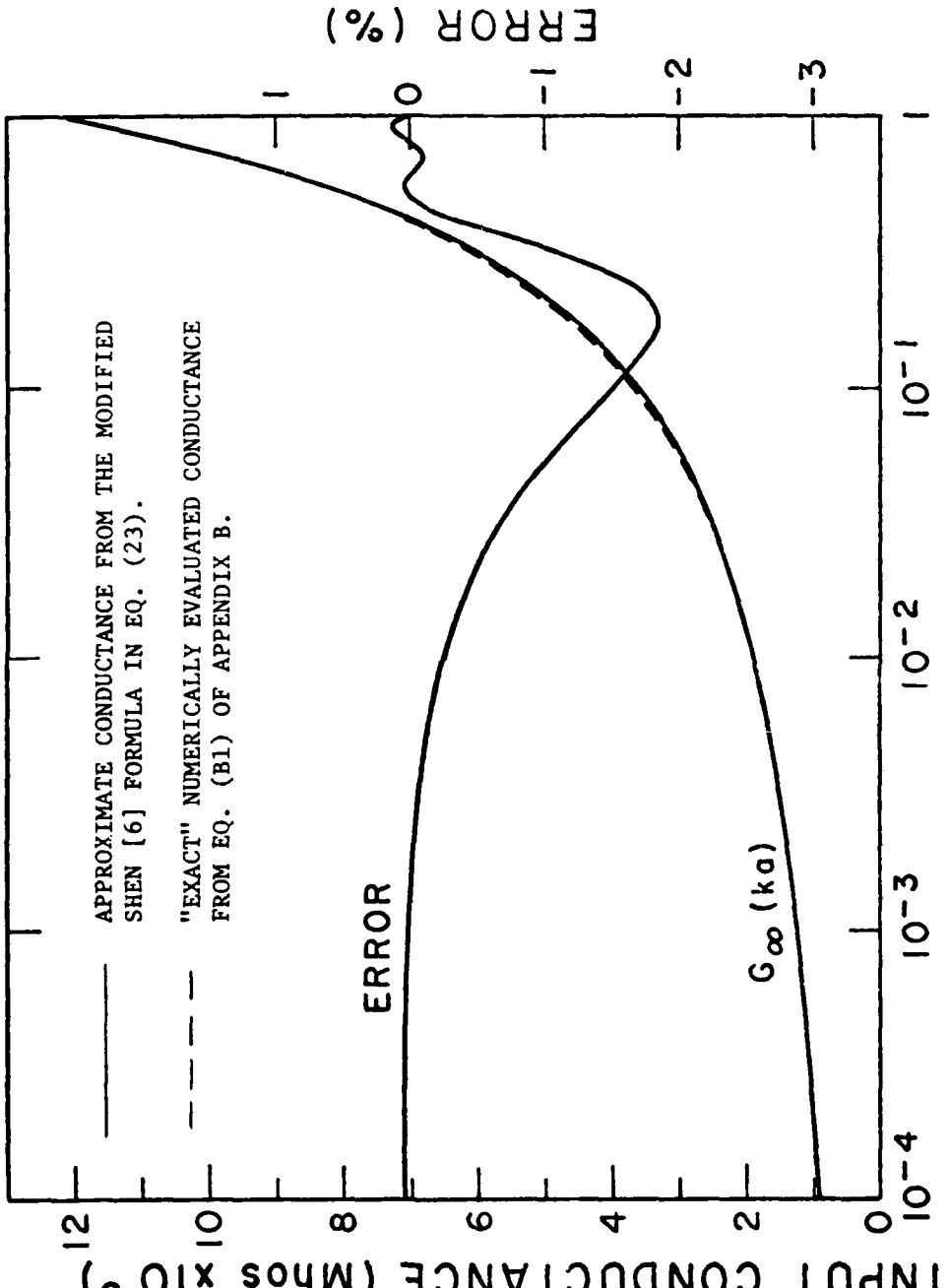

Figure 5. Input conductance of an infinitely long tubular cylinder.

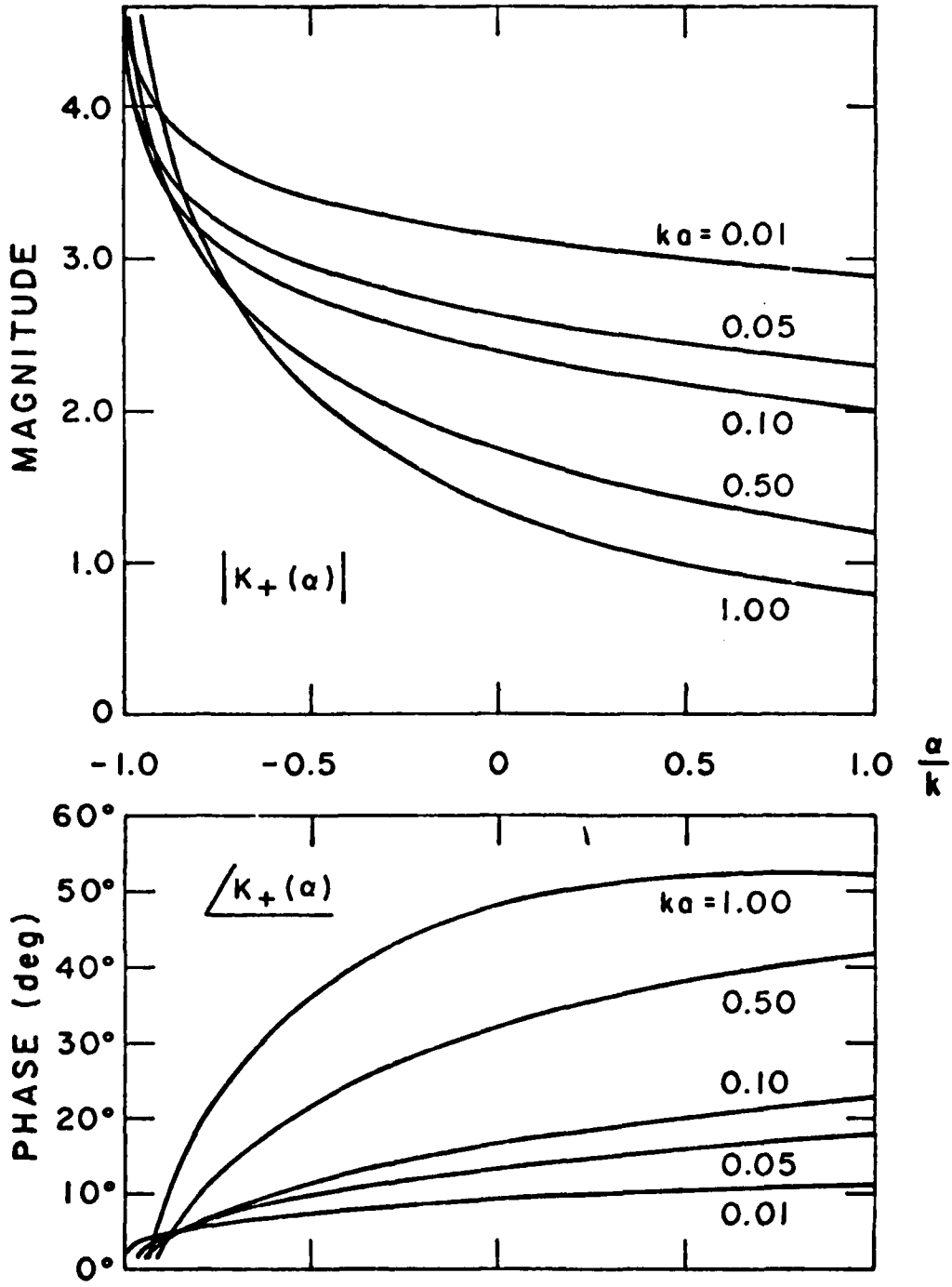

Figure 6. Magnitude and phase of $K_+(\alpha)$ in the range, $-k \leq \alpha \leq k$, calculated from the exact formula for $K_+(\alpha)$ in [15, 5-2,(3)], (See eq.(C11) of Appendix C of this report.)

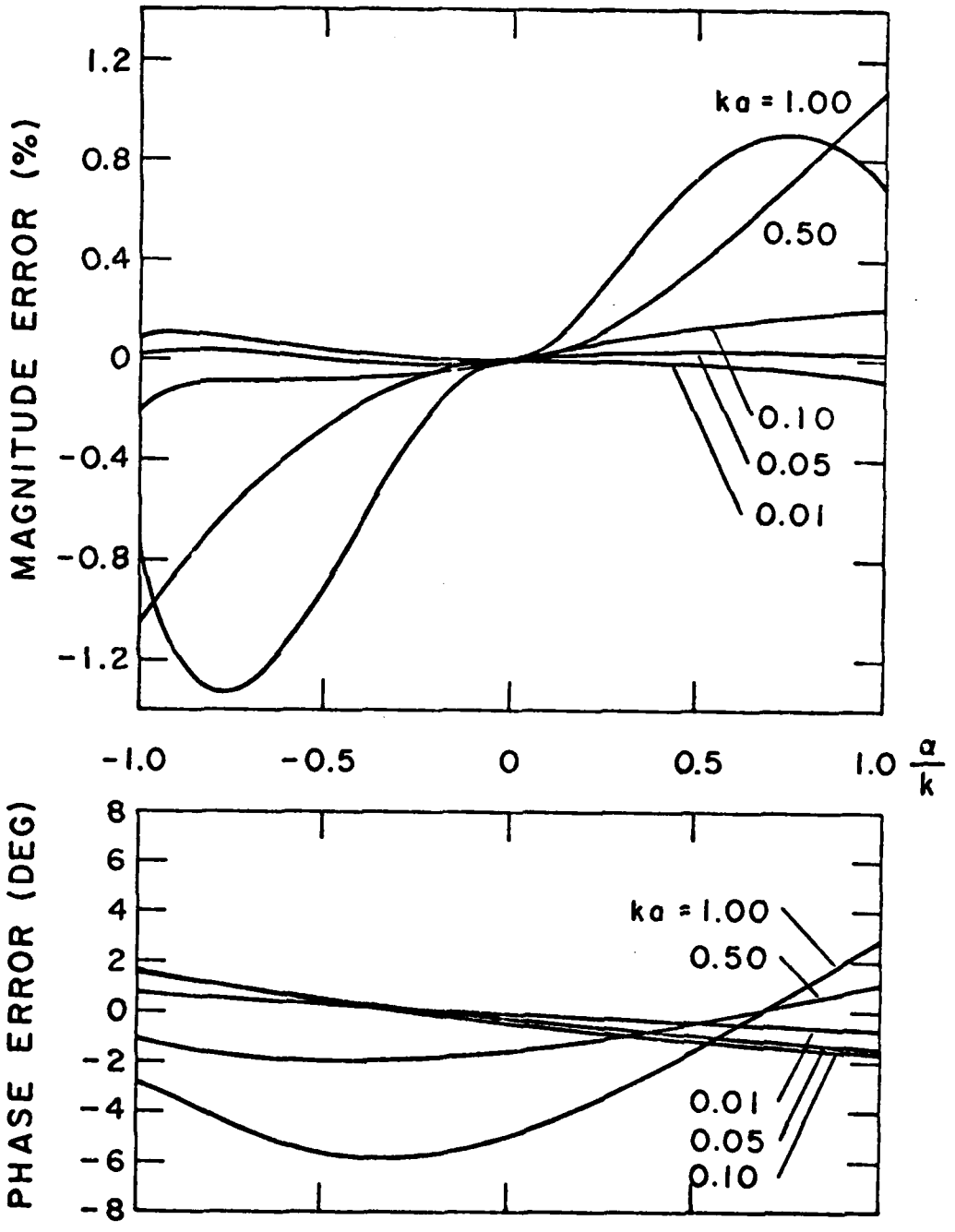

Figure 7. Magnitude and phase errors of the approximate form of $K_+(\alpha)$ in eq. (27) for the range $-k \leq \alpha \leq k$.

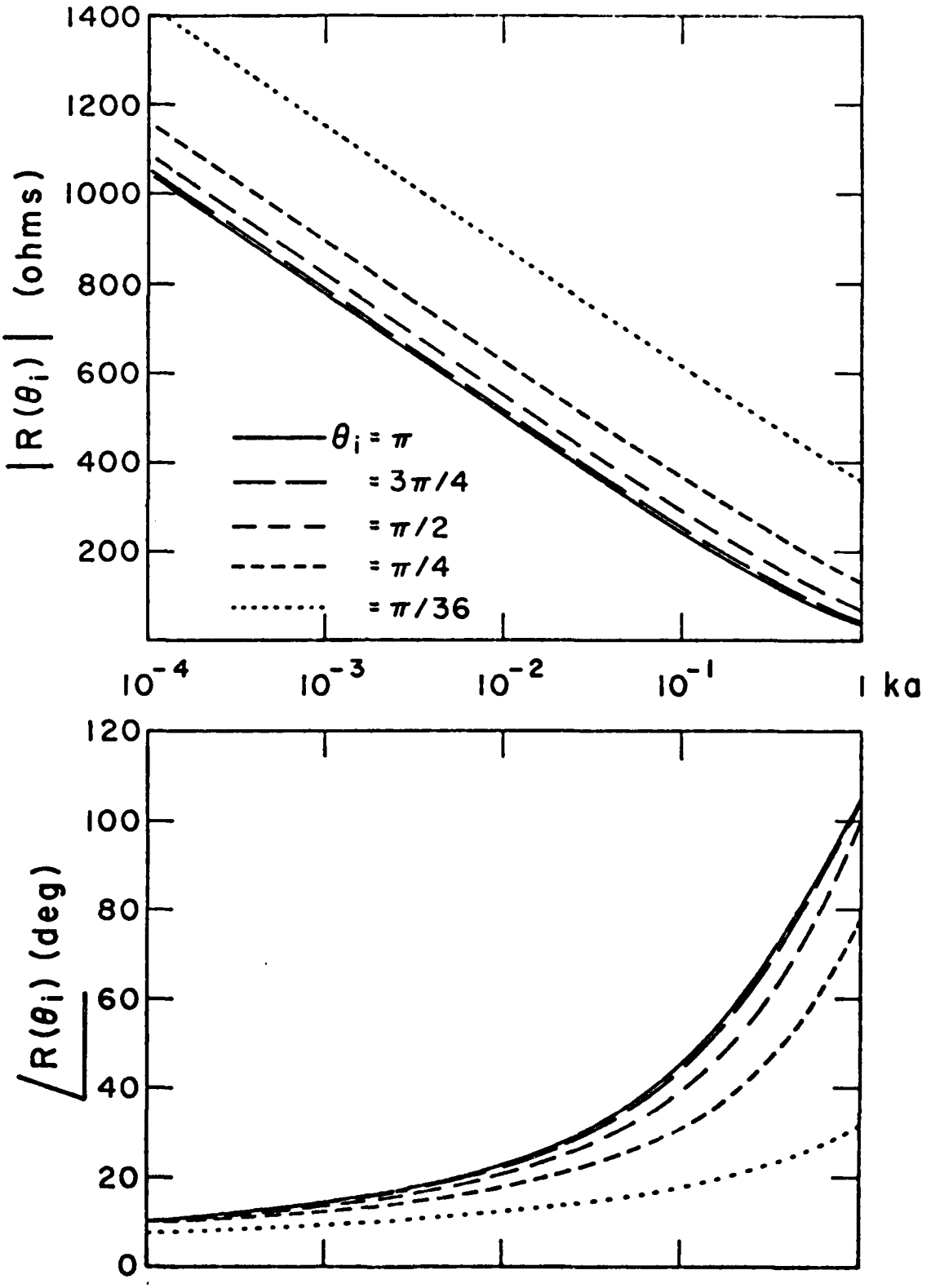

Figure 8. Magnitude and phase of the "reflection coefficient," $R(\theta_i) = (\eta/2\pi)K_+(k)K_+(-k\cos\theta_i)$, calculated from the exact formula for $K_+(\alpha)$ in [15, Sec 5-2.(3)] (See eq. (C11) of Appendix C of this report.)

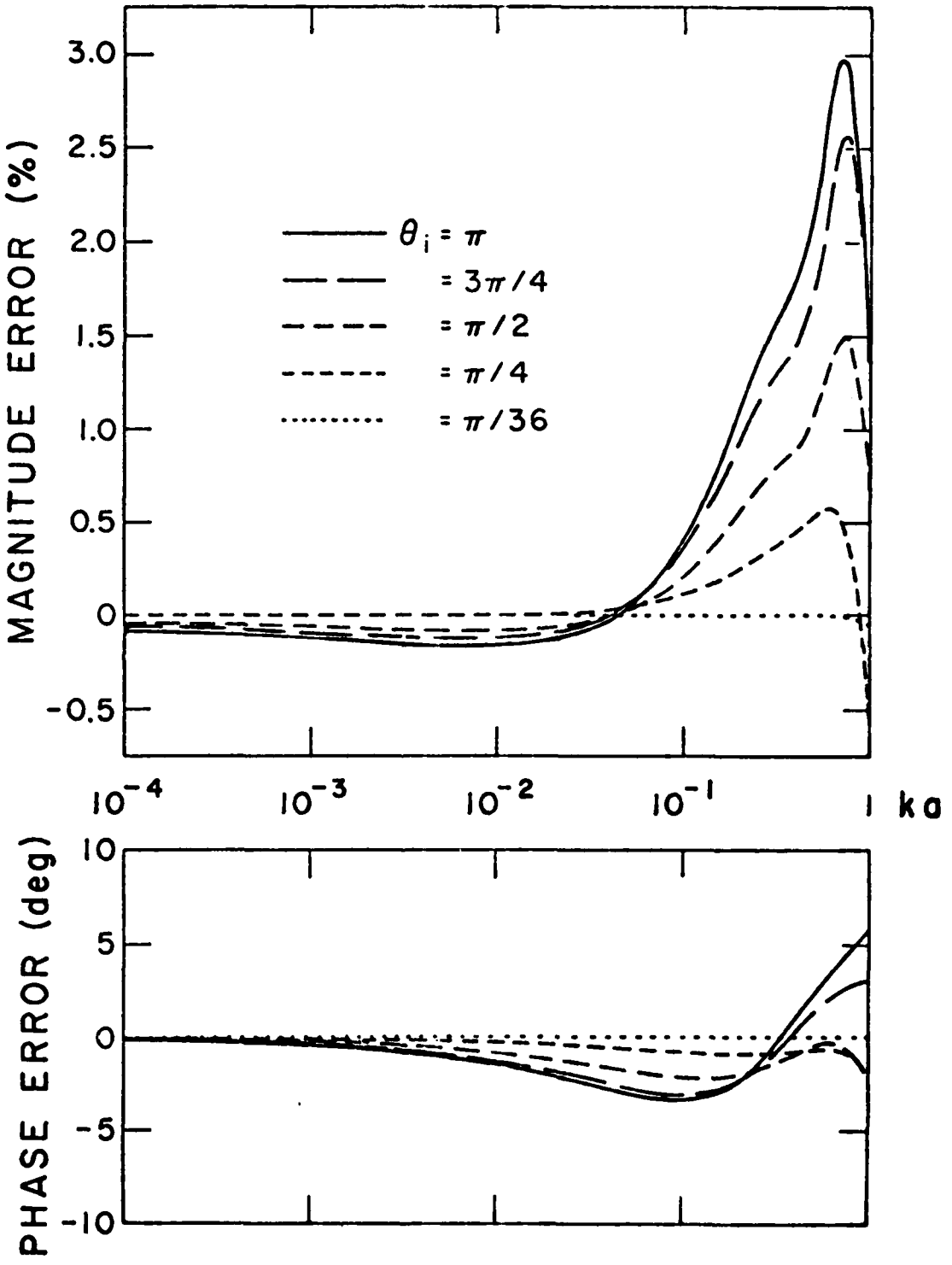

Figure 9. Magnitude and phase errors of the "reflection coefficient," $R(\theta_i) = (\eta/2\pi)K_+(k)K_+(-k \cos \theta_i)$, calculated using the approximate formula for $K_+(\alpha)$ in (27).

Data for $R(\theta_i)$ using the approximate formula for $K_+(\alpha)$ in (27) is not included in Figure 8 because of the very close agreement it has with the exact data. Instead, we show the error of this approximation with regard to the exact in Figure 9 for the same range and set of parameters as in Figure 8. The magnitude error is seen to be at most about 3% and typically much less while the very small phase error is never more than ±5°.

4.3 Reflected current distributions

Denoting the reflected current due to a unit incident current of the form $\exp[ikz \cos \theta_i]$ as $I^N_{refl}(\theta_i;z)$, we have from (6) and (24) the expression,

$$I^N_{refl}(\theta_i,z) = -\frac{\eta}{2\pi} K_+(-k \cos \theta_i)\, W(\theta_i;z) \quad ; \; 0 \le z \le \infty, \; 0 \le \theta_i \le \pi \qquad (33)$$

in both the receiving and transmitting situations. We note that (33) is an exact expression for the normalized reflected current in the receiving situation $(0 \le \theta_i \le \pi)$ and is a very good approximation for the normalized reflected current in the transmitting situation $(\theta_i = \pi)$ when the delta function voltage source is located sufficiently away from the end. From (7) and (26), the approximate form of (33) is given by

$$I^N_{refl}(\theta_i,z) = -R(\theta_i)U(\theta_i;z) \quad ; \; 0 \le z \le \infty, \; 0 \le \theta_i \le \pi \qquad (34)$$

To demonstrate the accuracy attained with our approximate formulas, Figures 10–14 show the behaviors of the "exact" reflected currents in (33) (with $K_+(-k \cos \theta_i)$ numerically determined using the formula of Mittra and Lee [15, Sec. 5-2.13] and $W(\theta_i;z)$ in (6) numerically integrated) and

Legend for Figures 10-14

○ $\theta_i=\pi$ □ $=\pi/2$ ⬡ $=\pi/4$ △ $=\pi/36$ — "Exact" numerically determined $I^N_{refl}(\theta_i;z)$ from (33) found by using the formula of Mittra and Lee [15, Sec. 5-2.(3)] for $K_+(\alpha)$ and by the numerical integration of $W(\theta_i;z)$ given in (6).

———— Approximate form of $I^N_{refl}(\theta_i;z)$ given in (35), with $R(\theta_i)$ from (26) determined by the approximate $K_+(\alpha)$ formula in (27) and the approximate formula (13) used for $U(\theta_i;z)$.

— — — Approximate form of $I^N_{refl}(\theta_i;z)$ given in (35), with $R(\theta_i)$ from (26) determined by the approximate $K_+(\alpha)$ formula in (27) and the approximate formula in (9) used for $U(\theta_i;z)$.

Note: In Figures 10-14, the traveling wave phase factor, e^{ikz}, has been suppressed to aid in improving the clarity of the information presented.

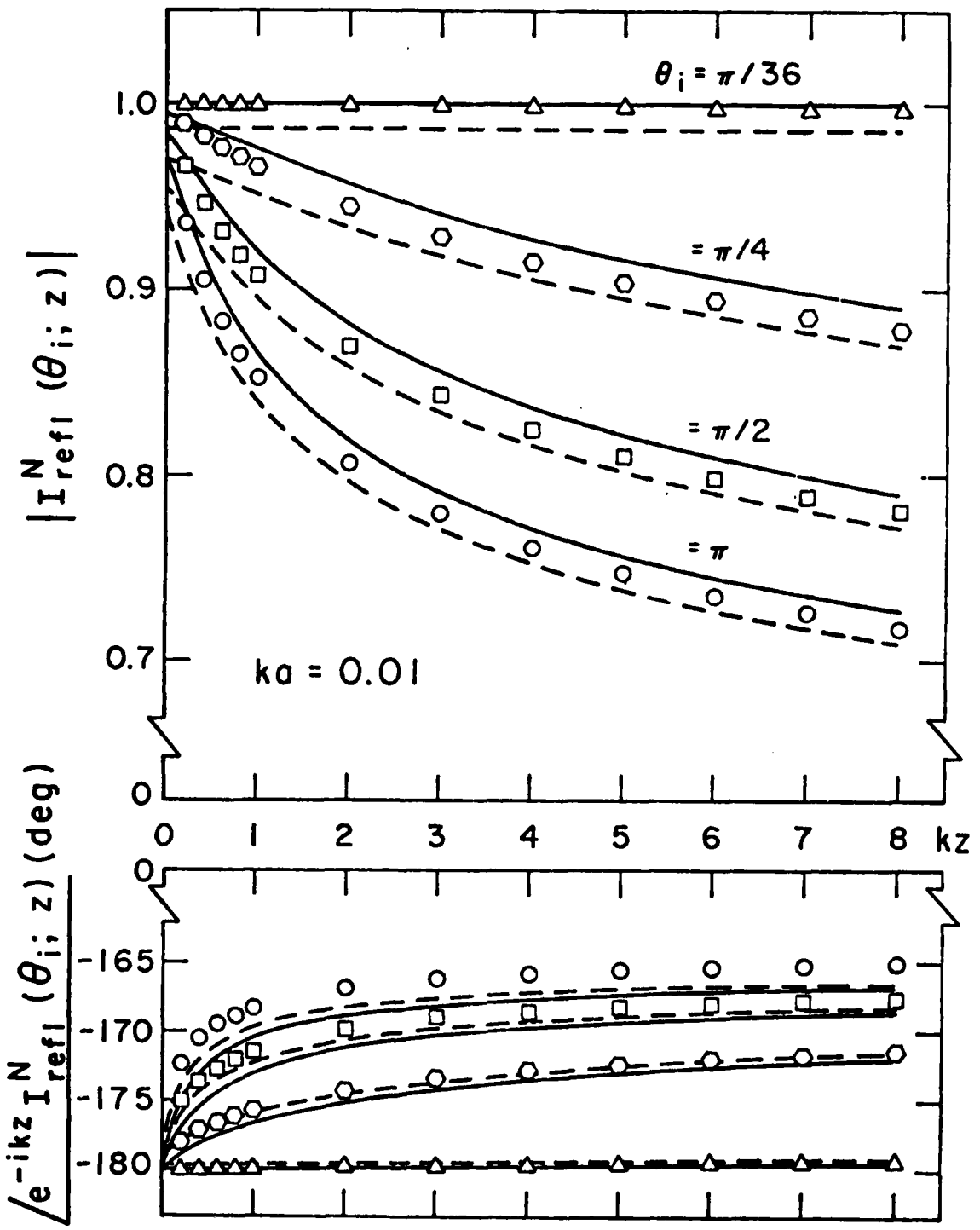

Figure 10. Magnitude and phase of the current reflected from the end of a semi-infinite tubular cylinder where ka = 0.01. (See accompanying Legend for further details.)

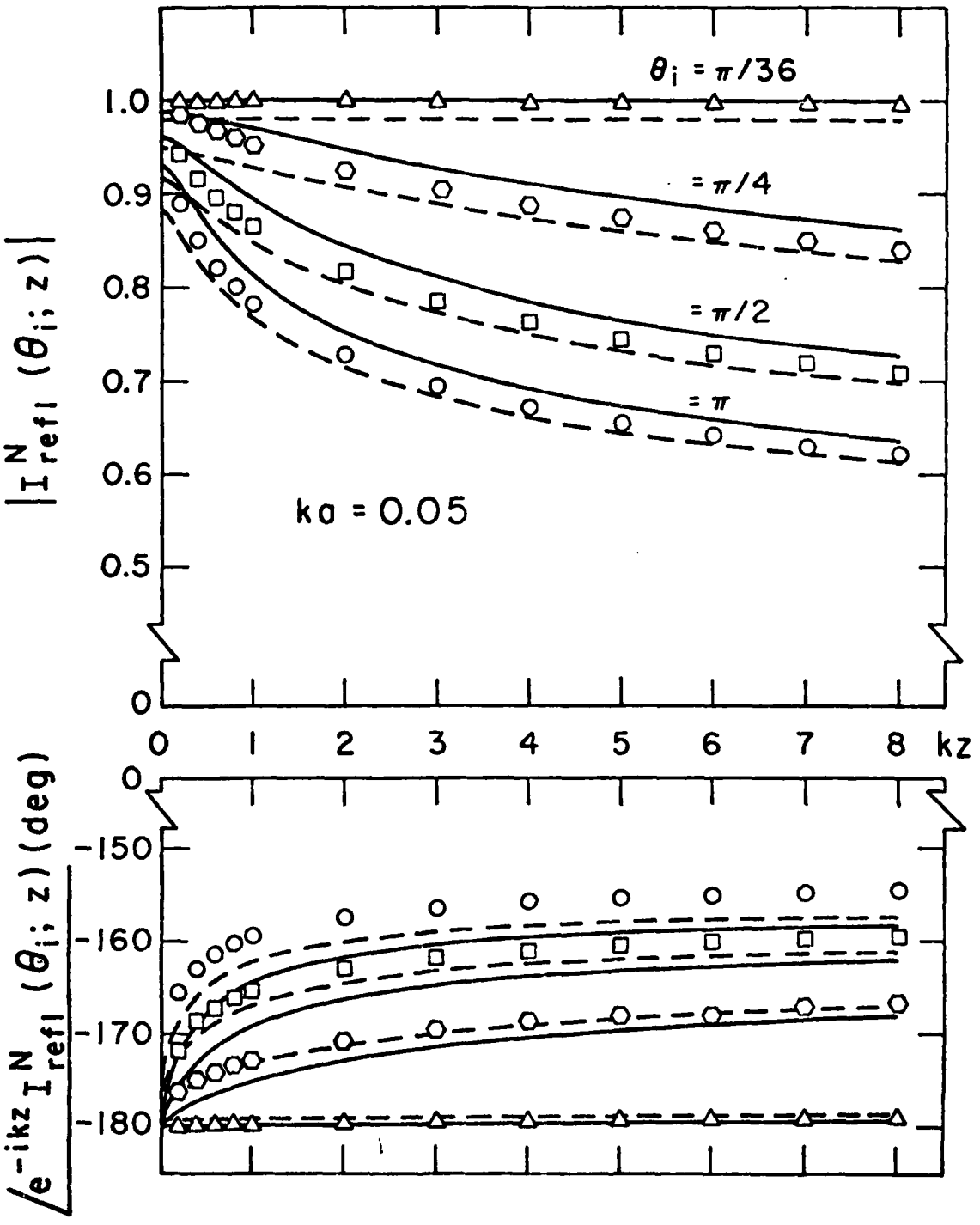

Figure 11. Magnitude and phase of the current reflected from the end of a semi-infinite tubular cylinder where ka = 0.05. (See accompanying Legend for further details.)

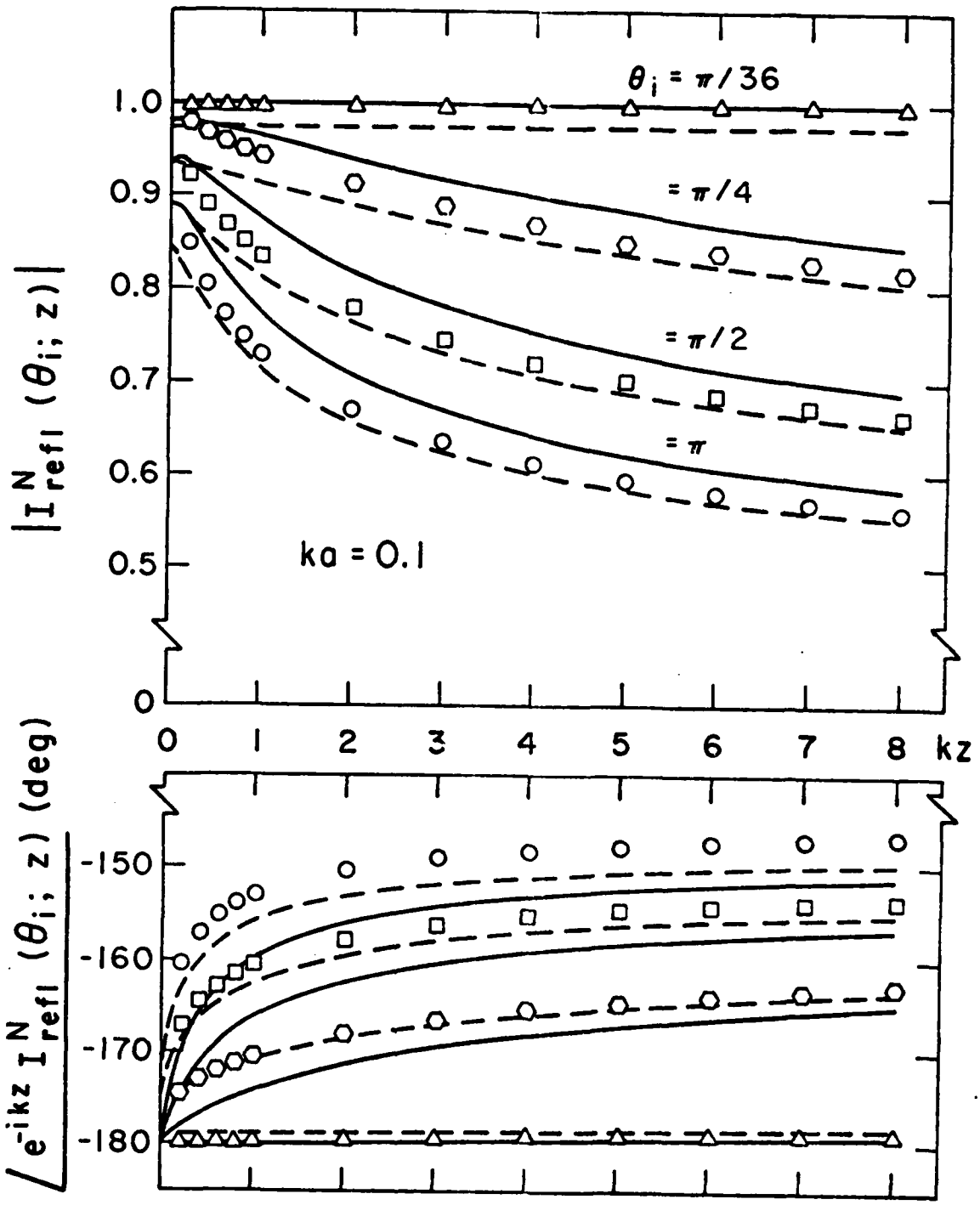

Figure 12. Magnitude and phase of the current reflected from the end of a semi-infinite tubular cylinder where ka = 0.1. (See accompanying Legend for further details.)

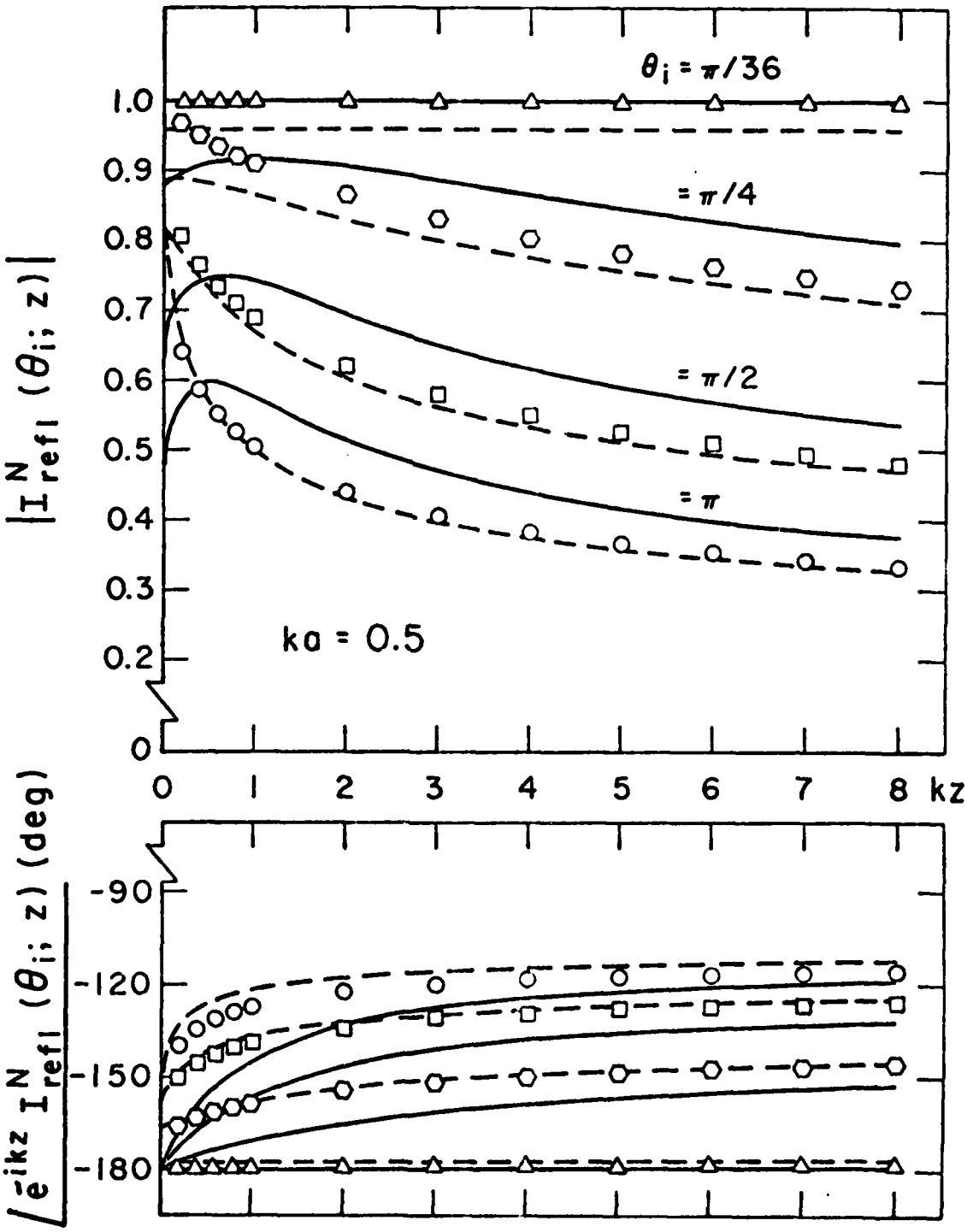

Figure 13. Magnitude and phase of the current reflected from the end of a semi-infinite tubular cylinder where ka = 0.5. (See accompanying Legend for further details.)

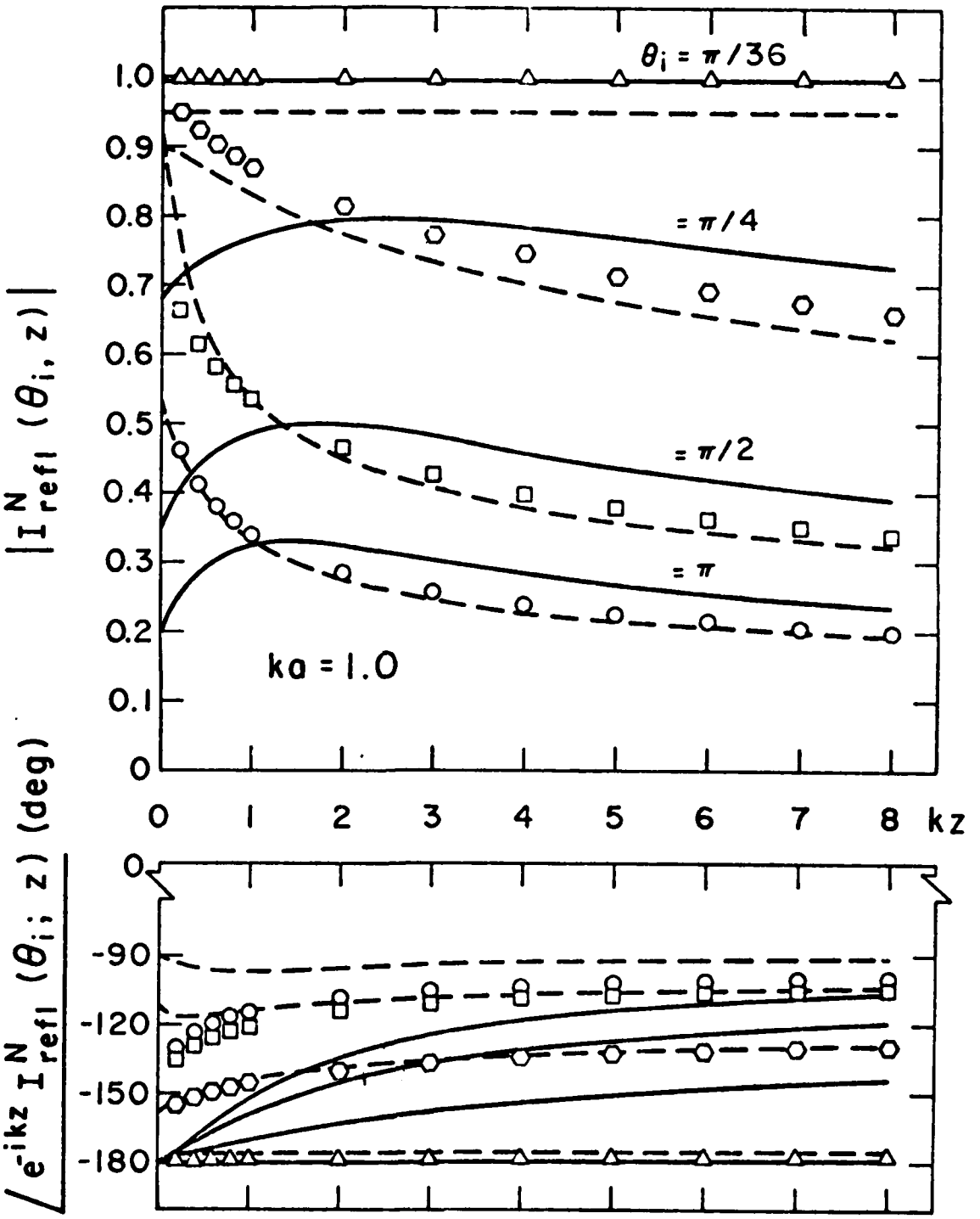

Figure 14. Magnitude and phase of the current reflected from the end of a semi-infinite tubular cylinder where ka = 1.0. (See accompanying Legend for further details.)

the approximate reflected currents in (34) using (27) for $K_+(\alpha)$ in (26) for $R(\theta_i)$ and using both (9) and (13) for $U(\theta_i;z)$ as function of kz in which $\theta_i = \pi/36$, $\pi/4$, $\pi/2$, and π for the values of ka equal to 0.01, 0.05, 0.1, 0.5, and 1.0, respectively. We note that in every case, the data obtained from the use of (9) for $U(\theta_i;z)$ appears to be closer to the numerical data than does results using (13) for $U(\theta_i;z)$. This is somewhat misleading, since in the finite length cylinder situation where multiple reflections of currents from the end are characterized by waves incident at an angle, $\theta_i = \pi$, and subsequently summed (see Section 5) slightly better results are obtained with (13) used for $U(\theta_i;z)$. This apparent incongruity must be a result of the summation procedure producing an error which is more compensitive for the error in (13) for $U(\theta_i;z)$ than it is for the error in (9). A more detailed clarification of this point will be forthcoming.

Section 5. Approximate expressions for the external currents on finite-length cylindrical antennas

Expressions for the currents on finite length cylindrical antennas are constructed by summing the primary and subsequent secondary currents reflected from the ends of the antenna.

5.1 Finite receiving antenna

Our theory can now be applied to the finite length receiving antenna with the understanding that only the average (over the circumference) z-directed current is obtained. As noted by Kao [18] specifically for normal incidence of the plane wave, this zero-order current is not coupled to any higher order variations of the current with respect to the azimuthal angle, ϕ, and may be considered independently from these higher order currents. Rispin and Chang [19] have also noted this to be true for arbitrary polarization and arbitrary incidence of the uniform plane wave.

The constituative currents on a finite length ($-h \le z \le h$), cylindrical receiving antenna with radius, a, are shown pictorially in Figure 15. Beginning with the plane wave induced primary current, $E^i_\theta V(\theta_i;z)$, shown in Figure 15a, the reflections of this current from the end at $z = -h$ and the $z = +h$ end are determined to be $-V(\pi-\theta_i;h)R(\theta_i)U(\theta_i,h+z)$ and $-V(\theta_i;h)R(\pi-\theta_i)U(\pi-\theta_i,h-z)$, respectively, as illustrated in Figure 15b. These reflected currents then propagate toward opposite ends of the cylinder (analogous to waves incident at an angle π with respect to a particular end) at which point they reflect again as $-V(\pi-\theta_i;h)R(\theta_i)U(\theta_i;2h)$ $R(\pi)U(\theta;h-z)$ and $-V(\theta_i;h)R(\pi-\theta_i)U(\pi-\theta_i;2h)R(\pi)U(\pi;h+z)$, respectively. Continuing this procedure leads to an infinite number of reflected currents eminating from each end of the cylinder, as suggested in Figure 15c. The infinite series expressing the current reflected from a particular end of

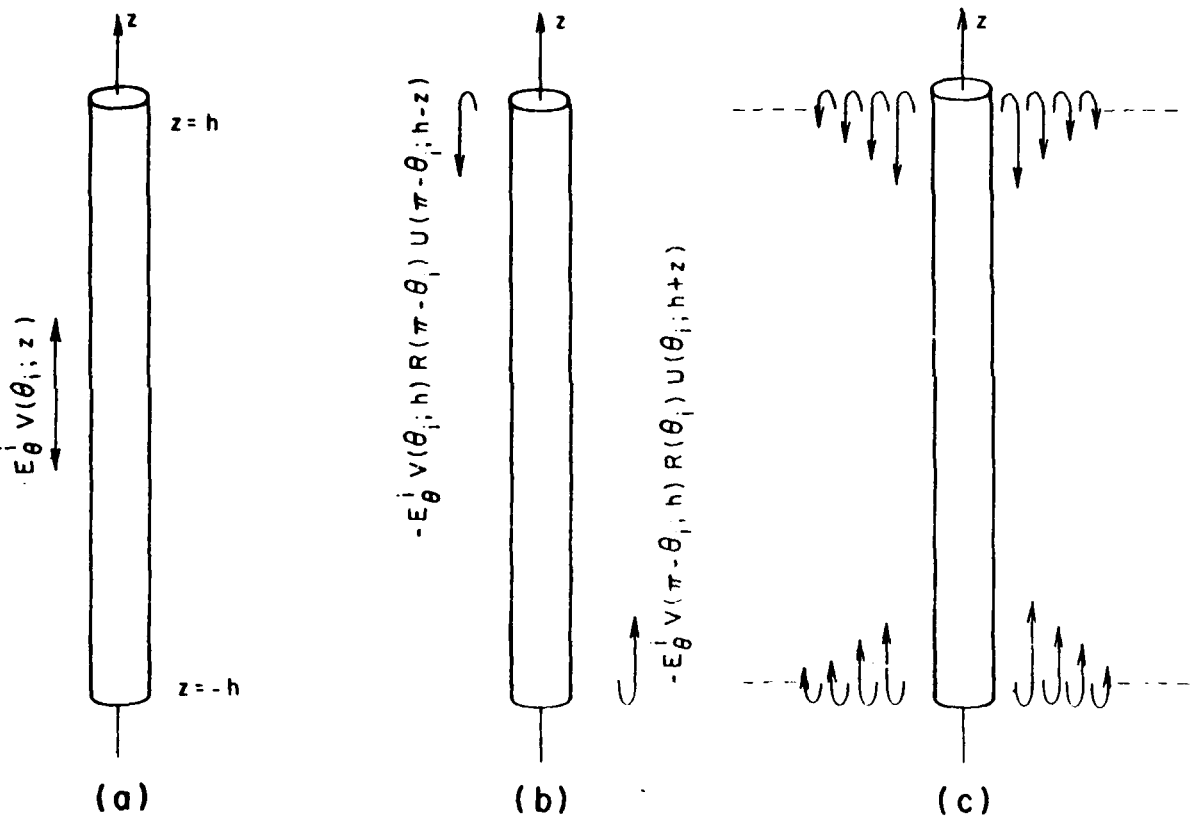

Figure 15. Illustration of the multiple reflection concept as applied to the finite length cylindrical receiving antenna.

a. Primary receiving current distribution from eq. (15).

b. Initial reflection of the primary current from each end from eq. (25).

c. Subsequent multiple reflections.

the cylinder are in the form of simple geometric series which may be readily summed. Hence, we arrive at the following expression for the total external current on the finite length cylindrical receiving antenna,

$$I^R(\theta_i;z) = E^i_\theta\{V(\theta_i;z) - V(\pi-\theta_i,h)R(\pi-\theta_i)U(\theta_i;h+z) - C^R(\pi-\theta_i)R(\pi)U(\pi,h+z)$$

$$- V(\theta_i;h)R(\pi-\theta_i)U(\pi-\theta_i,h-z) - C^R(\theta_i)R(\pi)U(\pi,h-z)\} \qquad (35)$$

where

$$C^R(\theta_i) = \frac{[V(\theta_i;h)R(\pi-\theta_i)U(\pi-\theta_i;2h)R(\pi)U(\pi;2h)-V(\pi-\theta_i;h)R(\theta_i)U(\theta_i;2h)]}{1 - [R(\pi)U(\pi;2h)]^2} \qquad (36)$$

represents the total incident current (with an analogous wave incidence of $\theta_i = \pi$) upon the end $z = +h$ due to current reflections eminating from the end at $z = -h$. $C^R(\pi-\theta_i)$ has a similar interpretation with the ends interchanged. The terms involving $R(\theta_i)U(\theta_i,h+z)$ and $R(\pi-\theta_i)U(\pi-\theta_i;h-z)$ represent the initial reflections of the primary current wave incident at the angles, θ_i and $\pi - \theta_i$, respectively. Thus, except for the primary term, $V(\theta_i;z)$, all the other terms in (35) represent reflected currents from the ends of the cylinder. Our expression for the receiving antenna current in (35) agrees in form with that of Weinstein [2] and can be shown to be consistent with our earlier result in [17] under the conventional thin wire approximations. A complete formal agreement between our result and that of Shen [7] occurs only when the terms $U(\theta_i;z)$ and $U(\pi-\theta_i,z)$ in (35) are approximated by $U_s(z)$ in (20) with the constant, g, deleted. The approximation of these terms in this manner is implicit in Shen's [7] analysis.

The limiting form of the current on a finite length receiving antenna as the angle, θ_i, approaches grazing incidence, i.e., $\theta_i \to 0$ or π, based upon both approximate forms of $U(\theta_i;z)$ in (9) and (13) is discussed in Appendix D. And it is found that, while our theory is not expected to be valid in this range because of the apparent violation of the restriction, $\Omega(z) >> |\ln(v_0)|$ in (8), the approximate form of $U(\theta_i;z)$ in (13) actually produces the very physically acceptable result of a vanishing current as $\theta_i \to 0$ or π. Also a smaller, magnitude-wise, result for the current near the ends of a cylinder for a fixed incident angle, θ_i, is obtained in Appendix D, when (13) is used for $U(\theta_i;z)$ rather than (9). These considerations are very important in the cases when the incident angle θ_i is near grazing, i.e., $\theta_i = 0$ or π, and when the length of the antenna becomes electrically short.

And, finally, we note the symmetrical behavior of (35) with respect to the incident angle of the uniform plane wave and the position, z,

$$I^R(\theta_i;-z) = I^R(\pi-\theta_i;+z) \tag{37}$$

5.2 Finite transmitting antenna

In much the same manner, the current on a finite length $(-h \le z \le +h)$ cylindrical transmitting antenna of radius, a, due to a delta function voltage source of strength, V_0, at $z = z_0$ (see Figure 16) may be expressed in terms of a primary current and the multiply reflected currents from the ends. Figure 16a illustrates the primary current, which we shall approximate by $U_s(|z-z_0|)$ from (20), eminating from the delta function voltage source at $z = z_0$. These waves are incident upon the ends of the cylinder at an angle of π respective to the particular end. Hence, the initial reflections of the primary current from $z = -h$ and $z = +h$ are,

$-V_0U_s(\pi,h+z_0)R(\pi)U(\pi,h+z)$ and $-V_0U_s(\pi,h-z_0)R(\pi)U(\pi,h-z)$, respectively, as is shown in Figure 16b. The reflections of these currents from the respective opposite ends and the subsequent reflections which follow (Figure 16c) lead to a pair of infinite series, which are again summable. The final result for the transmitting current distribution is given by,

$$I^T(z_0;z) = V_0\{U_s(|z-z_0|)$$

$$- U_s(h+z_0)R(\pi)U(\pi;h+z) - C^T(h+z_0)R(\pi)U(\pi;h+z)$$

$$- U_s(h-z_0)R(\pi)U(\pi;h-z) - C^T(h-z_0)R(\pi)U(\pi;h-z)\} \qquad (38)$$

where

$$C^T(z) = \frac{U_s(z)[R(\pi)U(\pi;2h)]^2 - U_s(2h-z)R(\pi)U(\pi;2h)}{1 - [R(\pi)U(\pi;2h)]^2} \qquad (39)$$

represents the sum of the currents incident upon the $z = -h$ and $+h$ ends of the antenna when z is taken as $h+z_o$ and $h-z_o$, respectively, due to current reflections eminating from the opposite end. Note that the initial reflection of the primary current from each end is explicitly stated in (38), the overall form of the transmitting current expression being the same as that for the receiving current in (35). Our transmitting current expression in (38) can be shown to be equivalent in form to those of many other authors [1, Sec. 35.7], [2], [6] and others.

However, unlike the expressions of these authors, our expression is more general and flexible, since we claim it may be used for electrically short as well as electrically thick antennas as long as the basic condition in (8), $\Omega(z') = 2\ln(2z'/a) \ll |\ln(2kz')|$ is satisfied (note here

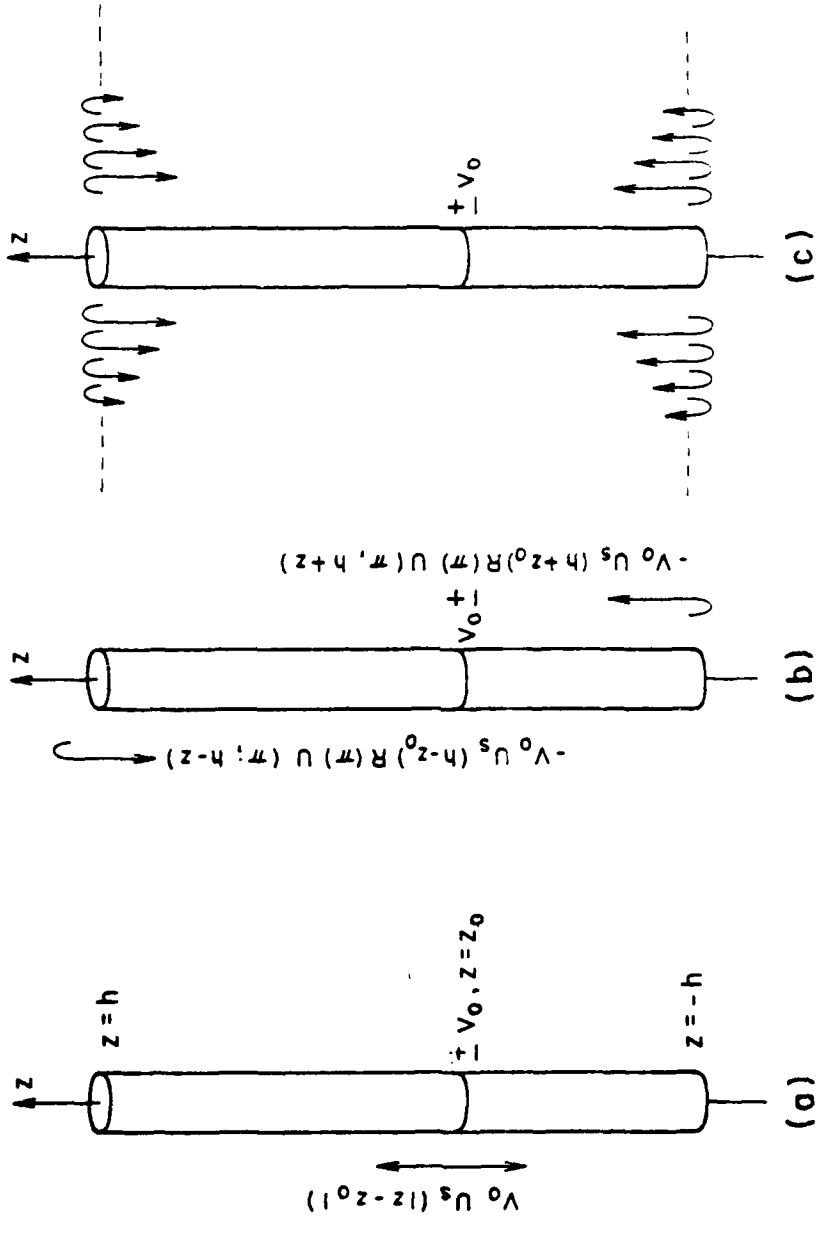

Figure 16. Illustration of the multiple reflection concept as applied to the finite length cylindrical transmitting antenna.

a. Primary transmitting current distribution from (19) and (20).

b. Initial reflection of the primary current from each end from eq. (32).

c. Subsequent multiple reflections.

z' refers to the distance to the source, $z-z_0$, and the distances to the cylinder ends, $h+z$ and $h-z$) and appropriately accurate values of $R(\pi)$ are used. And in this report, we often take the nominal measure, $z' = h$.

We note the symmetry in (38) with respect to the source and observation points, i.e.,

$$I^T(z_0;-z) = I^T(-z_0;z) \tag{40}$$

An approximate formula for the input admittance of an asymetrically driven cylindrical antenna of length, 2h, obtained by setting $z=z_0$ and $V_0 = 1$ volt in (38) is given by

$$\begin{aligned} Y_{in} = G - iB = {} & U_s(0) \\ & - U_s(h+z_0)R(\pi)U(\pi;h+z_0) - C^T(h+z_0)R(\pi)U(\pi;h+z_0) \\ & - U_s(h-z_0)R(\pi)U(\pi;h-z_0) - C^T(h-z_0)R(\pi)U(\pi;h-z_0) \end{aligned} \tag{41}$$

Here G is the input conductance and B is a "relative" input susceptance. The qualification to a "relative" input susceptance is necessary, due to the fact we employ a delta function voltage source for the excitation and the mathematically predicted behavior of the imaginary part of the input current for this excitation should exhibit a logarithmic singularity [20] and [21]. This singularity would indicate an infinite capacitance, the so-called "knife-edge capacitance" [22]. However, the particular way in which the primary current term, $U_s(z)$, was derived (discussed in Section 3.2) does not allow the possibility of such a singularity in this current at the source. In a realistic sense, though, this slice

capacitance is due to an idealization in the mathematical model rather than a physically occurring phenomenon in the practical situation and in general does not pose any difficulties in experimental studies. Thus, the absence of such a singularity in our formulation is not unwelcomed.

6. Approximate expressions for the internal currents on cylindrical antennas

Thus far our theory has considered only the external current distributions on cylindrical antennas, hence, it is appropriate at this time to include a complementary discussion of the current distributions on the internal walls of receiving and transmitting cylindrical antennas. By combining the external and internal current distributions, the total current on the antenna may be found. But a more important use of a knowledge of the internal current occurs in some electromagnetic compatibility studies where it is desirable to know the amount of penetration into a long thin metallic enclosure. In many cases, the penetration is into the end of a cylinder and one needs to know the induced current on the internal wall of the cylinder.

6.1 Internal current on a semi-infinite receiving antenna

The TM_{0n} mode currents on the internal wall of a semi-infinite ($0 \le z \le \infty$) cylinder due to a plane wave incident at an angle, θ_i, are easily determined by a Wiener-Hopf analysis [17, Eq. 27] to be given by

$$\{I^R_{s\infty}(\theta_i;z)\}_{int} = E^i_\theta V(\theta_i;0) \left[\frac{ik}{2\pi}(1-\cos\theta_i)K_+(-k\cos\theta_i)\right] \int_{\Gamma_1} \frac{K_+(-\alpha)e^{-i\alpha z}}{(k+\alpha)(k\cos\theta_i+\alpha)K(\alpha)}\, d\alpha \; ; \; 0 \le z \le \infty, \; 0 \le \theta_i \le \pi \qquad (42)$$

where $E^i_\theta V(\theta_i;0)$ is the incident current at the end and is given in (15). The contour, Γ_1, is shown in Figure 1 and K_+ is the "plus" factor of $K(\alpha)$ in (4), which is discussed in Appendix C. Since the contour, Γ_1, encloses only simple poles of $[K(\alpha)]^{-1}$, the integral may be easily

evaluated and (42) may be written in the form,

$$\{I^{R}_{s\infty}(\theta_i;z)\}_{int} = E^{i}_{\theta}\, V(\theta_i;0) \sum_{n=1}^{\infty} T_{0n}(\theta_i) e^{-\gamma_{0n} z} \tag{43}$$

where T_{0n} is a transmission coefficient given by,

$$T_{0n}(\theta_i) = +i \frac{k}{2} (1-\cos\theta_i) K_{+}(-k\cos\theta_i) \frac{(\gamma_{0n}-ik)}{\gamma_{0n}(\gamma_{0n}+ik\cos\theta_i)} K_{+}(i\gamma_{0n}) \tag{44}$$

and,

$$i\gamma_{0n} = i\sqrt{(\rho_{0n}/a)^2 - k^2} \tag{45}$$

is the propagation constant of the TM_{0n} circular waveguide mode. And finally, ρ_{0n} is the $n^{\underline{th}}$ ordered zero of the Bessel function, J_0. Several approximations are possible to allow us to state the internal current in a more convenient form. The first of which is from the approximate splitting of the asymptotic form of the kernel, $K(\alpha)$, for large αa and is given by

$$K_{+}(\alpha) \approx \sqrt{i/(k+\alpha)a} \quad ; \quad \text{for } \alpha a \text{ large} \tag{46}$$

Numerical data comparing (46) with the exact value of $K_{+}(\alpha)$ from the formula of Mittra and Lee [15, Sec. 5-2.(3)] has shown good agreement for $\alpha \geq i\gamma_{01}$ up to $ka \approx 1.0$. Also for $e^{-\gamma_{0n} z} \ll 1$, the infinite sum may be truncated at $n=N$ and the subsequent loss of information for the smaller values of z may be somewhat compensated for, by approximating the summation in (43) at $z=0$ using relevant Taylor series expansions for $ka \leq 1$ in the manner described in Appendix E. The summation in (43)

may then be approximately written as

$$\sum_{n=1}^{\infty} T_{0n}\, e^{-\gamma_{0n} z} = \begin{cases} \frac{1}{2}\,(1-\cos\theta_i) K_+(-k\cos\theta_i) \sum_{m=1}^{4} S_m(\theta_i)(ika)^m; & z=0 \\ \sum_{n=1}^{N} T_{0n}(\theta_i) e^{-\gamma_{0n} z} \quad ; \quad e^{-\gamma_{0n} z} \ll 1 \end{cases} \tag{47}$$

where

$$S_1(\theta_i) = 0.5831 \tag{48}$$

$$S_2(\theta_i) = -0.1364\ [\tfrac{1}{2} + \cos\theta_i] \tag{49}$$

$$S_3(\theta_i) = -0.0498\ [\tfrac{7}{8} - \tfrac{1}{2}\cos\theta_i - \cos^2\theta_i] \tag{50}$$

$$S_4(\theta_i) = 0.0198\ [\tfrac{9}{16} + \tfrac{11}{8}\cos\theta_i - \tfrac{1}{2}\cos^2\theta_i - \cos^3\theta_i] \tag{51}$$

which is sufficiently accurate for most engineering applications up to $ka \approx 1$.

6.2 Internal currents on a semi-infinite transmitting antenna

The current which penetrates into the end of a semi-infinite ($0 \le z \le \infty$) cylindrical transmitting antenna having a delta function voltage source of strength, V_0 volts, at $z=z_0$ is associated with TM_{0n} circular waveguide modes and may be written in an analogous manner with respect to the receiving case as,

$$\{I^T_{s\infty}(z)\}_{int} = I^T_{\infty}(z_0;0)\left[-\frac{ik}{\pi} K_+(k)\right] \int_{\Gamma_1} \frac{K_+(-\alpha)e^{-i\alpha z}}{(k^2-\alpha^2)K(\alpha)}\, d\alpha \ ; \ 0 \le z \le \infty \tag{52}$$

where $I^T_\infty(z_0;0)$ is the incident current from (19) at the end. Again the contour, Γ_1, is given in Figure 1 and K_+ is the plus factor of $K(\alpha)$ in (4) discussed in Appendix C. The integral may be evaluated exactly by finding the residues of the poles of $[K(\alpha)]^{-1}$ enclosed by Γ_1 and (52) may then be approximated by,

$$\{I^T_{s\infty}(z)\}_{int} = V_0 U_s(z_0) \sum_{n=1}^{\infty} T_{0n}(\pi)\, e^{-\gamma_{0n} z} \tag{53}$$

where we have replaced the exact incident current, $I^T_\infty(z_0;0)$ with the approximate quantity, $V_0\, U_s(z_0)$ from (20). T_{0n} and γ_{0n} have been defined in (44) and (45), respectively. Again, as in the receiving formulation, we may approximate the summation in (53) with the expression in (47).

It should be noted that there would also be internal wall currents on the semi-infinite transmitting antenna which would not come from penetration at the cylinder end but rather would be excited directly by the source. For a delta function voltage source, this internal current can be shown to possess a logarithmic singularity at the feed-point similar to the logarithmic singularity of the external current at the input. For a more realistic excitation, such as a finite gap, however, the internal current would be well-behaved everywhere and would be directly related to a capacitive susceptance component (assuming there to be negligible radiation from the open end of the cylinder which in turn implies, $e^{-\gamma_{01} z_0} << 1$) of the overall input admittance. And since we have not addressed ourselves to the task of specifically defining a "realistic" input susceptance, the internal current in the vicinity of the voltage source and its effect on the input admittance will not be pursued any further in this report.

6.3 Internal current on a finite-length receiving antenna

From the external receiving current expression in (35), we may write the internal penetrating current near $z = -h$ using the transmission characterization in (43) as,

$$I^R_{int}(\theta_i;z) = E^i_\theta \sum_{n=1}^{\infty} \{V(\pi-\theta_i,+h)\ T_{0n}(\theta_i) + C^R(\pi-\theta_i)\ T_{0n}(\pi)\}\ e^{-\gamma_{0n}(h+z)} \quad ; z \simeq -h \qquad (54)$$

while the penetrating current near the opposite end at $z = +h$ is obtained by replacing θ_i with $\pi-\theta_i$ and $(h+z)$ with $(h-z)$ in the above expression. The first term in the {brackets} above corresponds to TM_{0n} mode currents on the internal walls of the cylinder due to the primary current term, $E^i_\theta\ V(\pi-\theta_i;+h)$, while the second term corresponds to TM_{0n} mode currents due to the total external current incident upon $z = -h$ arising from reflections eminating from the opposite end at $z = +h$. These latter currents are analogous to waves incident at an angle, $\theta_i = \pi$. Hence, the transmission coefficient for these incident currents is evaluated at $\theta_i = \pi$. The expression in (47) may be used to approximate the summations in (54), thereby reducing the computational efforts required to find the internally penetrating current. Note, it is implicit in this formulation, that there is no internal interaction between the ends of the cylinder, thus implying that $e^{-\gamma_{01}2h} << 1$.

6.4 Internal current on a finite-length transmitting antenna

The internal penetrating current near the ends of a finite length $(-h \le z \le h)$ cylindrical transmitting antenna may be obtained by applying the transmission characterization in (53) to the respective incident currents from (38) with the result,

$$I^{T}_{int}(z = \mp h) = V_0 \{U_s(h \mp z_0) + C^{T}(h \pm z_0)\}$$

$$\sum_{n=1}^{\infty} T_{0n}(\pi)\, e^{-\gamma_{0n}(h \pm z)} \qquad (55)$$

Analogous to the receiving case, the first term in (55) corresponds to TM_{0n} mode currents on the internal walls of the cylinder due to the primary current, $V_0\, U_s(|z - z_0|)$ at $z = \mp h$ while the second term corresponds to TM_{0n} mode currents due to the total external current incident upon $z = \mp h$ arising from reflections eminating from the opposite end. Again, (47) may be used to approximate the summations in (55) and the restriction, $e^{-\gamma_{01}(h \pm z_0)} << 1$, is also implied in this formulation.

6.5 End conductance of a finite length cylindrical antenna

A quantity related to the internally penetrating current on a cylindrical antenna is the input conductance for a TM_{0n} mode incident upon one of the ends of the antenna. Unlike the cases treated by Weinstein [2, Chap. 1], Levin and Schwinger [23], Jones [24] and others, our analysis for the end conductance, discussed in Appendix F, deals with a TM_{0n} mode under cut-off, the radiation in this case necessarily coming from tunneling. The end conductance in this situation is relevant and very important to EMC studies involving the penetration into the end of a cylindrical enclosure [25]. A detailed discussion of this quantity is left to Appendix F, where the end conductance as seen by an evanescent TM_{0n} mode inside and near the end of a finite length cylinder based upon Wiener-Hopf analyses and the multiple reflection concept is derived.

Section 7 Numerical results for the finite length cylindrical antenna

Due to the restriction our theory places upon the electrical radius of $ka \lesssim 1$, the currents on the internal wall of the finite length cylindrical receiving or transmitting antenna are, in general, very much smaller in magnitude than the currents on the external wall, except in the near vicinities of the ends. From Section 6, it may be ascertained, that the internal current is significant only within a distance, 2a, (equal to one cylinder diameter) from either end. And since we cannot rely upon results from our external current expressions so close to the ends, where the internal currents are significant, the formation of total current distributions from the combinations of our receiving and transmitting external current distributions in (35) and (38), respectively, with the corresponding internal current distributions in (54) and (55) would be of little advantage. Hence, in most cases, the external current formulas in (35) and (38) will be sufficient to describe the current distribution, whether it be the total or external only, on finite length receiving or transmitting antennas, respectively. On the other hand, the internal current distributions given in (54) and (55) for the finite length receiving and transmitting cylindrical antennas may be accurately calculated using the approximate formula in (47) at practically any point on the antenna.

7.1 Current distribution on a receiving antenna

In order to examine differences in our receiving theory resulting from the use of either approximate form of $U(\theta_i;z)$ in (9) or (13) we have included Figure 17 which shows the magnitude of the induced current at the center of a receiving antenna where $\Omega(h) = 10$, illuminated by

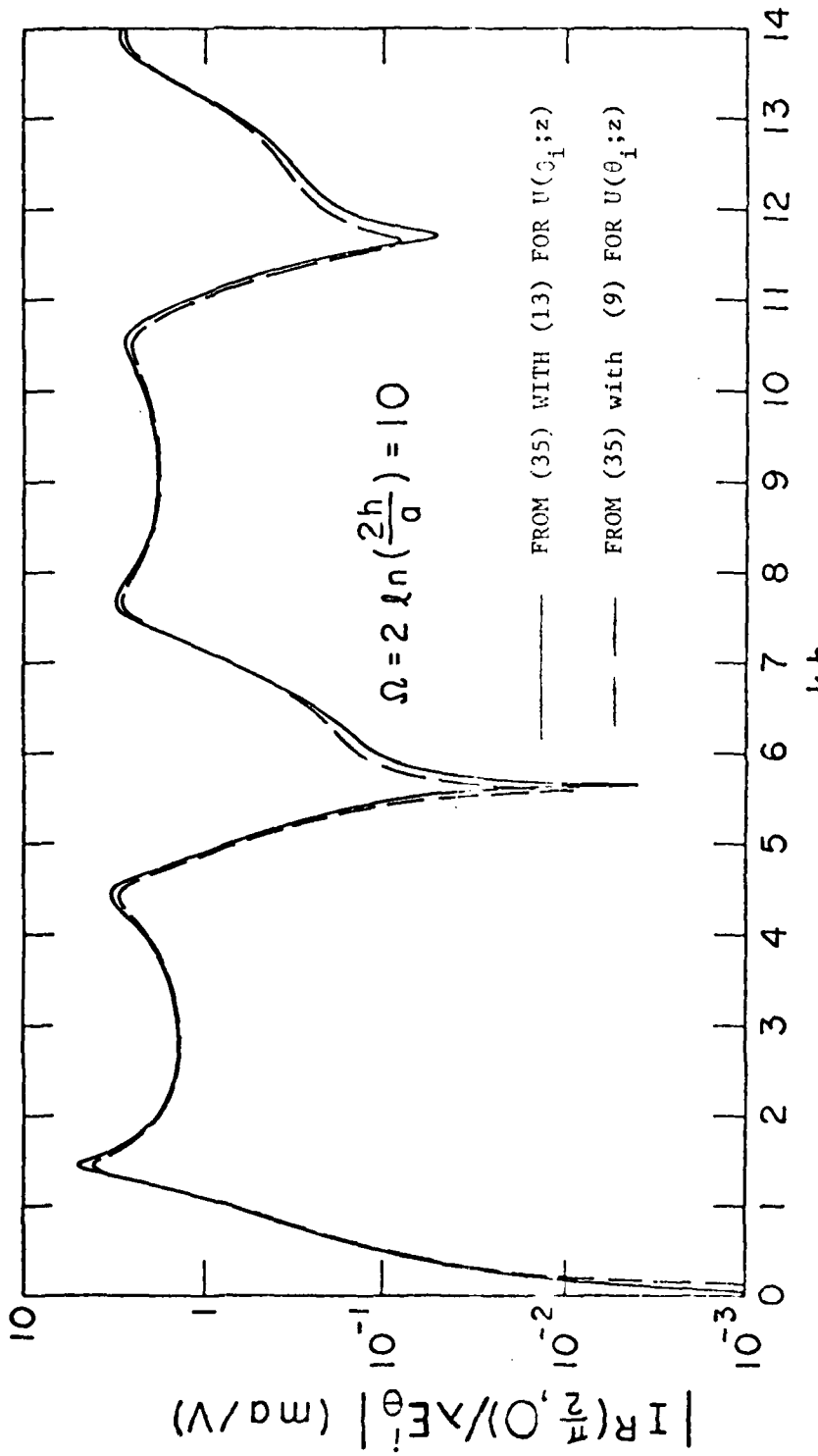

Figure 17. Magnitude of the current at the center of a cylindrical receiving antenna due to a normally incident uniform plane wave as a function of the electrical half-length, kh, and normalized to the incident electric field and the wavelength.

a normally incident ($\theta_i = \pi/2$) plane wave polarized parallel to the antenna as a function of the electrical length, using both (9) and (13) in the finite length receiving antenna current expression in (35). As expected, the agreement between both results is very good except near resonances and anti-resonances. And comparisons with existing analytical and numerical results for cylindrical antennas in which the condition, $\Omega(h) >> |\ell n(v_0)|$ in (8), is satisfied, have indicated that our theory yields slightly better results in almost every case when (13) is used for $U(\theta_i; z)$. For these reasons, in what follows we shall present only results obtained from the use of (13) for $U(\theta_i; z)$ in the receiving and transmitting expressions in (35) and (38), respectively.

The current distributions on a half-wave, $kh = \pi/2$, receiving antenna where $\Omega(h) = 2\ \ell n(2h/a) = 10$ for the incident angles, $\theta_i = \pi/36,\ \pi/6,\ \pi/3$ and $\pi/2$ as calculated from (35) are shown in Figure 18. For comparison, first order results from the King-Middleton theory [11, Chap. IV, Sec. 7] and results from King's three term theory [5] for the normal incidence case, $\theta_i = \pi/2$, are also shown. The agreement between the latter King theory and ours in this particular case is excellent. And the overall agreement between all theories is quite acceptable. We note that in spite of the condition in (8) which requires $\Omega(h) = 2\ \ell n(2h/a) >> |\ell n(v_0)|$, the current distribution predicted by our formulas in the near-grazing situation, $\theta_i = \pi/36$, is at a physically anticipated small level. This is further exemplified in Figure 19, where for the same antenna as in Figure 18 the currents at $z = 0$, $h/3$ and $2h/3$ are illustrated as a function of the incident angle, θ_i. And we note the near sinusoidal variation of the current with respect to the incident angle, θ_i, as would be expected for a thin half-wave dipole.

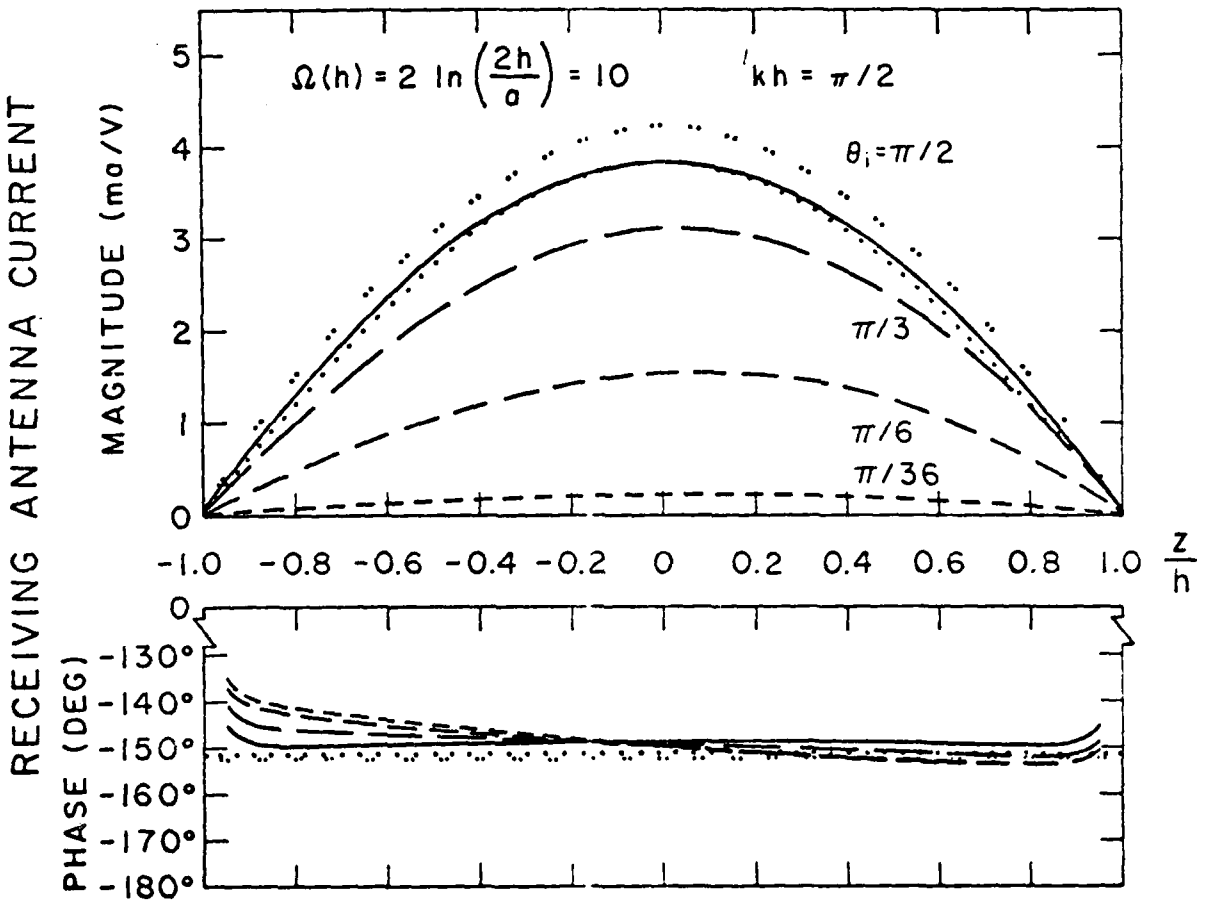

Figure 18. Current distribution on a thin half-wave receiving antenna normalized to the incident electric field and the wavelength, i.e., $I^R(\theta_i;z)/\lambda E^i_\theta$.

——————— $\theta_i = \pi/2$
— — — — $= \pi/3$
— — — — — $= \pi/6$
— — — — — — $= \pi/36$
} from eq. (35) with (13) used for $U(\theta_i;z)$

. . . . . $\theta_i = \pi/2$ Three term theory of King [5]

.. .. $\theta_i = \pi/2$ First order King-Middleton theory [II, Sec. IV.7]

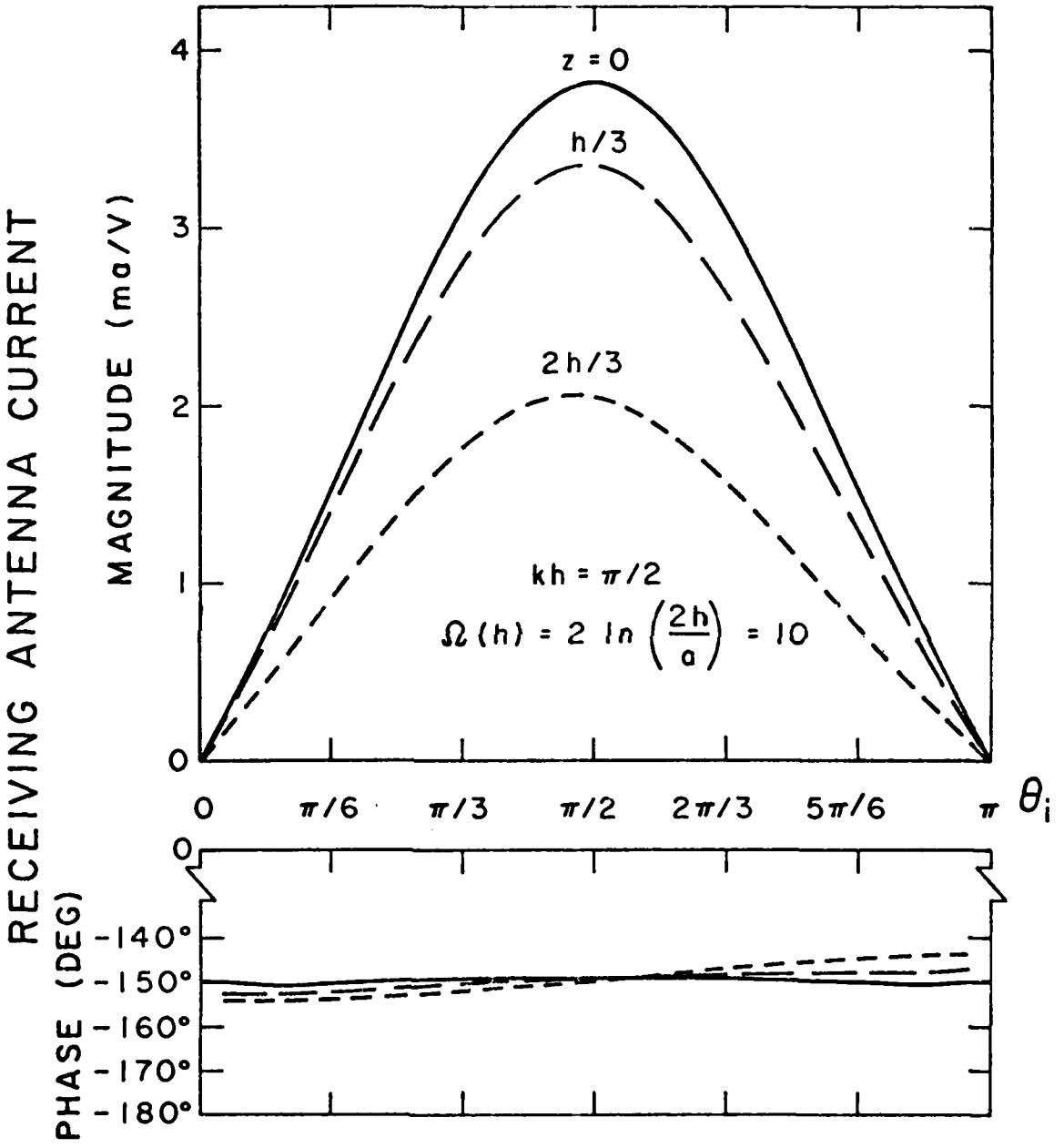

Figure 19. Current at specific positions on a thin half-wave receiving antenna as a function of the incident angle, θ_i, calculated from eq. (35) with (13) used for $U(\theta_i;z)$, and normalized to the incident electric field and the wavelength, i.e., $I^R(\theta_i;z)/\lambda E^i_\theta$.

The currents on the internal walls of the same receiving antenna ($kh = \pi/2$, $\Omega(h) = 10$) at the end, $z = -h$, and slightly away from the end, $z = -h + 2a$, as calculated from (54) with (47) are shown in Figure 20 as a function of the incident angle, θ_i. The internal current at the end, $z = -h$, represents an infinite summation of all the TM_{0n} mode currents at this point and is equal in theory to the negative of the external current at this end. While the internal current at $z = -h + 2a$ is predominantly associated with the TM_{01} circular waveguide mode, all the higher order modes being much more attenuated at this point. Thus beyond $z = -h + 2a$, the internal current will decay essentially as $e^{-\gamma_{01}(h+z)}$.

The current distribution on an electrically thick ($ka = 1.0$) receiving antenna three wavelengths in length as calculated from (35) is shown in Figure 21 for the incident angles, $\theta_i = \pi/36, \pi/6, \pi/3$, and $\pi/2$. Note that this distribution corresponds only to the external azimuthally uniform z-directed current on the cylinder. Note also that since $\Omega(h) = 2\,\ell n(2h/a) = 5.87$ and $|\ell n(v_0)| = 2.64$, 0.93, 2.24, and 3.63 for the respective angles considered, the condition that $\Omega(h) >> |\ell n(v_0)|$ as originally required in the analytical development, no longer holds. However, the correspondence with the data from Wu, et al., [35] based upon the integral equation and product integration formulation of Kao [18] for the azimuthally uniform z-directed current also shown in Figure 21 for the same antenna with a normally incident plane wave is surprisingly good. Again we bring attention to the relatively small level of current on the antenna predicted by our theory at near-grazing incidence, $\theta_i = \pi/36$. The behavior of the current at $z = 0$, $h/3$ and $2h/3$ with respect to the incident angle, θ_i, is shown in Figure 21 and

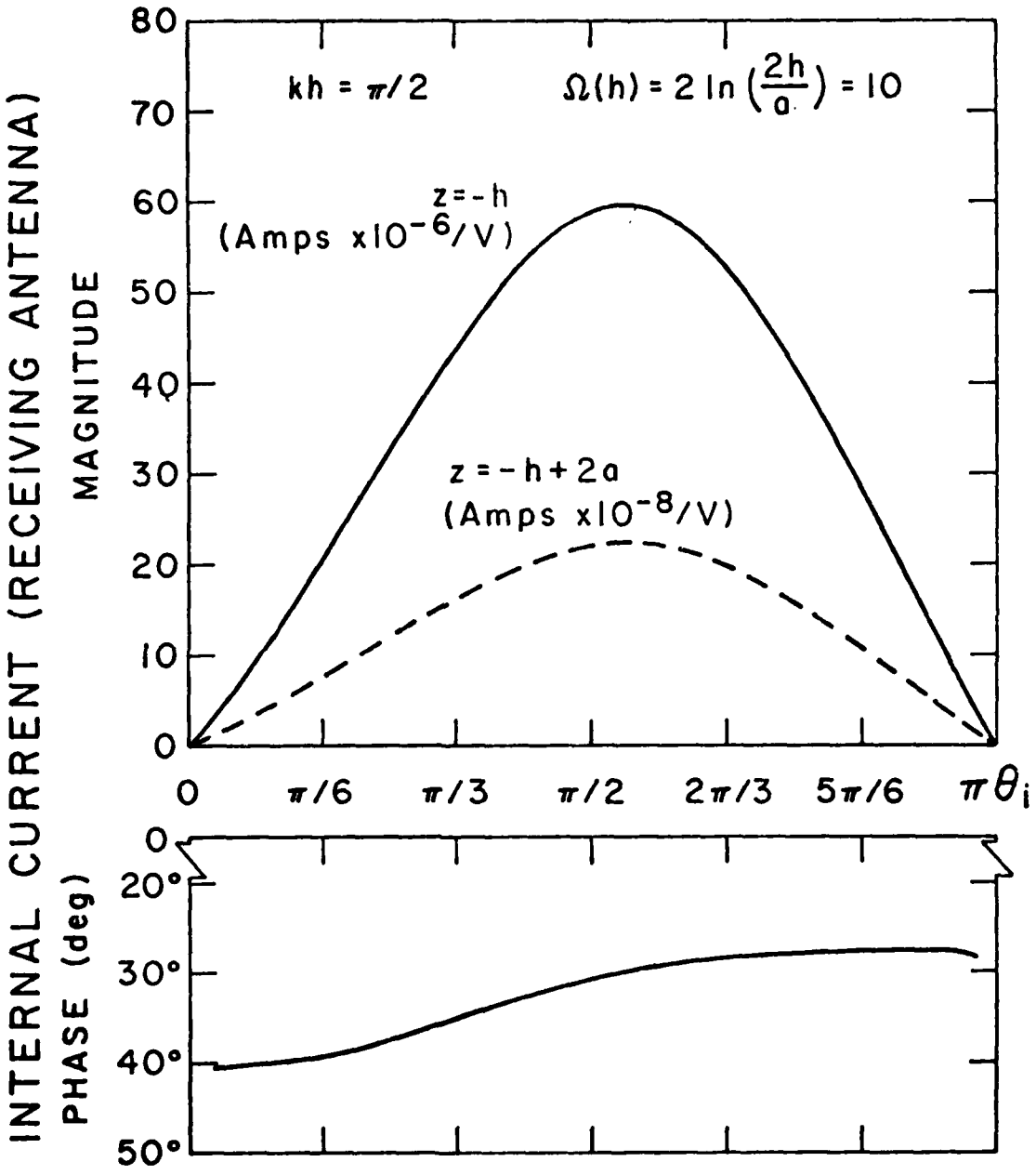

Figure 20. Internal current at the end and slightly within the end of a thin half-wave receiving antenna as a function of the incident angle, θ_i, calculated from eq. (35) with (13) used for $U(\theta_i;z)$, and normalized to the incident electric field and the wavelength, i.e., $I^R_{int}(\theta_i;z)/\lambda E^i$.

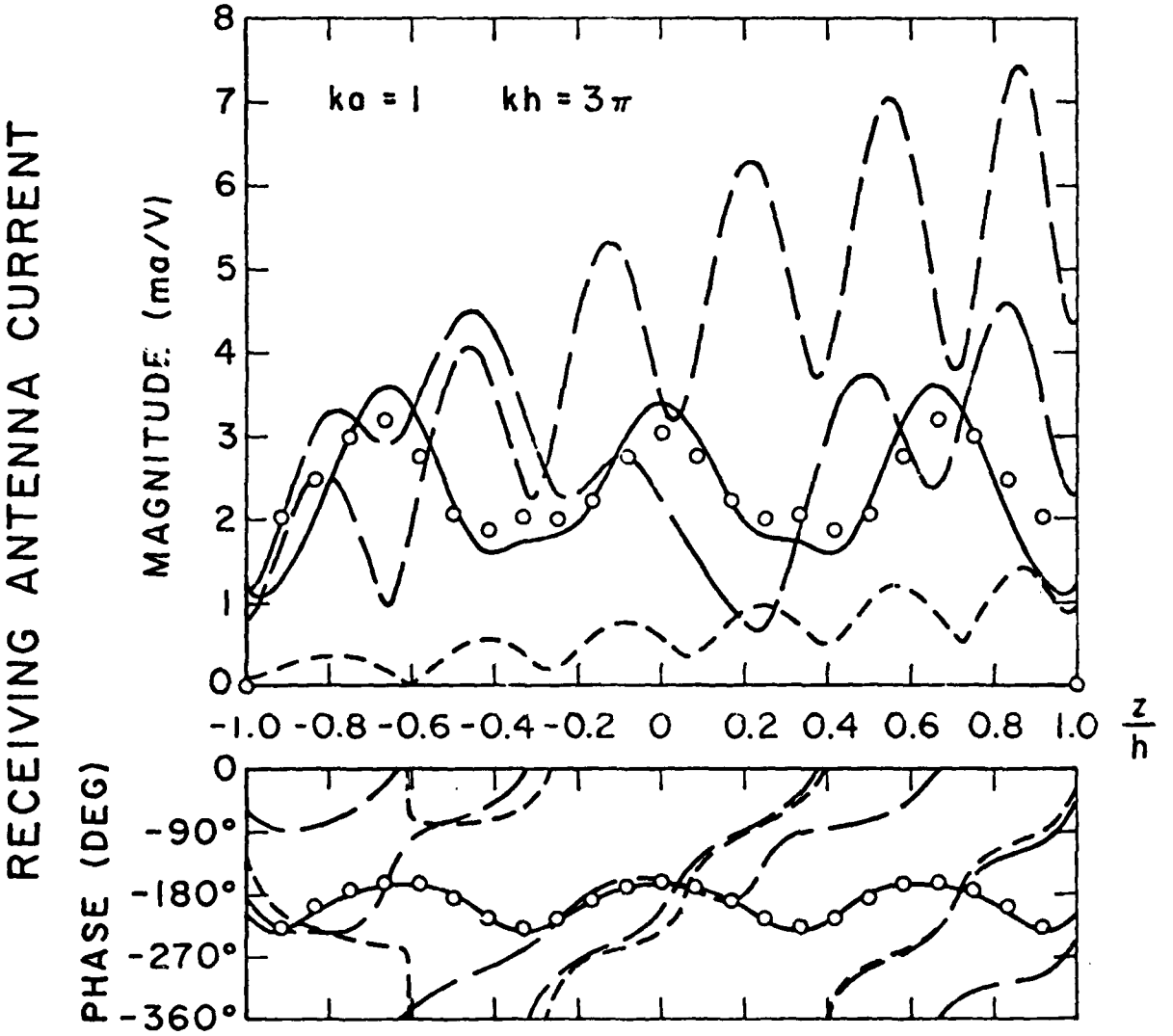

Figure 21. Current distribution on a three wavelengths long, electrically thick, receiving antenna normalized to the incident electric field and the wavelength, i.e., $I^R(\theta_i;z)/\lambda E^i_\theta$.

——————— $\theta_i = \pi/2$
——— ——— $= \pi/6$
— — — $= \pi/3$
- - - - - - $= \pi/36$

} from eq. (35) with (13) used for $U(\theta_i;z)$

o $\theta_i = \pi/2$ Numerically evaluated data from Wu, et al. [35]

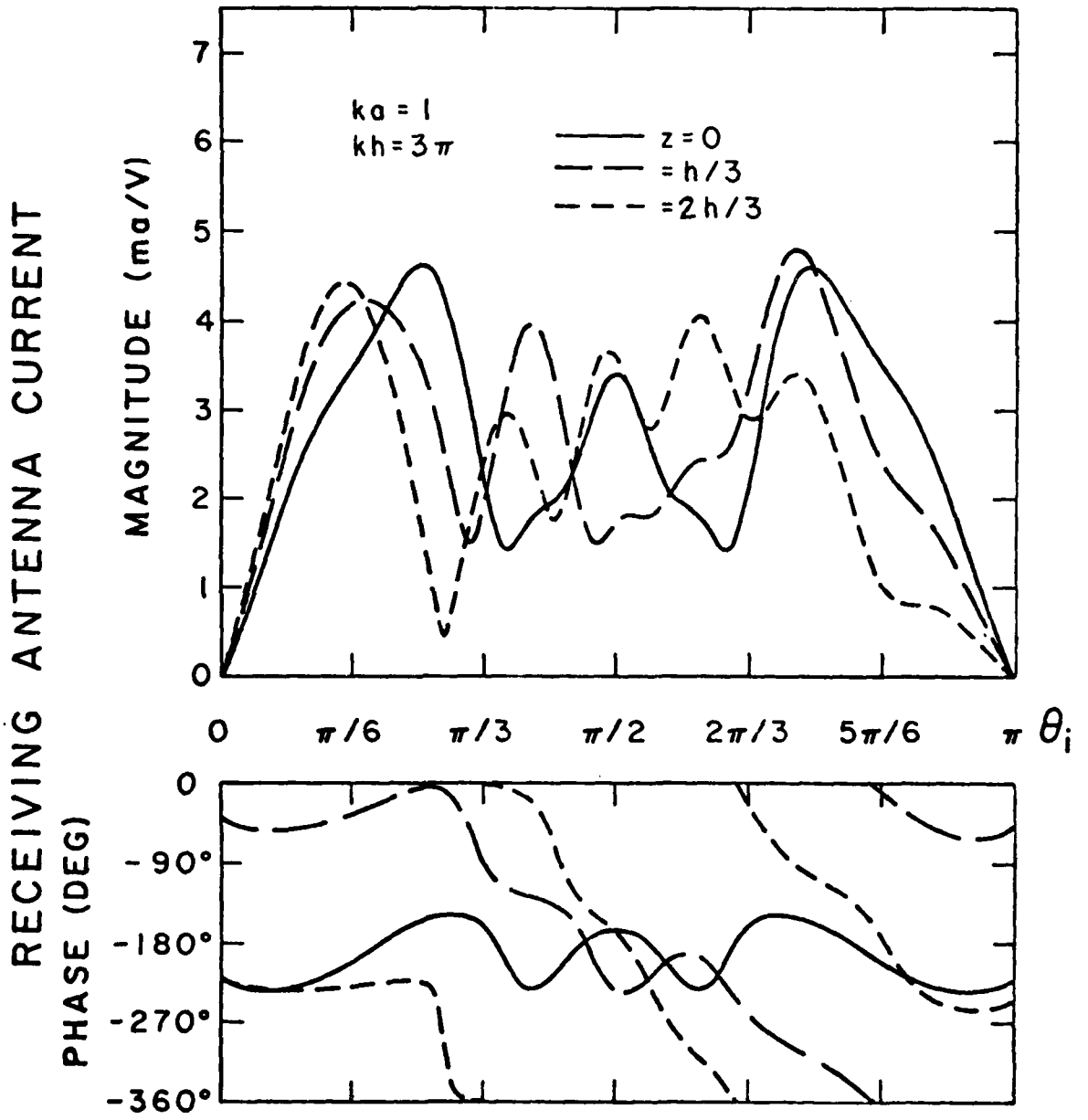

Figure 22. Current at specific positions on an electrically thick receiving antenna as a function of the incident angle, θ_i, calculated from eq. (35) with (13) used for $U(\theta_i;z)$, and normalized to the incident electric field and the wavelength, i.e., $I^R(\theta_i;z)/\lambda E^i_\theta$.

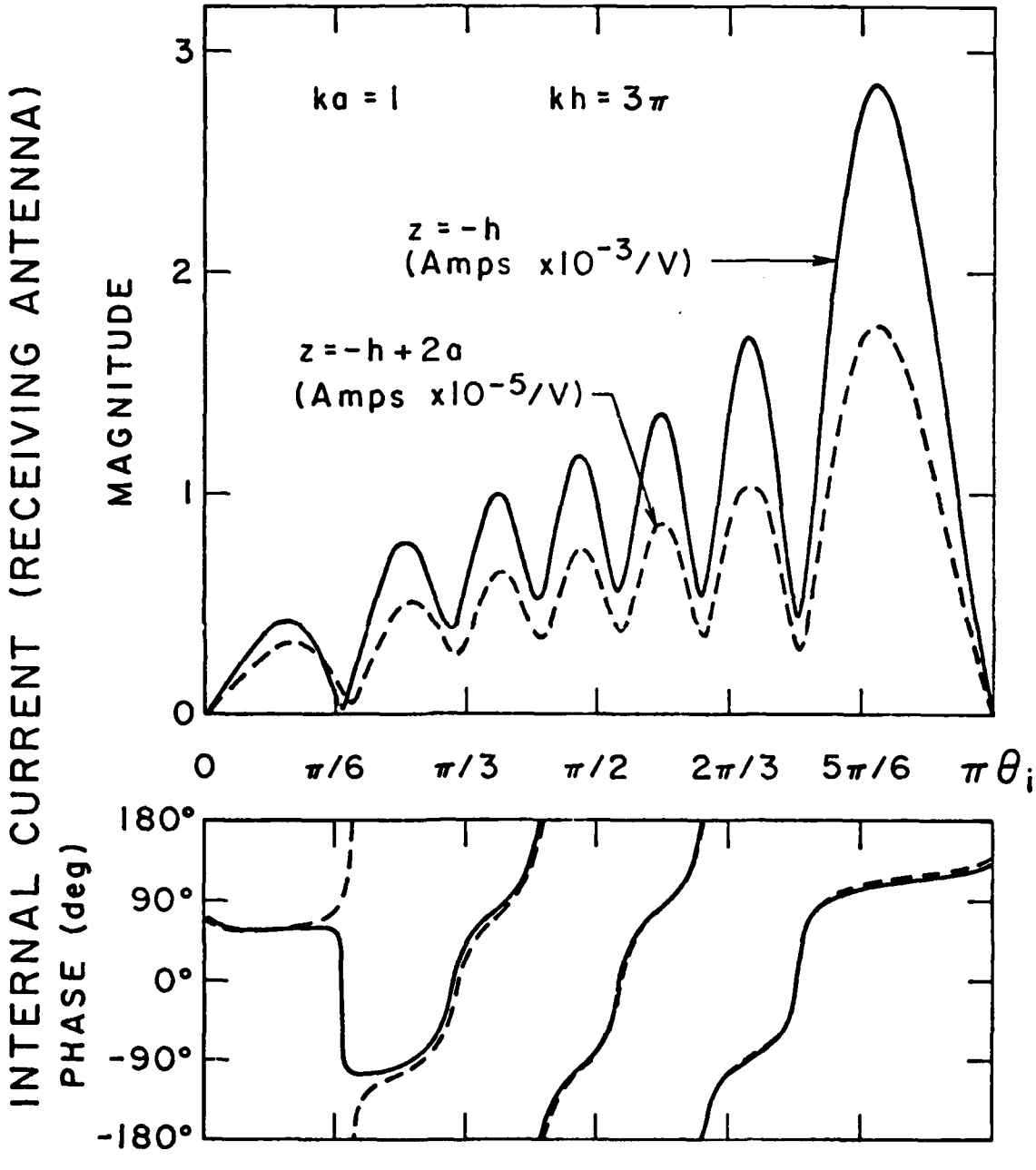

Figure 23. Internal current at the end and slightly within the end on an electrically thick receiving antenna as a function of the incident angle, θ_i, of the uniform plane wave, calculated from eq. (35) with (13) used for $U(\theta_i;z)$, and normalized to the incident electric field and the wavelength, i.e., $I^R_{int}(\theta_i;z)/\lambda E^i_\theta$.

is seen to exhibit the physically expected result of zero current at grazing incidence, $\theta_i = 0$ and π. The currents on the internal walls of this receiving antenna ($kh = 3\pi$, $ka = 1$) at the end, $z = -h$, and slightly away from the end, $z = -h + 2a$, as calculated from (54) with (47) are shown in Figure 23 as a function of the incident angle, θ_i. Comments similar to the ones given for the internal currents illustrated in Figure 20 are also applicable to this much thicker and longer antenna.

7.2 Current distribution on a transmitting antenna

As discussed at the beginning of this section, the total (internal + external) current distribution on those cylindrical antennas (both transmitting and receiving) for which out theory is applicable is for all practical purposes given by the external current distribution alone, except in the near vicinity of the ends. An additional exception to this, which is particular to the transmitting antenna, is the region very close to the source where internal currents are directly excited by the source, itself. A brief disucssion of this localized internal current has already been given in Section 6.4, where it was deemed inappropriate to pursue an in depth study of this current, which is of secondary importance.

The current distribution on a center-driven half-wave antenna where $\Omega(h) = 2\ \ell n(2h/a) = 10$ as calculated from (38) is shown in Figure 24 along with corresponding data from the three-term theory of King [5] and the approximate second order iteration procedure of King and Middleton [11, Chap. II, Sec. 22]. The agreement between our results and the latter theory with regard to the real component of the current is excellent. And although the agreement between the imaginary components is acceptable, the discrepancy here was not totally unexpected since in the process of

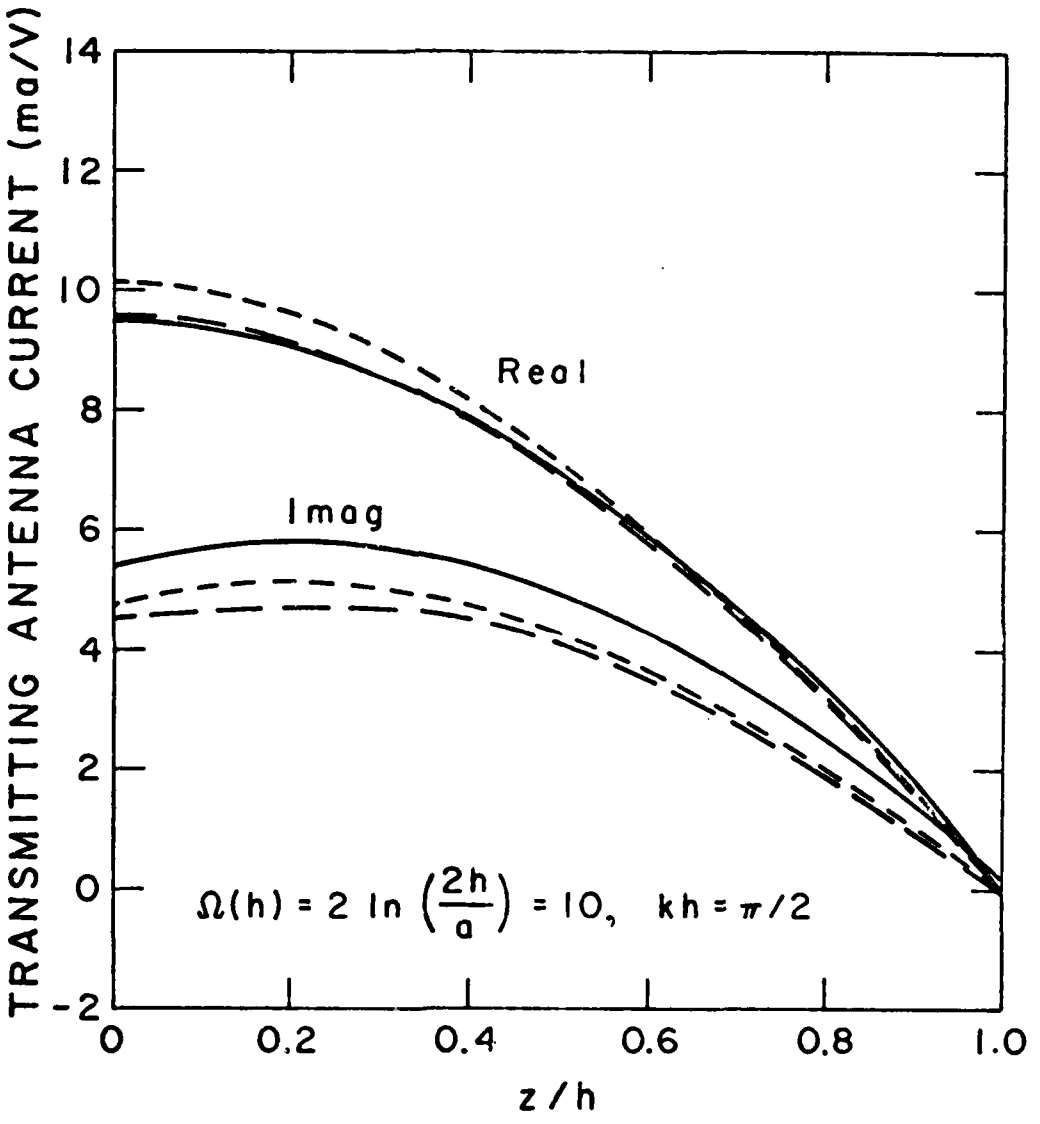

Figure 24. Current distribution on a thin, center fed, half wave transmitting antenna.

———— from eq. (38) with (13) used for $U(\pi;z)$.

— — approximate second order King-Middleton theory [11, Chap. II, Sec. 22]

— — — — King three-term theory [5]

achieving an accurate value for the real component of the primary current discussed in Section 3.2, a less accurate "physically acceptable" value of the imaginary current near the source resulted. The correspondence between the three-term theory of King (which may be judged to be less accurate [5] than the King-Middleton results) and our theory is also quite acceptable.

Perhaps more important than the transmitting current distribution, is the input admittance to the antenna. Therefore, in Figures 25 and 26 we show the input conductance and susceptance, respectively, as calculated from (41) for a center-driven cylindrical antenna where $\Omega(h) = 2\,\ell n(2h/a) = 10$, as a function of the electrical length, kh. Corresponding admittance data from the three-term theory of King [5] and second order results from the iterative method of King and Middleton [11, Chap. II, Sec. 30] are also shown in these figures. The agreement between the conductances predicted by all three theories in Figure 25 is seen to be very good. The agreement between the input susceptances is also very good for the smaller values of kh where the "realistic" imaginary component of the primary current is small compared to imaginary current arising from the multiple reflections from the ends. At the larger values of kh, where ka is proportionally larger, we find larger discrepancies between our results and the King three term and King-Middleton results. Here the imaginary component of the primary current significantly affects the overall input susceptance. And since our approximate expression for the primary transmitting current in (20) is not expected to accurately estimate the "realistic" value for the imaginary input current, this discrepancy will also appear in the finite length antenna susceptance calculated from (41) in which (20) is used.

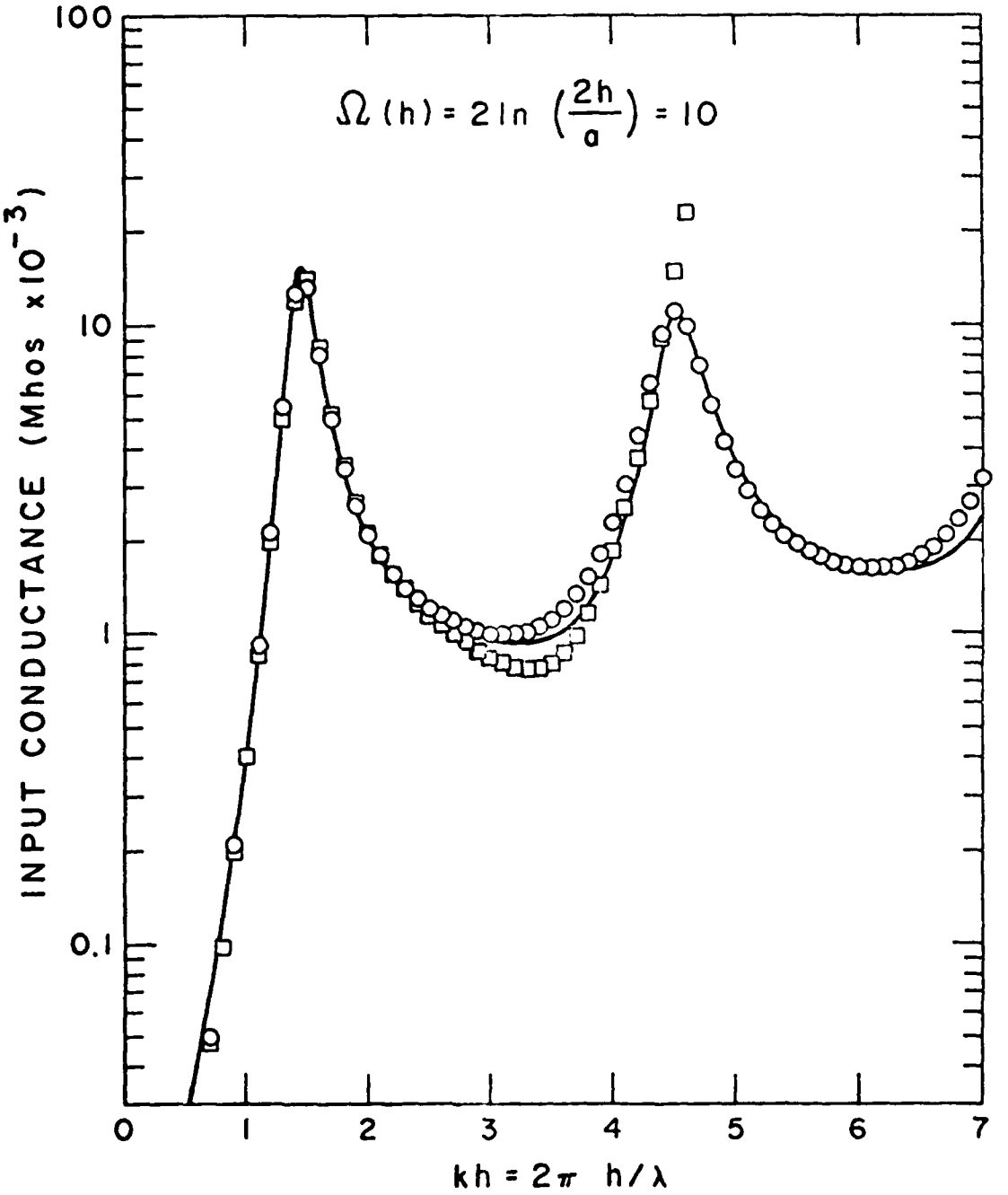

Figure 25. Input conductance of a thin center fed cylindrical antenna.

——— from eq. (41) with (13) used for $U(\pi;z)$

○ Second order King-Middleton theory [11, Chap. II, Sec. 30]

□ King three-term theory [5]

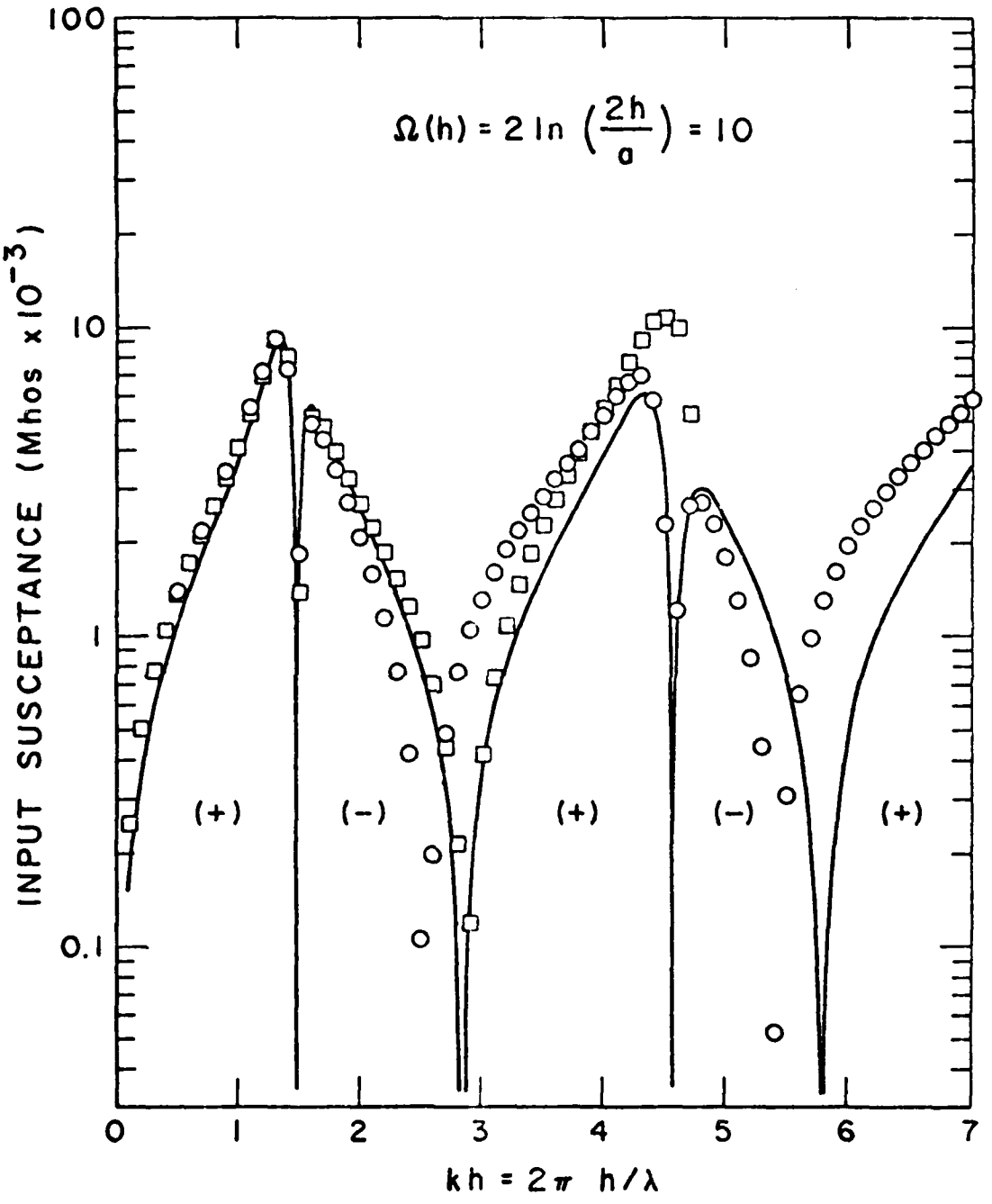

Figure 26. Input susceptance of a thin center fed cylindrical antenna.

——— from eq. (41) with (13) used for $U(\pi;z)$

○ Second order King-Middleton theory [11, Chap. II, Sec.30]

□ King three-term theory [5]

However, in practical situations the input susceptance may be eliminated by appropriate matching leaving the input conductance essentially unchanged and the most important quantity of consideration.

To provide further comparison of our theory with existing approaches we offer Figure 27 which shows the input conductance to a center-driven cylindrical antenna where the ratio of antenna half-length to radius is $h/a = 100$ as calculated by (41) and the corresponding numerically evaluated (via the moment method) results of Harrington and Mautz [26]. The agreement between our results and the accurate numerically-determined data is excellent. Further evidence to substantiate our theory is given in Figure 28, which is the same as the previous figure except the driving point is now located at $z = \pm h/2$. Excellent correspondence with the numerically determined data of Harrington and Mautz [26] is once more attained.

We extend our considerations to much thicker antennas with Figure 29, which shows the input conductance of cylindrical antennas as calculated from (41) for the radii normalized to wavelength, $a/\lambda = 0.0159$, 0.078, and 0.164 ($ka = 0.1$, 0.49 and 1.03, respectively) as a function of the normalized half-length, h/λ, between 0.1 and 0.5. And although these antennas are out of the applicable range of our theory due to the basic condition in (8), we find behavior still consistent with the numerically-obtained results of Chang [27] and [28] (one-sided delta function excitation data), and the experimental results of Hartig [29]. This further enhances the feeling that the derived result actually has a much wider application than had been assumed analytically. And we note the very good agreement between our theory and the others for the larger values of h/λ, where the ratio of h/a is also larger.

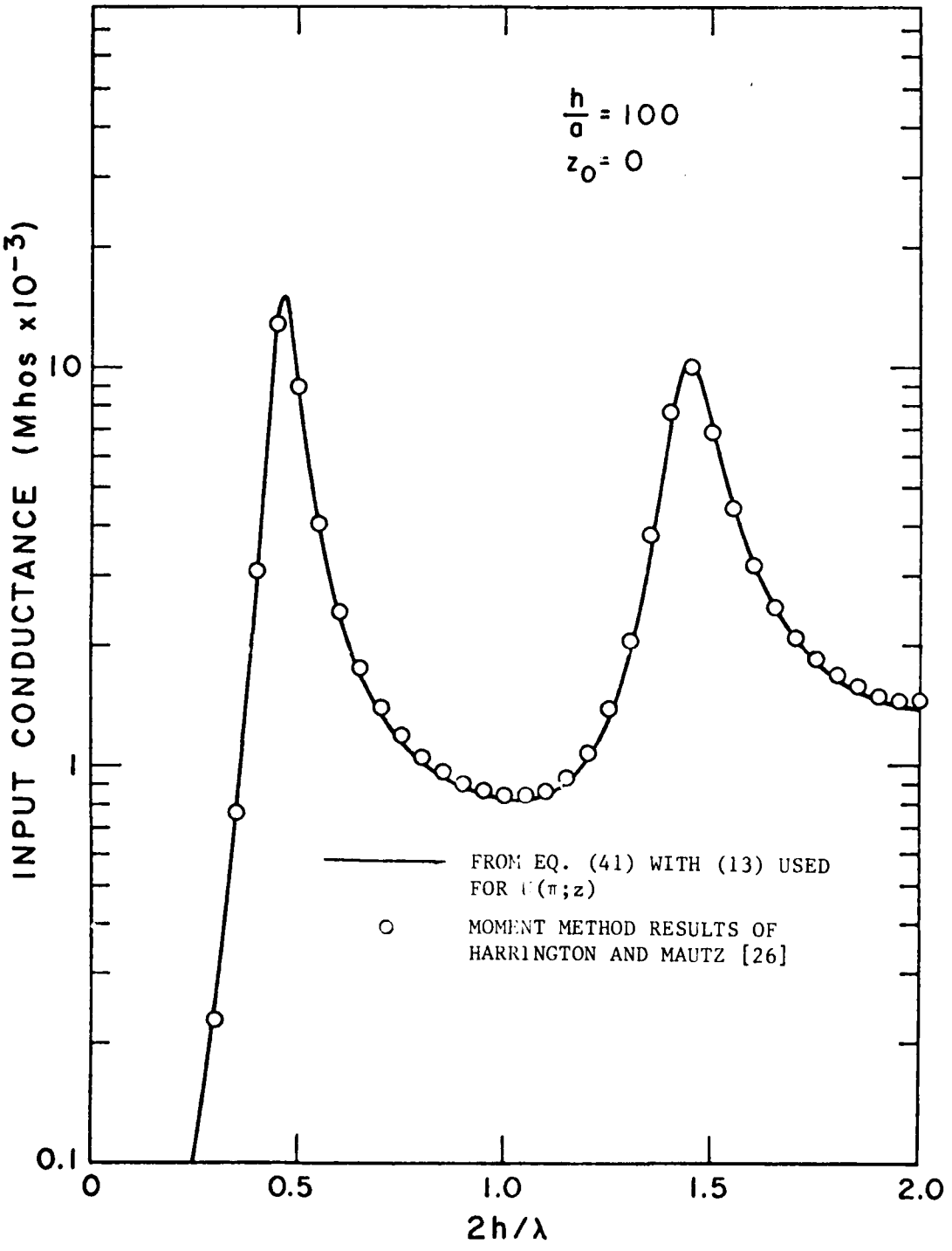

Figure 27. Input conductance of a center fed cylindrical antenna as a function of the normalized length, $2h/\lambda$.

However, in practical situations the input susceptance may be eliminated by appropriate matching leaving the input conductance essentially unchanged and the most important quantity of consideration.

To provide further comparison of our theory with existing approaches we offer Figure 27 which shows the input conductance to a center-driven cylindrical antenna where the ratio of antenna half-length to radius is $h/a = 100$ as calculated by (41) and the corresponding numerically evaluated (via the moment method) results of Harrington and Mautz [26]. The agreement between our results and the accurate numerically-determined data is excellent. Further evidence to substantiate our theory is given in Figure 28, which is the same as the previous figure except the driving point is now located at $z = \pm h/2$. Excellent correspondence with the numerically determined data of Harrington and Mautz [26] is once more attained.

We extend our considerations to much thicker antennas with Figure 29, which shows the input conductance of cylindrical antennas as calculated from (41) for the radii normalized to wavelength, $a/\lambda = 0.0159$, 0.078, and 0.164 ($ka = 0.1$, 0.49 and 1.03 , respectively) as a function of the normalized half-length, h/λ , between 0 1 and 0.5 . And although these antennas are out of the applicable range of our theory due to the basic condition in (8), we find behavior still consistent with the numerically-obtained results of Chang [27] and [28] (one-sided delta function excitation data), and the experimental results of Hartig [29]. This further enhances the feeling that the derived result actually has a much wider application than had been assumed analytically. And we note the very good agreement between our theory and the others for the larger values of h/λ , where the ratio of h/a is also larger.

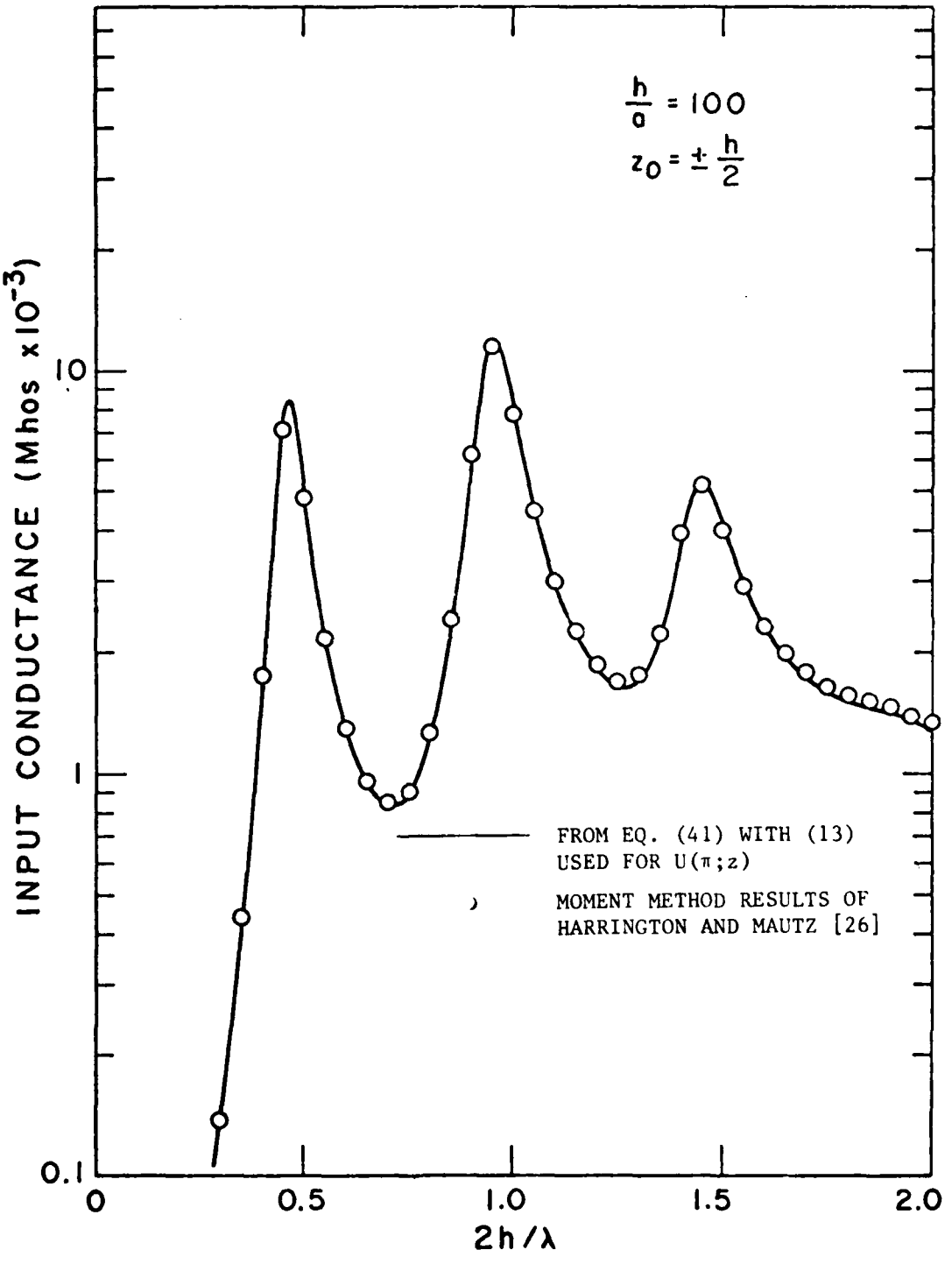

Figure 28. Input conductance of a off-center fed cylindrical antenna as a function of the normalized length, $2h/\lambda$.

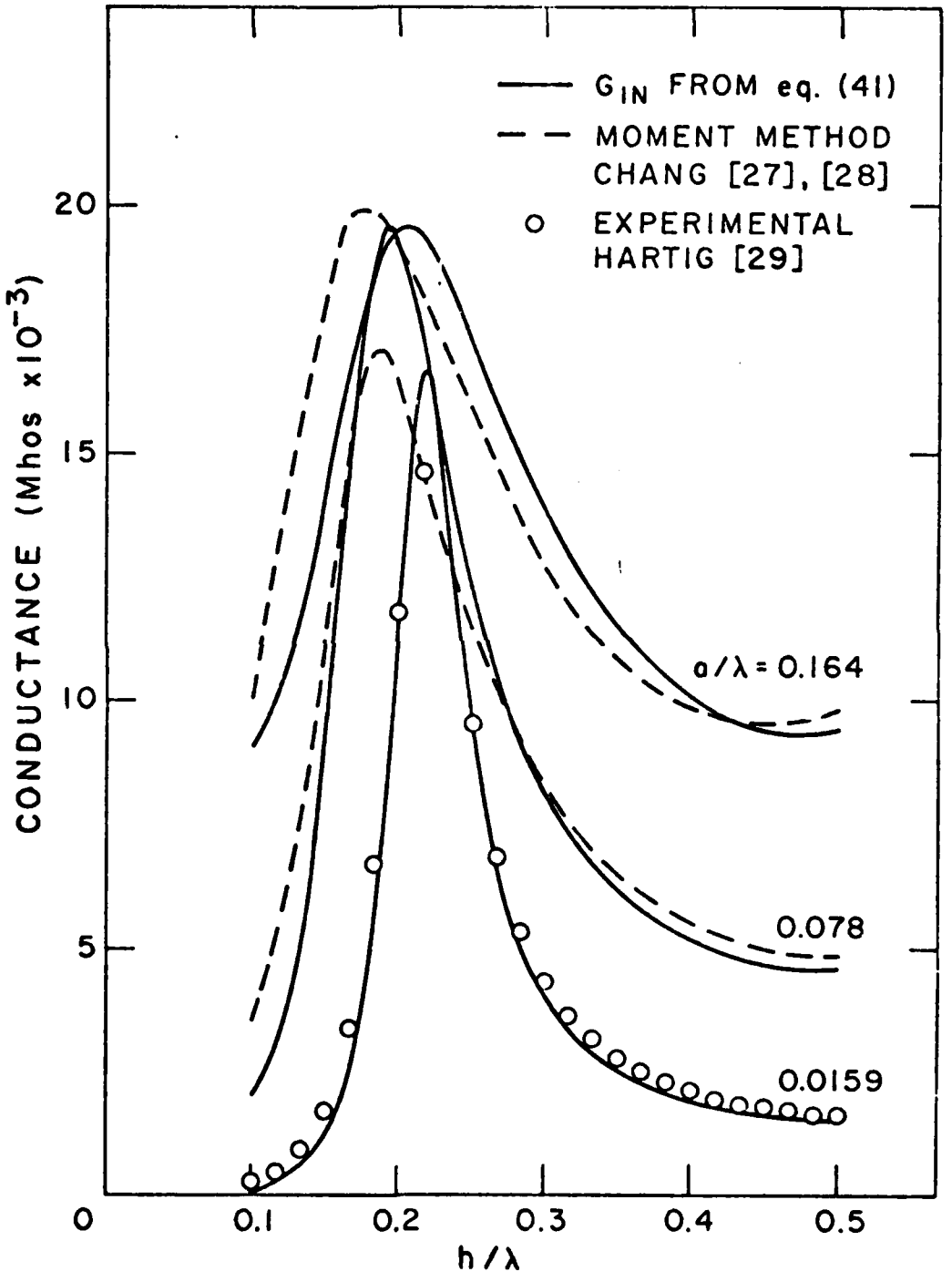

Figure 29. Input conductance of three electrically thick center fed cylindrical antennas as a function of the normalized half-length, h/λ .

The application of our theory to the thicker cylindrical antennas is more successful when the antenna length is significantly larger than the antenna radius. Hence, the input admittance to a center-driven cylindrical antenna having a half-length to radius ratio of $h/a = 10$ as calculated from (41) is shown in Figure 30, as a function of the normalized length, $2h/\lambda$. Comparison of this data to the numerically obtained results of Harrington and Mautz [26] also included in the figure is very good, even near $2h/\lambda = 2.0$ where the electrical radius approaches $ka = 1.256$. This value of electrical radius is slightly beyond the range of our formulas, however, because the attenuation rate of the secondary currents on an electrically thick cylinder is so pronounced, as may be observed in Figure 14, the input conductance for the finite length electrically thick antenna is predominantly determined by $U_s(0)$ in (20), which obviously still predicts the input conductance of an infinite cylindrical antenna to a sufficient degree of accuracy.

Further, we offer Figure 31, which is similar to the previous figure except the feed point is taken to be at $z_0 = \pm h/2$. Again the agreement with the numerical moment method results of Harrington and Mautz [26] is quite good.

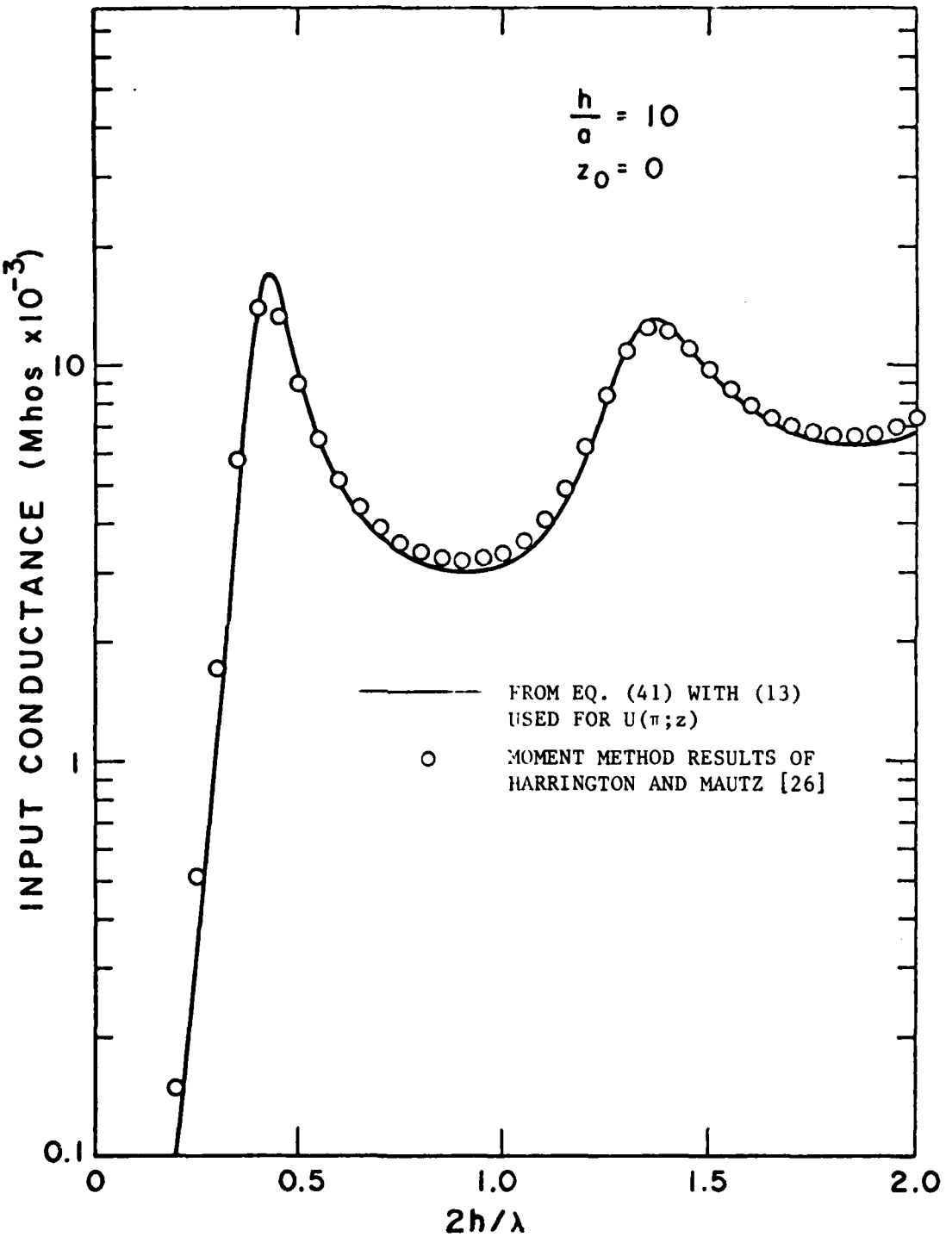

Figure 30. Input conductance of a center fed cylindrical antenna as a function of the normalized length, $2h/\lambda$.

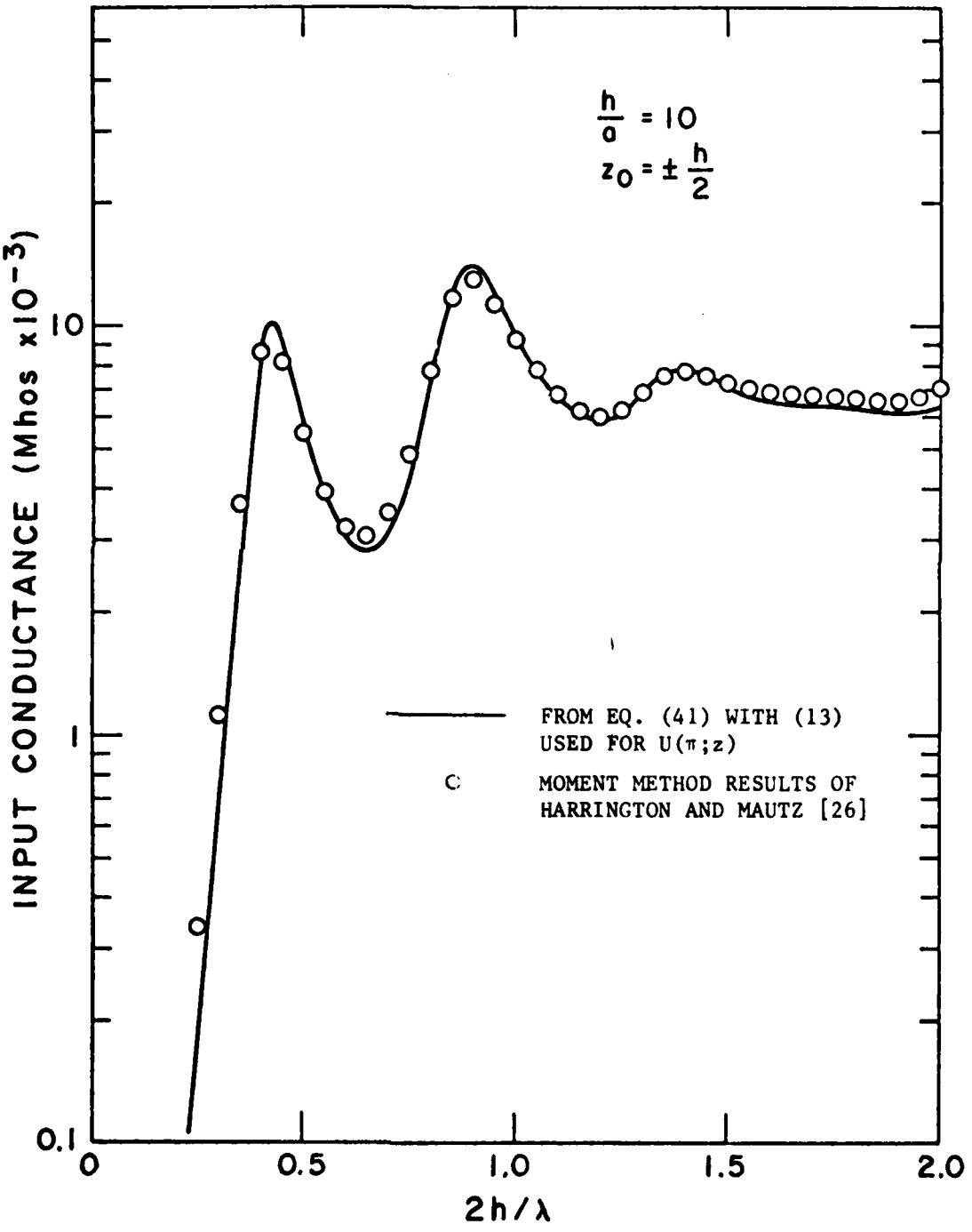

Figure 31. Input conductance of an off-center fed cylindrical antenna as a function of the normalized length, $2h/\lambda$.

Section 8 Electrically short cylindrical antennas

8.1 Short receiving antenna

The current distribution on an electrically short ($kh = 0.4$) thin ($\Omega(h) = 2\,\ell n(2h/a) = 10$) cylindrical receiving antenna calculated from (35) with (13) is shown in Figure 32 for the incident angles of the uniform plane wave of $\theta_i = \pi/36$, $\pi/6$, $\pi/3$, and $\pi/2$. For comparison the current distribution for normal incidence ($\theta_i = \pi/2$) predicted by the short antenna theory of King [11, Chap. IV, Sec. 7] is also shown. The agreement between the two normal incidence magnitude distributions is quite acceptable, especially in light of the fact that the basic condition in (8) is only moderately satisfied, i.e., $\Omega(h) = 10$ while $|\ell n(2kh)| = 0.92$. On the other hand, the phase of the current predicted by our theory is less than 90° along most of the antenna as opposed to the phase predicted by King which is always slightly more than 90°. However, since the phase of the receiving current is quite inconsequential compared to the magnitude in most applications, this slight inconsistency is not seen as a serious drawback to our receiving theory.

The behavior of the current at the positions $z = 0$, $h/3$, and $2h/3$ on the same electrically short ($kh = 0.4$ and $\Omega(h) = 10$) receiving antenna just discussed is shown in Figure 33 as a function of the incident angle, θ_i. The sinusoidal variation of the current at each position, with respect to the angle, θ_i, is readily apparent in this figure and is consistent with the expected behavior.

8.2 Short transmitting antenna

Figure 34 illustrates the current distribution on an electrically short ($kh = 0.4$) thin ($\Omega(h) = 2\,\ell n(2h/a) = 10$) center driven cylinder

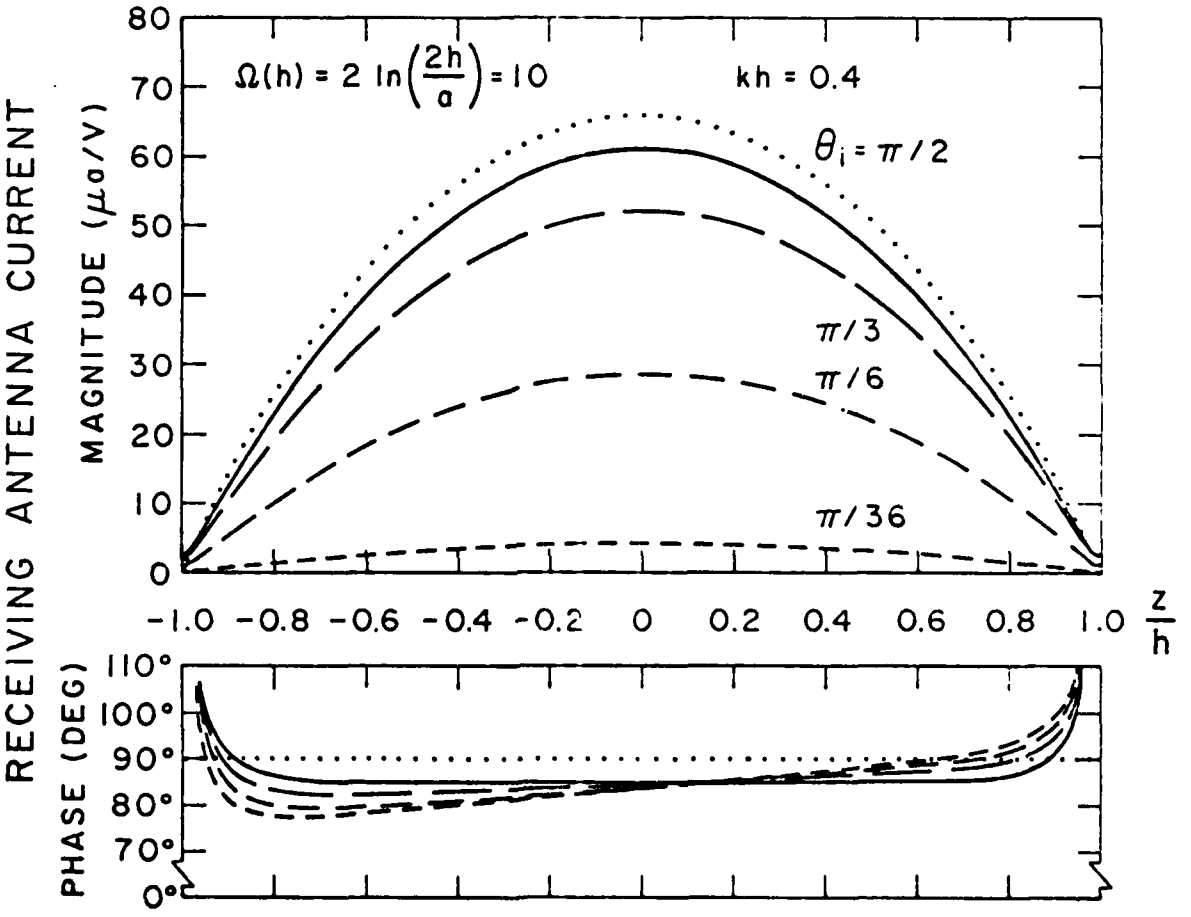

Figure 32. Current distribution on an electrically short receiving antenna normalized to the incident electric field and the wavelength, i.e., $I^R(\theta_i;z)/\lambda E^i_\theta$.

——————— $\theta_i = \pi/2$
— — — — $= \pi/3$
— — — — — $= \pi/6$
— — — — — $= \pi/36$

} from eq. (35) with (13) used for $U(\theta_i;z)$.

. . . . . $\theta_i = \pi/2$ Short antenna theory of King [11, Chap. IV, Sec. 8]

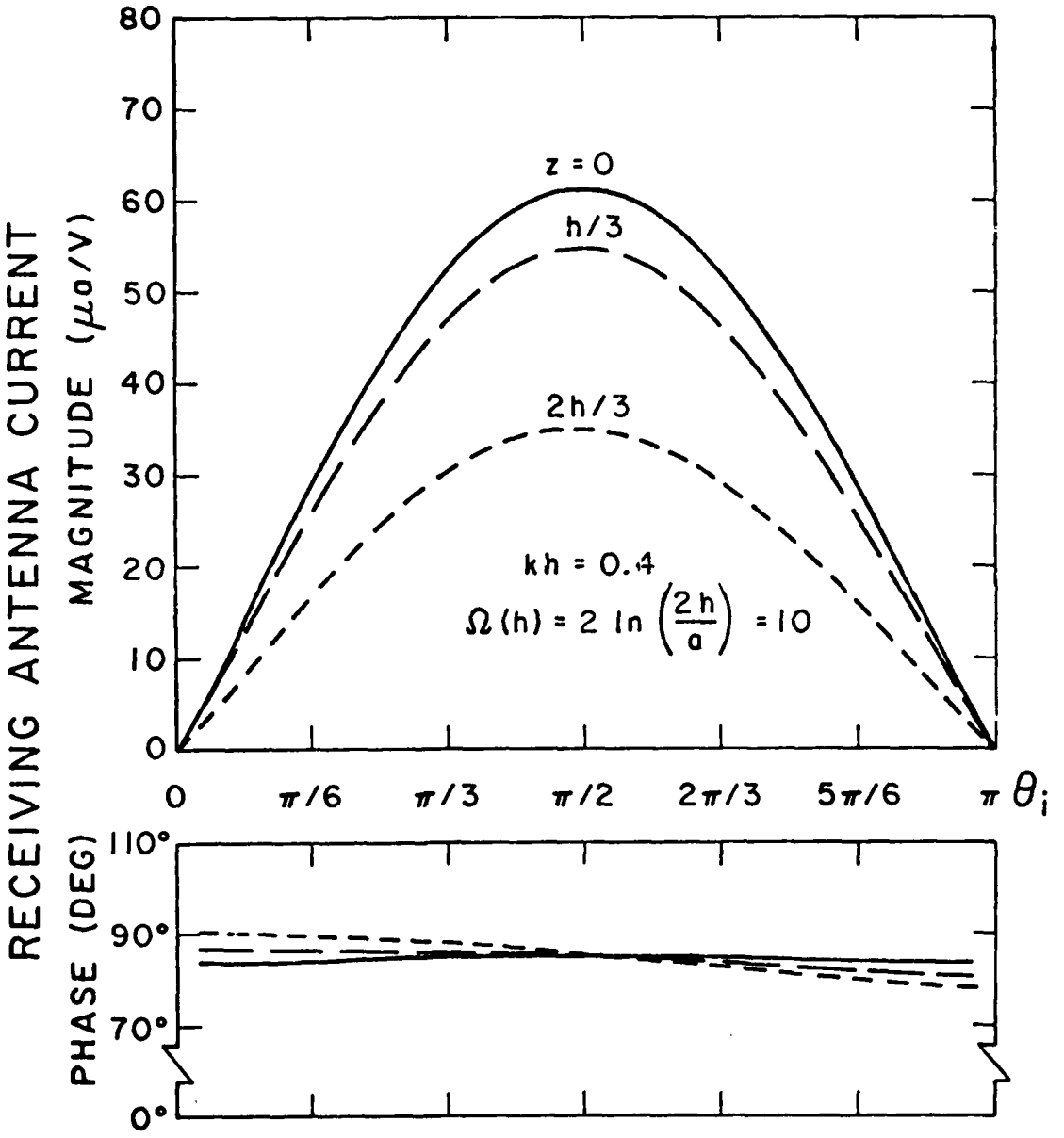

Figure 33. Current at specific positions on an electrically short receiving antenna as a function of the incident angle, θ_i, calculated from (35) with (13) used for $U(\theta_i;z)$ and normalized to the incident electric field and the wavelength, i.e., $I^R(\theta_i;z)/\lambda E^i_\theta$.

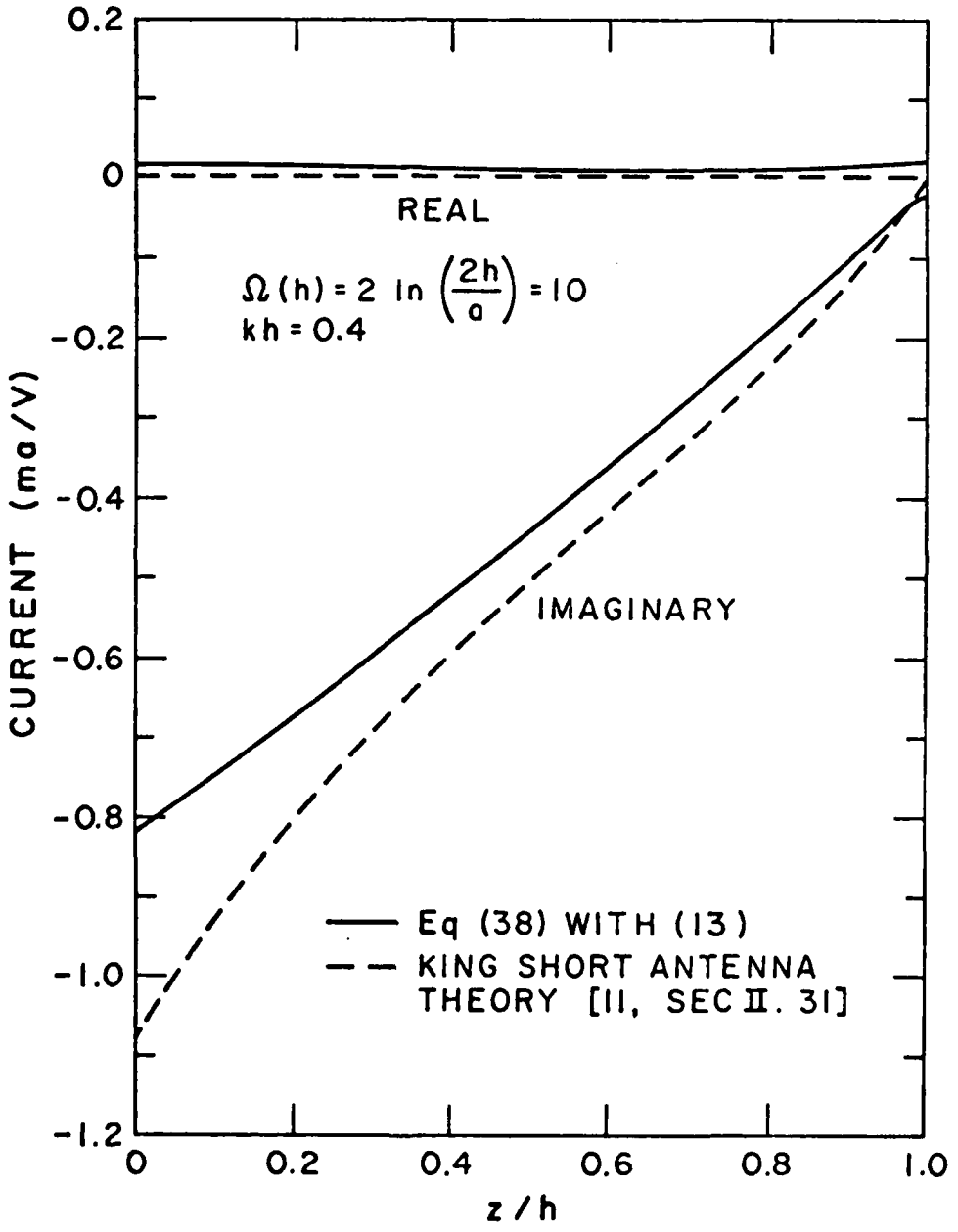

Figure 34. Current distribution on a center-fed electrically short cylindrical transmitting antenna.

calculated from (38). Also shown in this figure is the current distribution on the same antenna as predicted by the short antenna theory of King [11, Chap. II, Sec. 31]. The agreement between our result and that of King is, in general, fairly good, especially since we have again only moderately satisfied the basic restriction in (8). Of particular interest here is the inability of our formulation to predict an accurate real component of current at the source. This situation results from the fact that our transmitting current formulation in (38) is good only to $(C_W)^{-2}$ for short antennas, while the input conductance for these antennas is given by higher order terms. We may easily recover the input conductance, however, by turning to the input conductance formulation of Chang and Rispin in [30] which is based upon the effective aperture of the antenna and requires a knowledge of only the magnitude of the receiving current on the same antenna illuminated by a normally incident uniform plane wave. Their approximate result for the electrically short receiving antenna may be written as

$$G \approx \eta \frac{k^2}{6\pi} \left| I^R(\pi/2 , z_0)/E^i_\theta \right|^2 \tag{56}$$

where $\left|I^R(\pi/2 , z)/E^i_\theta\right|$ is the magnitude of the receiving current normalized to the incident field, at the feedpoint, z_0, due to a normally incident $(\theta_i = \pi/2)$ plane wave. As seen in the previous sub-section, the magnitude of our receiving current is of sufficient accuracy for these short electrical lengths to permit the above calculation. Figure 35 shows the input conductance predicted by (56) using our receiving current formula in (35) along with comparable data from the short antenna theory of King [11, Chap. II, Sec. 31] for electrically short antennas characterized by $\Omega(h) = 2\ \ell n(2h/a) = 10$ as a function of the electrical

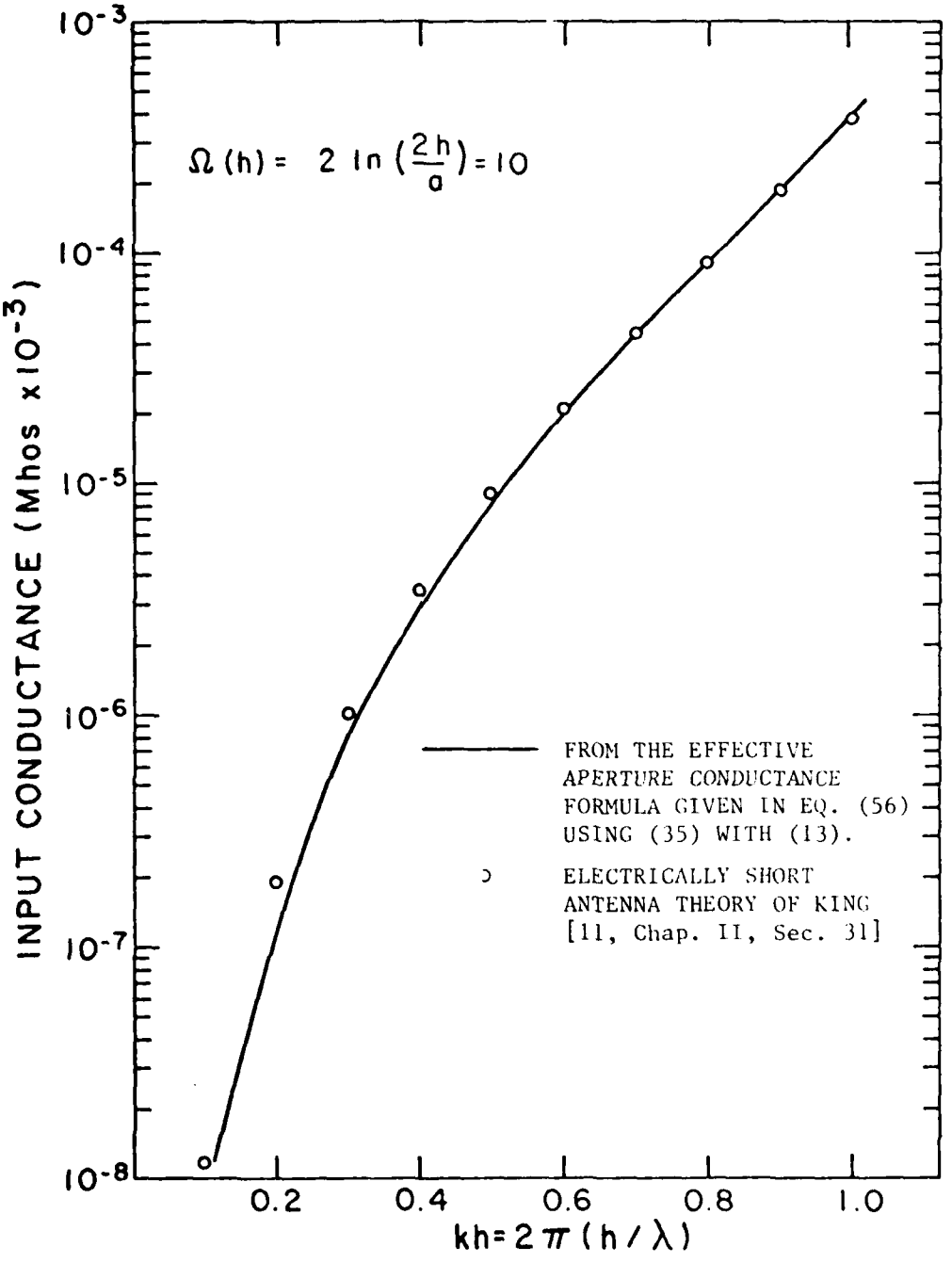

Figure 35. Input conductance of a center-fed electrically short cylindrical antenna.

length, between kh = 0.1 and 1.0. Obviously the two theories appear to be in relatively good agreement. Thus, even though our transmitting current formula in (38) failed to yield an acceptable input conductance for the electrically short cylindrical antenna, the alternate procedure described above that relies upon our complementary receiving current formula in (35) has yielded successful results.

9. Concluding remarks

Through a re-examination of the conditions necessary to obtain simple asymptotic solutions based upon a Wiener-Hopf analysis for the reflected current distribution on semi-infinite tubular cylindrical antennas, we have broken away from the traditional "thin wire" assumptions, $ka \ll 1$ and $kh \gtrsim 1$, and extended these asymptotic Wiener-Hopf solutions to include antennas as thick as $ka = 1$ and as short as $kh = 0.4$. These extended solutions have been derived subject primarily to the satisfaction of the condition, $\Omega(h) = 2\,\ell n(2h/a) >> |\ell n[2kh \sin^2(\theta_i/2)]|$. Although for the thicker antennas, we have observed a significant relaxation of this condition. Our simple receiving current formula is applicable for all angles of incidence of a uniform plane wave, i.e., $0 \le \theta_i \le \pi$, and we have constructed our simple transmitting formula in such a way so that an accurate input conductance is obtained over our entire range of interest. Numerical comparisons of our theory with the work of many other authors have shown very good overall agreement. Hence our theory, which requires primarily only arithmetic calculations, permits easy and inexpensive calculations of the current distribution on cylindrical transmitting and receiving antennas, thus providing an excellent basis for statistical and transient studies. As a consequence, the transient aspects of a cylindrical antenna based upon our present theory shall be covered in a forthcoming report.

Although only the unloaded transmitting and receiving antenna has been analyzed in this report, the extension to the loaded situation in both cases is straightforward. The voltage developed across a load admittance, Y_ℓ, located at $z = z_\ell$ along a cylindrical transmitting or receiving antenna would be given by $V_\ell^T = -I_\ell^T(z_0;z_\ell)/Y_\ell$ or $V_\ell^R = -I_\ell^R(\theta_i;z_\ell)/Y_\ell$, respectively, where $I_\ell^T(z_0,z_\ell)$ and $I_\ell^R(\theta_i;z_\ell)$ are the transmitting and receiving currents,

respectively, at $z = z_\ell$ in the loaded situation. The potential difference across $z = z_\ell$ in either the transmitting or receiving situations acts as a voltage generator for which our transmitting antenna theory can be used to obtain the current distribution. Adding this current distribution to the unloaded current distribution yields the total (external) current distribution which may in turn be solved at $z = z_\ell$ to obtain $I_\ell^T(z_0;z_\ell)$ or $I_\ell^R(\theta_i;z_\ell)$. Subsequently the loaded receiving and transmitting current distributions may be written as [11, Sec. IV.7],

$$I_\ell^R(\theta_i;z) = I^R(\theta_i;z) - \frac{I^R(\theta_i;z_\ell)}{Y_\ell + Y_{in}(z_\ell)} \frac{I^T(z_\ell;z)}{V_0} \tag{57}$$

and,

$$I_\ell^T(z_0;z) = I^T(z_0;z) - \frac{I^T(z_0;z_\ell)}{Y_\ell + Y_{in}(z_\ell)} \frac{I^T(z_\ell;z)}{V_0} \tag{58}$$

respectively. The unloaded receiving current, $I^R(\theta_i;z)$ is given in (35) and the unloaded transmitting current, $I^T(z_0;z)$ in (38). The term, $I^T(z_\ell;z)/V_0$, corresponds to the transmitting antenna current distribution due to a voltage source of unit strength at $z = z_\ell$. And $Y_{in}(z_\ell)$ is the input admittance to the antenna at $z = z_\ell$ which is approximately given by (41). Although (41) has been shown to give an excellent result for the input conductance, i.e., $\mathrm{Re}\{Y_{in}\}$, the input susceptance, $-\mathrm{Im}\{Y_{in}\}$ from (41) is subject to error. Thus in some cases a more accurate expression for the input admittance $Y_{in}(z_\ell)$ may be desired. The error in our admittance formula in (41) comes mainly from the inaccurate prediction of the input susceptance by $U_s(0)$ for an infinitely long antenna. For the smaller values of ka ($ka \lesssim 0.1$) the imaginary part of the term, $-U_s(0)$ in (41), may be replaced by the susceptance formula of Fanté [21], which has been shown to be a good approximation for the input susceptance by Miller [32] and may be

written as,

$$B_{\infty} = - \frac{2ka}{\eta} \ell n(k\delta) \tag{59}$$

where δ is the physical width of the load region and is assumed to be very small. As noted by Miller [32], the input conductance to an infinite cylinder is relatively insensitive to variations in the gap width, δ, when δ is small compared to the cylinder radius, a. Hence, $Re\{U_s(0)\}$ may be retained in (41) to determine the infinite cylinder input conductance. The current distributions on antennas with multiple-loads can be found by generalization of the single-load approach outlined here.

Another quantity of interest for which our approximate cylindrical antenna theory proves useful is the far field radiation pattern of a cylindrical transmitting antenna. It is well known that the far field radiation pattern of a transmitting antenna bears the same angular dependencies as the received current at the same feed point when the antenna is used as a receiving element. A derivation of this principle as applied to the cylindrical antenna is contained in Appendix H. From Appendix H, we have the far field radiation from a finite length, $-h \leq z \leq h$, cylindrical transmitting antenna with a delta function voltage source of strength, V_0 volts, at $z = z_0$ given in terms of,

$$E_{\theta}(r,\theta,\phi) = \frac{+ik\eta}{4\pi} \frac{e^{ikr}}{r} V_0 \frac{I^R(\pi - \theta ; z_0)}{E^i_{\theta}} \quad ; \quad kr >> 1 \tag{60}$$

(r,θ,ϕ) refers to a spherical co-ordinate system coincident with the cylindrical co-ordinate system implied in Figure 16, i.e., the positive z-axis corresponds to $\theta = 0$. And $I^R(\pi - \theta ; z_0)/E^i_{\theta}$ is the received current at $z = z_0$ on the same antenna when illuminated by a uniform plane wave of

unit amplitude incident at an angle, $\pi - \theta$, with respect to positive z-axis. Hence the far field radiation from a transmitting antenna may be approximately determined from (60) using our approximate formula for the receiving current distribution in (35) for the same antenna parameters. For example, for a center-fed, $z_0 = 0$, transmitting antenna where $\Omega(h) = 2\ \ell n(2h/a) = 10$ and $kh = \pi/2$ (the approximate current distribution of which is shown in Figure 24), the far field radiation is shown in the $z = 0$ curve (apart from the constant $\frac{+ik\eta}{4\pi r}\exp(ikr)$) of Figure 19 with θ_i replaced by $\pi - \theta$. Similarly all of the receiving antenna current distributions shown in graphical form in this report may be related to the far field of the same antenna when it is used as a transmitting element.

The basic approach utilized in this report to develop a simple approximate cylindrical antenna theory is currently being applied to other types of linear antennas, such as the co-axial and parallel thin-wire antennas. Results of this research should appear in the not-too-distant future. In the same respect, since our present theory deals only with the azimuthally uniform axial current on cylindrical antennas, a further extension of our theory which also considers the higher-order variations of axially-directed currents as well as the circumferentially-directed currents is currently being prepared.

References

[1] Hallén, E., Electromagnetic Theory, John Wiley and Sons, New York, 1962. Original works which include, "Theoretical investigations into the transmitting and receiving qualities of antennas," Nova Acta (Uppsala) (4), vol. 11, pp. 1-44, Nov. 1938 are referenced in Chap. 35.

[2] Wienstein, L.A., The Theory of Diffraction and the Factorization Method, the Golem Press, Boulder, Colorado, 1969, Sec. 62. Original (translated) papers are "Waves of current in a thin cylindrical conductor; I. Currents and impedance of a transmitting antenna, II. The current in a passive oscillator, and the radiation of a transmitting antenna," Soviet Physics, Technical Physics (translated), Vol. 4, No. 6, pp. 601-626, December 1959.

[3] Wu, T.T., "Theory of the dipole antenna and the two wire transmission line," J. of Math. Physics, Vol. 2, No. 4, pp. 550-574, July-Aug., 1961.

[4] Chen, Y.M. and J.B. Keller, "Current on and input impedance of a cylindrical antenna," J. Res. NBS, Radio Prop., Vol. 66D pp. 15-21, Jan.-Feb., 1962.

[5] King, R.W.P. and T.T. Wu, "Currents, charges, and near fields of cylindrical antennas," Radio Science, Vol. 69D, No. 3, pp. 429-446, Mar., 1965.

[6] Shen, L.C., T.T. Wu, and R.W.P. King, "A simple formula for current in dipole antennas," IEEE Trans. Ant. and Prop., Vol. AP-16, pp. 543-547, Sept., 1968.

[7] Shen, L.C., "A simple theory of receiving and scattering antennas," IEEE Trans. Ant. and Prop., Vol. AP-18, No. 1, pp. 112-114, Jan., 1970.

[8] Einarsson, O., "Electromagnetic scattering by a thin finite wire," Acta Polytech. Scandinavia, Elect. Eng. Series 23, Stockholm, 1969.

[9] Chen, C.-L., "On the scattering of electromagnetic waves from a long wire," Radio Sci., Vol. 3 (New Series), No. 6, pp. 585-598, June, 1968.

[10] Andersen, J.B., "Admittance of infinite and finite cylindrical metallic antenna," Radio Sci., Vol. 3 (New Series), No. 6, June, 1968.

[11] King, R.W.P., The Theory of Linear Antennas, Harvard Univ. Press, Cambridge, Mass., 1956.

[12] King, R.W.P. and C.W. Harrison, Antennas and Waves, A Modern Approach, The MIT Press, Cambridge, Mass., 1969.

[13] Harrington, R.F., Field Computation by Moment Methods, The Macmillan Co., New York, 1968.

[14] Nobel, B., Methods Based on the Wiener-Hopf Technique for the Solution of Partial Differential Equations, Pergamon Press, New York, 1958.

[15] Mittra, R. and S.W. Lee, Analytical Techniques in the Theory of Guided Waves, The Macmillan Co., New York, 1971.

[16] Abramovitz, M. and A. Stegun, Handbook of Mathematical Functions, Dover Publications, New York.

[17] Chang, D.C., S.W. Lee and L.W. Rispin, "Simple formula for current on a receiving antenna," IEEE Trans. Ant. and Prop., Vol. AP-26, No. 5, pp. 683-690, Sept., 1978.

[18] Kao, C.C., On the Electromagnetic Scattering from a Finite Cylinder, Ph.D. Thesis, Harvard Univ., Cambridge, Mass., 1969. Portions of this work have appeared in "Three dimensional electromagnetic scattering from a circular tube of finite length," J. Appl. Phys., Vol. 40, No. 12, pp. 4732-4740, Nov., 1969; "Electromagnetic scattering from a finite tubular cylinder: numerical solutions," Radio Sci., Vol. 5, no. 3, pp. 617-624, March, 1970; and "Currents on a semi-infinite tube illuminated by electromagnetic waves," Radio Science, Vol. 5, No. 5, pp. 853-859, May, 1970.

[19] Rispin, L.W. and D.C. Chang, "Analytical solutions to the cylindrical antenna based upon the Wiener-Hopf technique," to be submitted to IEEE Trans. on Ant. and Prop.

[20] Duncan, R.H., "Theory of the infinite cylindrical antenna including the feedpoint singularity in antenna current," J. Res. NBS D. Radio. Prop., Vol. 66D, No. 2, Mar.-Apr., 1962.

[21] Fante, R.L., "On the admittance of the infinite cylindrical antenna," Radio Science, Vol. 1 (New Series), No. 9, pp. 1041-1044, Sept., 1966. And correction, Radio Science, Vol. 1 (New Series), No. 10, pp. 1234, Oct., 1966.

[22] Wu, T.T., "Introduction to Linear Antennas," Chap. 8 of Antenna Theory Pt. 1, edited by R.E. Collin and F.J. Zucker, McGraw-Hill, New York, 1969.

[23] Levin, H. and J. Schwinger, "On the radiation of sound from an unflanged circular pipe," Phys. Rev., Vol. 73, No. 4, pp. 383-406, 1948.

[24] Jones, D.S., The Theory of Electromagnetism, Sec. 9.10, The Macmillan Co., New York, 1964.

[25] Rispin, L.W. and D.C. Chang, "Electromagnetic penetration into a finite coaxial cylinder with a recessed inner conductor," Sci. Rept. No. 29, (N0014-76-C-0318), Dept. of Elect. Engr., Univ. of Colorado, Boulder, Colorado, June, 1978.

[26] Harrington, R.F. and J. Mautz, "Matrix methods for solving field problems," Tech. Rept. No. RADC-TR-66-351, Vol. II, Rome Air Development Center, Griffiss Air Force Base, Rome, N.Y., DDC No. AD 639745, Aug., 1966.

[27] Chang, D.C., "On the electrically thick cylindrical antenna," Radio Sci., Vol. 2 (New Series), No. 9, pp. 1043-1060, Sept., 1967.

[28] Chang, D.C., "On the electrically thick monopole. Part I - Theoretical solution, and Part II - Experimental study," IEEE Trans. Ant. and Prop., Vol. AP-16, No. 1, pp. 58-71, Jan., 1968.

[29] Hartig, E.O., Circular Apertures and their Effects on Half-Dipole Impedances, doctoral dissertation, Harvard Univ., Cambridge, Mass., 1950. Experimental data from the above may also be found in Ref. [11].

[30] Chang, D.C. and L.W. Rispin, "A method of computing the input conductance of an electrically small antenna," to be published in IEEE Trans. Ant. and Prop.

[31] Rispin, L.W. and D.C. Chang, "Electromagnetic penetration into a finite coaxial cylinder with a recessed inner conductor," to be submitted to IEEE Trans. on Ant. and Prop.

[32] Miller, E.K., "Admittance dependence of the infinite cylindrical antenna upon exciting gap thickness," Radio Science, Vol. 2 (New Series), No. 12, pp. 1431-1435, Dec., 1967.

[33] Harrington, R.F., Time Harmonic Electromagnetic Fields, McGraw-Hill, New York, 1961.

[34] Schelkunoff, S.A. and H.T. Friis, Antennas and Theory and Practice, John Wiley and Sons, New York, 1952.

[35] Wu, T.T., R.W.P. King, D.J. Blejer, S.-K. Wan, M. Owens, R.W. Burton, L.C. Shen, and M.E. Burton, "Advanced aircraft EMP model development: Surface currents and charges induced on cylinders, crossed cylinders and cylinders crossed with horizontal flat plates by a normally incident plane electromagnetic field," Interaction Note No. 336, Oct., 1977.

Appendix A. Approximate solutions for the canonical integral, $U(\theta_i;z)$

Before the "so-called" canonical integral for $U(\theta_i;z)$ in (3) is considered, let us first of all begin with the closely related auxiliary canonical integral, $W(\theta_i;z)$, given in (6) and repeated here,

$$W(\theta_i;z) = \frac{-ik}{\eta}(1-\cos\theta_i)\int_{\Gamma_0}\frac{K_+(-\alpha)e^{-i\alpha z}}{(k+\alpha)(k\cos\theta_i+\alpha)K(\alpha)}\,d\alpha \quad ;$$

$$0 \le z < \infty, \quad 0 \le \theta_i \le \pi \tag{A1}$$

where,

$$K(\alpha) = i\pi J_0(\xi a)H_0^{(1)}(\xi a) \tag{A2}$$

and

$$\xi = \sqrt{k^2-\alpha^2} = i\sqrt{\alpha^2-k^2} \tag{A3}$$

K_+ is the "plus" factor of $K(\alpha)$ which is analytic and free of zeros in the upper half α-plane, (see Appendix C), and the contour, Γ_0, is shown in Figure 1. We shall find approximate solutions for $W(\theta_i;z)$ in (A1) and a similar integral for $U(\theta_i;z)$, which is stated later, that require the satisfaction of the condition,

$$\Omega(z) = 2\,\ell n(2z/a) >> |\ell n[2kz\sin^2(\theta_i/2)]| \tag{A4}$$

Actually, the restriction in (A4), which will be referred to as the "basic condition" on our analysis, expresses the most severe restriction encountered in the derivation of the approximate solutions for the canonical integral, $U(\theta_i;z)$, and the auxiliary canonical integral, $W(\theta_i;z)$. Many of the approximations to follow require lesser restrictions than the one in (A4) and, therefore, are automatically satisfied

when (A4) is true.

Since $K_+(-\alpha)$ is analytic in the lower half α-plane, combining the contributions from both sides of the branch cut, which is due to the term $[K(\alpha)]^{-1}$ in the integrand, allows (A1) to be written as,

$$W(\theta_i;z) = \frac{e^{ikz}}{\pi\eta} \int_0^\infty \left[\frac{1}{u} - \frac{1}{u - iv_0}\right] \frac{K_+\left[k + \frac{iu}{z}\right]}{J_0\left[\frac{a}{z}\sqrt{u(u - i2kz)}\right]} e^{-u}$$

$$\left[\frac{1}{H_0^{(1)}\left[\frac{a}{z}\sqrt{u(u - i2kz)}\right]} + \frac{1}{H_0^{(2)}\left[\frac{a}{z}\sqrt{u(u - i2kz)}\right]}\right] du \quad (A5)$$

where the change of variable, $\alpha = -k - iu/z$, has been utilized. v_0 is defined by,

$$v_0 = v_0(\theta_i;z) = 2kz \sin^2(\theta_i/2) \quad (A6)$$

and,

$$-\pi/4 < \arg(\sqrt{u(u - i2kz)}) < 0 \quad (A7)$$

Due to the exponential decay of the integrand in (A5), the meaningful range of integration is limited to the values of u of order unity or less. And since the term $K_+(\alpha)$ depends only upon the parameters, ka and αa, (see Appendix C for a discussion of $K_+(\alpha)$), then under the basic condition in (A4) (which implies $a/z << 1$) the term $K_+(k + iu/z)$ appearing in (A7) may be accurately represented by the first term of its Taylor series expansion about $u = 0$, i.e., $K_+(k)$. This term may then be removed from the integrand in (A5) yielding,

$$W(\theta_i;z) = K_+(k)U(\theta_i;z) \quad (A8)$$

where $U(\theta_i;z)$ is the canonical integral given by,

$$U(\theta_i;z) \approx \frac{e^{ikz}}{\pi\eta} \int_0^\infty \left[\frac{1}{u} - \frac{1}{(u - iv_0)} \right] \frac{e^{-u}}{J_0\left[\frac{a}{z}\sqrt{u(u - i2kz)}\right]}$$

$$\left[\frac{1}{H_0^{(1)}\left[\frac{a}{z}\sqrt{u(u - i2kz)}\right]} + \frac{1}{H_0^{(2)}\left[\frac{a}{z}\sqrt{u(u - i2kz)}\right]} \right] du \qquad (A9)$$

and is equivalent to the expression for $U(\theta_i;z)$ in (3) of Section 2.

The evaluation of $U(\theta_i;z)$ in (A9) requires numerical integration, since an exact analytical solution to the integral involved is not known. Hence, we seek a simple approximate solution for $U(\theta_i;z)$ which possesses a wide range of applicability. To this end, we assume the satisfaction of the basic condition on $\Omega(z)$ in (A4), which allows the Bessel functions in (A9) to be approximated by the leading terms of their respective small argument expansions. The resulting approximate expression for $U(\theta_i;z)$ can be written as,

$$U(\theta_i;z) \approx \mu(0;z) - \mu(\theta_i;z) \qquad (A10)$$

where,

$$\mu(\theta_i;z) = \frac{ie^{ikz}}{\eta} \int_0^\infty \frac{e^{-u}}{(u - iv_0)} \left[\frac{1}{\Omega(z) - 2\gamma + i\pi - \ell n[u(u - i2kz)]} \right.$$

$$\left. - \frac{1}{\Omega(z) - 2\gamma - i\pi - \ell n[u(u - i2kz)]} \right] du \qquad (A11)$$

and $\Omega(z)$ is given in (A4). The [bracketed] term behaves essentially like a slowly-varying function, both magnitude and phase, over the integration range, $0 < u < 1$, where the integrand has its major contribution, except of course very near $u = 0$. Thus, provided v_0

is not very small, we can approximate (A11) up to order $[\Omega(z)]^{-2}$ by,

$$\mu(\theta_i;z) \approx \frac{ie^{ikz}}{\eta}\left[\frac{1}{\Omega(z) - 2\gamma - \ell n(2kz) + i3\pi/2}\right.$$

$$\left. - \frac{1}{\Omega(z) - 2\gamma - \ell n(2kz) - i\pi/2}\right] e^{-iv_0} E_1(-iv_0) \qquad (A12)$$

where E_1 is the exponential integral of the first kind defined in [16, Eq. 5.1.1].

The situation is somewhat different for the case when $\theta_i = 0$ because the integrand now blows up at $u = 0$. To evaluate this integral properly, we must retain the logarithmic behavior of the integrand near $u = 0$, while approximating the term $\ell n(u - i2kz)$ by $\ell n(-i2kz)$. This procedure can be shown to lead to a solution for $\mu(0;z)$ good to order $[\Omega(z)]^{-2}$ consistent with the $\mu(\theta_i;z)$ solution. Proceeding, we obtain,

$$\mu(0;z) \approx \frac{ie^{ikz}}{\eta}\int_0^\infty \frac{e^{-u}}{u}\left[\frac{1}{\Omega(z) - 2\gamma - \ell n(2kz) + i3\pi/2 - \ell n(u)}\right.$$

$$\left. - \frac{1}{\Omega(z) - 2\gamma - \ell n(2kz) - i\pi/2 - \ell n(u)}\right] du \qquad (A13)$$

which has been previously given by Shen [6] whose subsequent solution was based upon the observation that the integration of a smooth function weighted by an exponential decay over an infinite interval can be approximated by the unweighted integration of the same function over a judiciously chosen integration range. The same result, however, can be obtained in a more straightforward manner if we replace u^{-1} by

$\int_1^\infty e^{-wu}\,dw$ and interchange the order of integration in (A13) which yields,

$$\mu(0;z) = \frac{ie^{ikz}}{\eta}\int_1^\infty \frac{dw}{w}\left\{\int_0^\infty e^{-t}\left[\frac{1}{\Omega(z) - 2\gamma + \ell n(w) - \ell n(2kzt) + i3\pi/2}\right.\right.$$

$$\left.\left. - \frac{1}{\Omega(z) - 2\gamma + \ell n(w) - \ell n(2kzt) - i\pi/2}\right] dt\right\} \qquad (A14)$$

Now since the term $|\ell n\ t|$ is typically small compared with $|\Omega(z)|$ for $t < 1$, except very close to $t \approx 0$ where the integration is rather insignificant, a two term Taylor series expansion followed by straightforward integrations on t yields,

$$\mu(0;z) = \frac{ie^{ikz}}{\eta}\int_1^\infty \frac{dw}{w}$$

$$\left\{\frac{1}{\Omega(z) - 2\gamma + \ell n(w) - \ell n(-i2kz) + i\pi}\left[1 - \frac{\gamma}{\Omega(z) - 2\gamma + \ell n(w) - \ell n(-i2kz) + i\pi}\right]\right.$$

$$\left. - \frac{1}{\Omega(z) - 2\gamma + \ell n(w) - \ell n(-i2kz) - i\pi}\left[1 - \frac{\gamma}{\Omega(z) - 2\gamma + \ell n(w) - \ell n(-i2kz) - i\pi}\right]\right\}$$

(A15)

Now taking the [bracketed] terms in (A15) as being the first two terms of a Taylor series expansion of a function of the form $[1+x]^{-1}$ for small x, the integrals in (A15) can be evaluated to order $[\Omega(z)]^{-2}$, with the result for $\mu(0;z)$ being given by,

$$\mu(0;z) \approx \frac{ie^{ikz}}{\eta}\,\ell n\left\{\frac{\Omega(z) - \gamma - i\pi - \ell n(-i2kz)}{\Omega(z) - \gamma + i\pi - \ell n(-i2kz)}\right\} \qquad (A16)$$

(A12) and (A16) may be combined to give a solution for (A10) good to order $[\Omega(z)]^{-2}$ which is given by,

$$U(\theta_i;z) = \frac{ie^{ikz}}{\eta} \ln \left\{ \frac{\Omega(z) - \gamma - i\pi - \ln(-i2kz) + e^{-iv_0} E_1(-iv_0)}{\Omega(z) - \gamma + i\pi - \ln(-i2kz) + e^{-iv_0} E_1(-iv_0)} \right\} \quad (A17)$$

Note that, although this approximate expression for $U(\theta_i;z)$ was derived under the assumptions that $v_0 = 2kz \sin^2(\theta_i/2)$ cannot be too small and that $|\Omega(z)| >> |\ln(v_0)|$, the particular method of combining $\mu(0;z)$ and $\mu(\theta_i;z)$ into $U(\theta_i;z)$ in (A17) actually gives a smooth function as $z \to 0$.

Although $U(\theta_i;z)$ is expressed in fairly simple terms in (A17), a simpler form (also good up to $O[\Omega(z)]^{-2}$) may be obtained by expressing the $\ln$ in terms of an arctangent, which in turn may be approximated by the leading term of its Taylor series expansion when the basic condition in (A4) is satisfied. This procedure yields the alternate formula for $U(\theta_i;z)$ given by,

$$U(\theta_i,z) \approx \frac{2\pi}{\eta} \frac{e^{ikz}}{\Omega(z) - \gamma - \ln(-i2kz) + e^{-iv_0} E_1(-iv_0)} . \quad (A18)$$

Appendix B. Input conductance of an infinitely long cylinder

The input conductance (which is associated with radiation from the external surface) of an infinitely long hollow cylindrical antenna may be formulated by means of considering the real part of the source current for a delta function voltage source of unit strength (i.e., 1.0 volt), [22]. The resulting expression may be written as,

$$G_\infty(ka) = \frac{4ka}{\pi\eta} \int_0^{ka} \frac{1}{x\sqrt{(ka)^2 - x^2}} \frac{dx}{J_0^2(x) + Y_0^2(x)} \qquad (B1)$$

where η is the intrinsic impedance of the surrounding medium, a is the cylinder radius, and J_0 and Y_0 are the zero order Bessel and Neumann functions, respectively. Although several asymptotic solutions (which assume $ka << 1$) for $G_\infty(ka)$ exist, [3], [4], [20] and [21], an exact solution to the integral in (B1) is not known to the authors. However, in their Wiener-Hopf approach to thin dipole antennas Shen, Wu, and King [6] constructed the surprisingly accurate formula for $G_\infty(ka)$ given by,

$$G_\infty(ka) = \mathrm{Re}\left\{\frac{i}{\eta}\left[\ell n(2C_w - i\pi/2) - \ell n(2C_w + i3\pi/2)\right]\right\} \qquad (B2)$$

which agrees with the asymptotic expression of Wu [3] to order C_w^{-3}. ($C_w = -\ell n(ka) - \gamma$, $\gamma = 0.577...$) . However, the constructed expression for $G_\infty(ka)$ in (B2) is fairly accurate even when $|C_w|$ is not large. In Figure B1, we have illustrated the input conductance predicted by both Shen's [6] curve-fitting formula and the exact expression in (B1) over the range of electrical radii, $10^{-4} \leq ka \leq 1.0$. This figure reveals the remarkable ability of Shen's approximate formula to predict an accurate input conductance not only in the conventional thin-wire regions but

AD-A142 291 A UNIFIED THEORY FOR THIN WIRE ANTENNAS OF ARBITRARY LENGTH(U) COLORADO UNIV AT BOULDER ELECTROMAGNETICS LAB L RISPIN ET AL. FEB 80 SCIENTIFIC-38 N00014-76-C-0318 2/2

UNCLASSIFIED F/G 9/1 NL

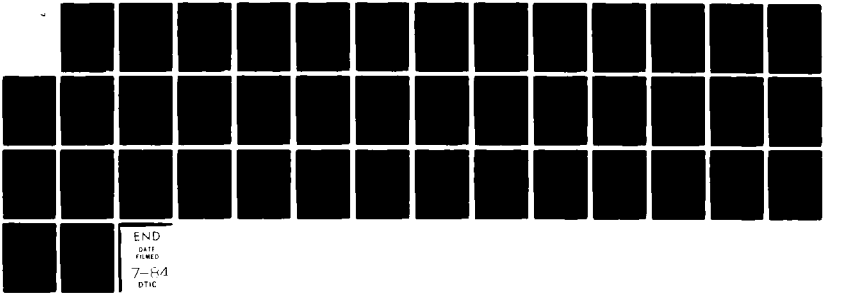

END

DATE FILMED

7-84

DTIC

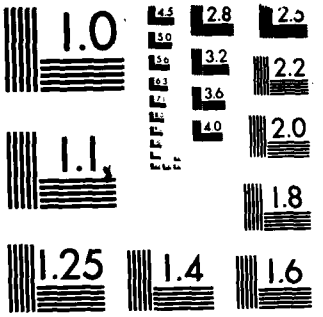

MICROCOPY RESOLUTION TEST CHART
NATIONAL BUREAU OF STANDARDS-1963-A

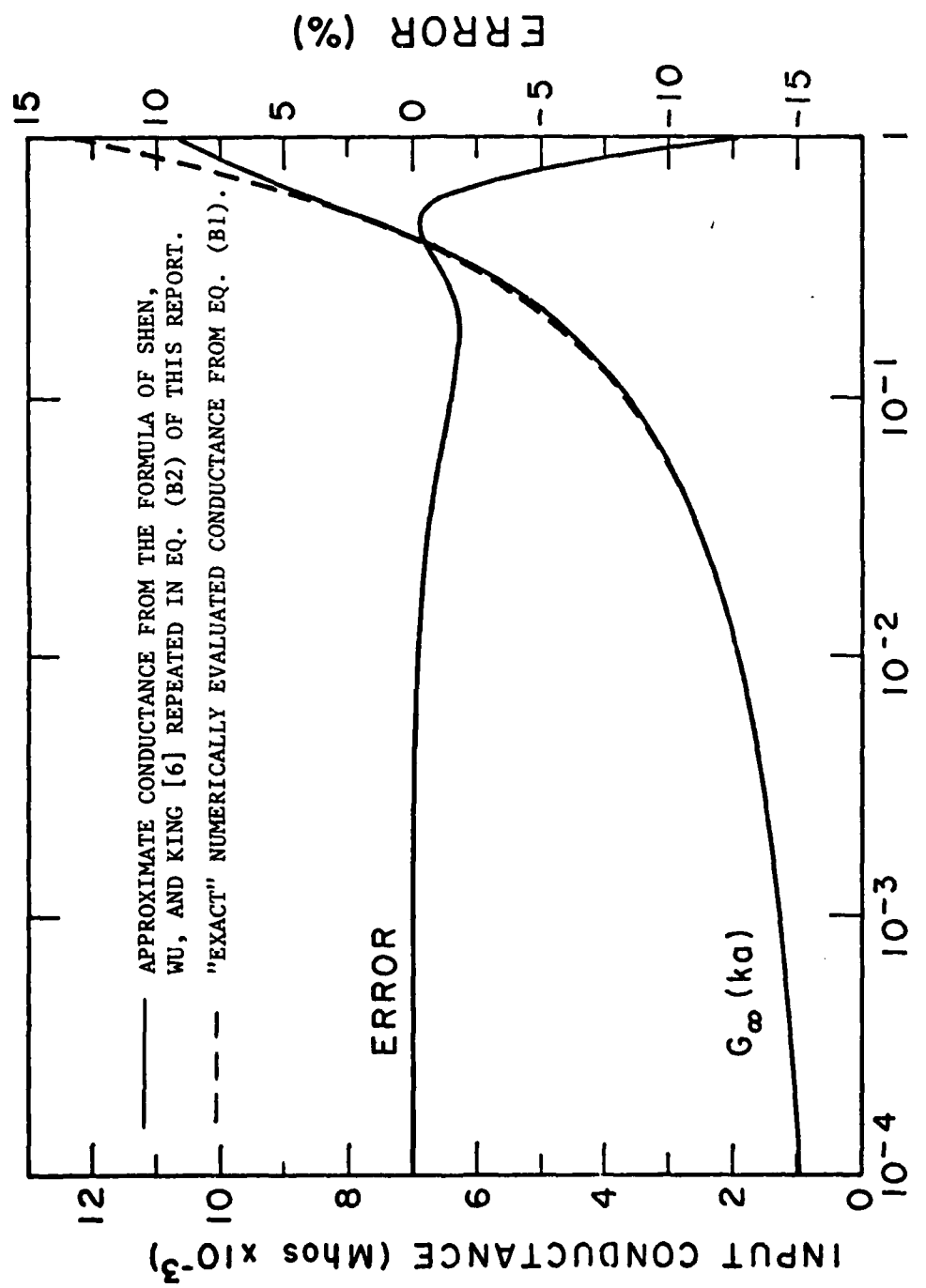

Figure B1. Input conductance of an infinitely long tubular cylinder.

for cylinders as thick as $ka \approx 0.7$, where $C_w = -0.22$! Furthermore, as $ka \to 0$, the approximate formula given in (B2) becomes asymptotic to,

$$G_\infty(ka) \sim \frac{\pi}{\eta} (C_w)^{-1} ; \quad \text{as} \quad ka \to 0 \tag{B3}$$

which corresponds to the asymptotic behavior of the results of many other authors, [3], [4], [20] and [21].

In order to further extend the applicable range of the basic approximate formula in (B2) to include values of ka as high as unity, we have employed a curve-fitting procedure to produce the modified formula,

$$G_\infty(ka) \approx \text{Re} \{ \frac{i}{\eta} [\ell n(2C_w - g - i\pi/2) - \ell n(2C_w - g + i3\pi/2)] \} \tag{B4}$$

where

$$g = 33.88(ka)^2 \exp [- \frac{3.26}{ka}] \tag{B5}$$

Obviously the insertion of g in (B5) into the approximate expression for $G_\infty(ka)$ in (B2) has little effect below $ka \approx 0.5$, however, above this point, all the way up to $ka \approx 1.0$, this modification allows for a quite accurate prediction for the input conductance as can be observed in Figure 5, which is discussed in the text of this report.

Consequently, in order to achieve this accurate value of input conductance from our primary transmitting current formula in (19) at $z = z_0$, we follow the lead of Shen, et al. [6] and restate the approximate form of $U(\pi;z)$ in (9) in the modified form,

$$U_s(z) = \frac{i}{\eta} e^{ikz} \{ \ell n[f_s(z) - i\pi] - \ell n[f_s(z) + i\pi] \} \tag{B6}$$

where,

$$f_s(z) = 2C_w + \gamma + i\pi/2 + \ell n[kz + \sqrt{(kz)^2 + \exp(-2\gamma - 2g)}\ ] \qquad (B7)$$

As given in (B6), $U_s(z)$ corresponds exactly to Shen's Eq. 6 in [6] except for the additional term, $-2g$, in the square root, which enables (B6) to yield a very accurate value for the real component of the input current up to $ka = 1.0$. And we note that $U(\pi;z)$ in (9) and the modified form denoted by $U_s(z)$ in (B6) differ insignificantly for $kz > 1$.

Appendix C. The kernel, $K(\alpha)$, and the factorized functions, $K_+(\alpha)$ and $K_-(\alpha)$

Consider the Wiener-Hopf kernel,

$$K(\alpha) = i\pi J_0(\xi a)H_0^{(1)}(\xi a) \tag{C1}$$

where

$$\xi = \sqrt{k^2-\alpha^2} = i\sqrt{\alpha^2-k^2} \tag{C2}$$

A small argument approximate form of (C1) which proves useful when dealing with conventionally thin ($ka<<1$) cylindrical antennas is given by,

$$K(\alpha) \approx 2C_w + i\pi - 2\,\ell n\left(\frac{\sqrt{k^2-\alpha^2}}{2k}\right) ; \; ka, \; \alpha a<<1 \tag{C3}$$

where

$$C_w = -\ell n(ka) - \gamma \; , \; \gamma = 0.57721566 \tag{C4}$$

In the Wiener-Hopf procedure, the kernel in (C1) is factorized into the form,

$$K(\alpha) = K_+(\alpha)K_-(\alpha) \tag{C5}$$

in which $K_+(\alpha)$ is analytic and free of zeroes in the upper half α-plane, $-Im(k) < Im(\alpha) < \infty$, and $K_-(\alpha)$ is analytic and free of zeroes in the lower half α-plane, $-\infty < Im(\alpha) < Im(k)$. We assume a symmetrical factorization which gives the relationship,

$$K_-(-\alpha) = K_+(\alpha) \tag{C6}$$

Thus the "minus factor", $K_-(\alpha)$, is known once $K_+(\alpha)$ is found. Another property imposed upon the factorization of $K(\alpha)$ is the asymptotic behaviors,

$$K_+(\alpha) \sim \alpha^{-\frac{1}{2}} \quad ; \text{ as } |\alpha| \to \infty \text{ in the upper half } \alpha\text{-plane} \tag{C7}$$

and

$$K_-(\alpha) \sim \alpha^{-\frac{1}{2}} \quad ; \text{ as } |\alpha| \to \infty \text{ in the lower half } \alpha\text{-plane} \tag{C8}$$

For the special case where ka and αa are much less than unity, $K_+(\alpha)$ may be approximated by the leading term of Hallen's exact formula for $K_+(\alpha)$, [1,Sec.38], given by,

$$K_+^0(\alpha) \approx \sqrt{2C_w+i\pi}\ \left[1 - \frac{1}{2C_w+i\pi}\ \ell n\left(\frac{k+\alpha}{2k}\right)\right] ; \ ka,\ \alpha a \ll 1 \tag{C9}$$

where C_w is given in (C4). The superscript "0" is used here to signify this as being the small argument (i.e., thin wire) approximate formula for $K_+(\alpha)$. And we note that $K_+^0(\alpha)$ in (C9) may also be identified as the plus factor in the approximate factorization of the small argument approximation of $K(\alpha)$ in (C3) given by:

$$K(\alpha) \approx (2C_w+i\pi)\ \left[1 - \frac{1}{2C_w+i\pi}\ \ell n\left(\frac{k+\alpha}{2k}\right)\right]\left[1 - \frac{1}{2C_w+i\pi}\ \ell n\left(\frac{k-\alpha}{2k}\right)\right]$$
$$; \ ka,\ \alpha a \ll 1 \tag{C10}$$

which is valid to order $(C_w)^{-2}$.

On the other hand, the exact value of $K_+(\alpha)$ may be obtained numerically from the formula of Mittra and Lee [15,Sec.5-2.(3)] which

is given by

$$K_+(\alpha) = \sqrt{i\pi}\ [J_0(\xi a)]_+\ \ [H_0^{(1)}(\xi a)]_+ e^{\chi(\alpha)} \tag{C11}$$

where ξ is given in (C2). The plus factors of $J_0(\xi a)$ and $H_0^{(1)}(\xi a)$ are given by

$$[J_0(\xi a)]_+ = \sqrt{J_0(ka)} \prod_{n=1}^{\infty} \left(1 + \frac{\alpha}{i\gamma_{0n}}\right) e^{i\frac{a}{n\pi}\alpha} \tag{C12}$$

and

$$[H_0^{(1)}(\xi a)]_+ = \sqrt{H_0^{(1)}(ka)}\ \ \exp\left\{-i\,\frac{ka}{2} + \frac{\xi a}{2}\,\ln\left(\frac{\alpha+i\xi}{k}\right) + q(\alpha)\right\} \tag{C13}$$

respectively. Here $i\gamma_{0n}$ corresponds to the propagation constant of the TM_{0n} mode within a circular waveguide of radius a and is given by

$$i\gamma_{0n} = i\sqrt{\left(\frac{\rho_{0n}}{a}\right)^2 - k^2}\ ;\ \rho_{0n} = n^{\text{th}} \text{ ordered zero of } J_0. \tag{C14}$$

The convergence factor $e^{\chi(\alpha)}$ in (C11) insures the correct asymptotic behavior described in (C7) and is given by

$$\chi(\alpha) = -i\,\frac{a}{\pi}\,\alpha\left[-1 + \gamma - \ln\left(\frac{2\pi}{ka}\right) - i\,\frac{\pi}{2}\right] \tag{C15}$$

where $\gamma = 0.577215.....$. And finally $q(\alpha)$ is given by

$$q(\alpha) = \frac{1}{\pi}\int_0^{\infty}\left[1 - \frac{2}{\pi\chi}\,\frac{1}{J_0^2(x) + Y_0^2(x)}\right]\ln\left(\frac{\sqrt{(ka)^2 - x^2} + \alpha a}{\sqrt{(ka)^2 - x^2}}\right)dx \tag{C16}$$

The specific application of $K_+(\alpha)$ in this paper is to calculate the reflection coefficient $R(\theta_i) = (n/2\pi)K_+(k)K_+(-k\cos\theta_i)$ in the range

$0 \le \theta_i \le \pi$; thus we require an accurate formula for $K_+(\alpha)$ for the corresponding range $-k < \alpha \le k$. Such a formula may be obtained by observing the behavior of the ratio of the small argument approximation, $K_+^0(\alpha)$ in (C8), with respect to the exact form of $K_+(\alpha)$ in (C11) over the range $-k < \alpha \le k$. Since the behavior of the small argument formula could be qualitatively argued as being at least partially inherent in the exact formula for $K_+(\alpha)$ for these values of α , the ratio, $K_+^0(\alpha)/K_+(\alpha)$, would be expected to be a fairly smooth function of α . This preassumption is verified in Figure C1 in which we show the real and imaginary parts of the ratio $K_+^0(\alpha)/K_+(\alpha)$ for $ka = 0.01$, 0.05, 0.1, 0.5, and 1.0, as a function of α between $-k$ and $+k$. Noting the behavior of this ratio and its predominantly real nature, we may assume the approximate relationship,

$$\frac{K_+^0(\alpha)}{K_+(\alpha)} = \begin{cases} A[1 + B(\alpha/k)] & ; 0 \le \alpha \le k \\ A[1 + B(\alpha/k) + C(\alpha/k)^2] & ; -k \le \alpha \le 0 \end{cases} \tag{C17}$$

where A, B, and C are coefficients yet to be determined. The above linear relationship for $0 \le \alpha \le k$ appears to describe the behavior of the imaginary component of $K_+^0(\alpha)/K_+(\alpha)$ for the cases where $ka \le 0.1$ in Figure C1, while it appears that higher order terms in α/k are necessary above $ka \approx 0.1$. However, due to the relatively large linear real component of $K_+^0(\alpha)/K_+(\alpha)$, neglecting this higher order variation in the imaginary component will not produce a significant error. The constant A is found by setting $\alpha = 0$ in (C17) yielding

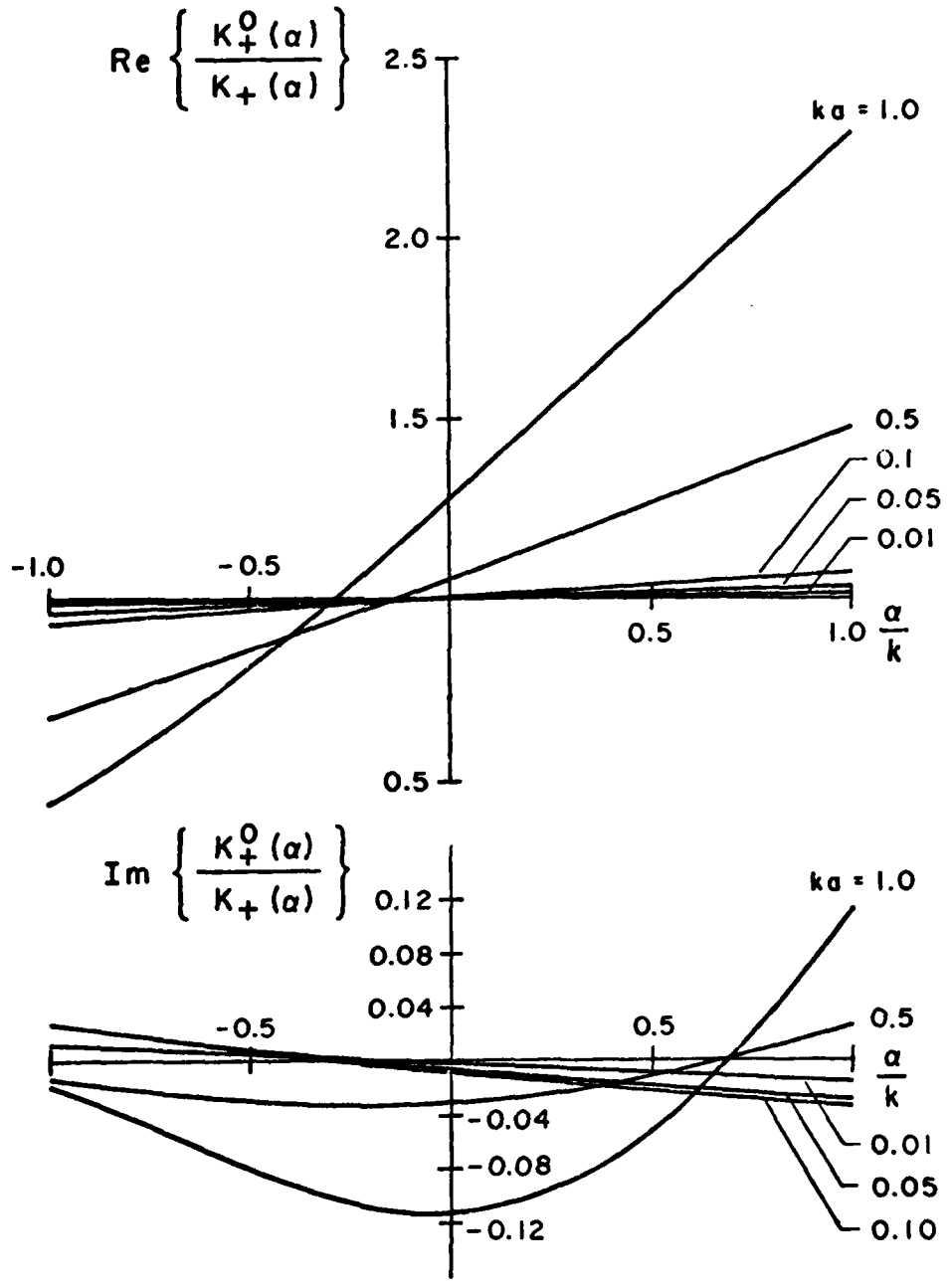

Figure C1. Real and imaginary components of the ratio of the small argument formula for $K_+(\alpha)$ in (C9) to the exact formula for $K_+(\alpha)$ in (C11).

$$A = \frac{\sqrt{2C_w + i\pi}\left[1 + \frac{\ell n(2)}{2C_w + i\pi}\right]}{\sqrt{i\pi J_0(ka)\, H_0^{(1)}(ka)}} \tag{C18}$$

The coefficient B is found by differentiating (C17) with respect to α and setting $\alpha = 0$, the result being

$$B = \frac{ika}{\pi} \sum_{n=1}^{\infty} \left(\frac{\pi}{a\gamma_{0n}} - \frac{1}{n} \right) - \chi(k) + \frac{ika}{\pi} - \frac{1}{2C_w + i\pi + \ell n(2)} \tag{C19}$$

$$+ \frac{ka}{\pi} \int_0^{\infty} \frac{1}{\sqrt{(ka)^2 - x^2}} \left[1 - \frac{2}{\pi x} \frac{1}{J_0^2(x) + Y_0^2(x)} \right] dx$$

As it stands, it appears as though a numerical integration is necessary in (C19) to evaluate B. However, one may recognize that the real part of the integral in question is directly related to the integral contained in the expression for the input conductance of an infintely long cylinder, $G_{\omega}(ka)$, in (B1) of Appendix B. And since a very good approximation for $G_{\infty}(ka)$, good up to $ka = 1.0$, has been found and is stated in (B4), we know the real part of B in (C19) to a very good degree of approximation. Furthermore, noting from Figure C1 that the imaginary component of $K_+^0(\alpha)/K_+(\alpha)$ for all the values of ka considered is relatively small, we may conclude that the imaginary part of B and the neglected higher order imaginary components are not important. Specifically for the constant B we may state that,

$$B_i^2 << (1 + B_r)^2 \tag{C20}$$

where B_r and B_i are the real and imaginary parts of B in (C19). Thus, we shall approximate B in (C19) by its real part given by

$$B_r = \frac{\eta}{2\pi} G_\infty(ka) - \mathrm{Re}\left\{ \frac{1}{2C_w} \frac{1}{+ i\pi + \ell n(2)} \right\} \tag{C21}$$

The above approximation of the coefficient B does introduce some phase error in our final formula (to follow shortly) which may be partially compensated by taking the absolute value of A in (C18) in the final formula. This compensation, however, is not seen until our curve-fit formula for $K_+(\alpha)$ is used in the context of the reflection coefficient $R(\theta_i) = \eta/2\pi\ K_+(k)K_+(-k\cos\theta_i)$.

With the above approximation for the coefficients A and B duly noted, we may write from (C17),

$$K_+(\alpha) = \begin{cases} \dfrac{K_+^0(\alpha)}{|A|\ [1 + B_r(\frac{\alpha}{k})]} & ;\ 0 < \alpha < k \\ \dfrac{K_+^0(\alpha)}{|A|[1 + B_r(\frac{\alpha}{k}) + C(\frac{\alpha}{k})^2]} & ;\ -k < \alpha < 0 \end{cases} \tag{C22}$$

which leaves only the coefficient C undetermined. An expression for C is easily obtained by matching the singularity at $\alpha = -k$ in (C22) with the actual singularity in $K(\alpha)$ at $\alpha = -k$. Using the relationship

$$\lim_{\alpha \to -k} K(\alpha) = K_+(k) \lim_{\alpha \to -k} K_+(\alpha) \tag{C23}$$

it is not difficult to show that

$$C = \frac{1 - |A|^2\ (1 - B_r^2)}{|A|^2\ (1 + B_r)} \tag{C24}$$

Numerical comparisons between our approximate expression for $K_+(\alpha)$ in (C22) and the exact formula in (C11) as well as between the subsequent approximate and exact reflection coefficients $(R(\theta_i) = \eta/2\pi\ K_+(k)\ K_+(-k\cos\theta_i))$ are found in Section 4 and show (C22) to be a very good approximation for $K_+(\alpha)$ in the range $-k < \alpha \leq k$ for ka as large as 1.0.

Appendix D. Limiting forms of the currents on cylindrical antennas near grazing incidence and near the ends

It is interesting to examine the limiting forms of our current expressions for semi-infinite as well as finite length cylindrical antennas as the incident angle of the uniform plane wave approaches grazing incidence in the receiving situation or as an end is approached in either the receiving or transmitting situations, even though these limits will violate the basic condition placed upon our theory in (8). It is noted that in the limits to follow, the value of the electrical radius, ka, has been necessarily taken to be small. This condition was imposed to avoid complications which would only serve to obliviate our original purpose of seeking a qualitative feeling for the behavior of our formulas beyond their expected analytical ranges.

D.1 Semi-infinite receiving antenna

The internal current on a semi-infinite $(0 \leq z \leq \infty)$ cylindrical receiving antenna predicted by (43) in the near-grazing situation, $\theta_i \to 0$, may be expressed as,

$$\{I^R_{S\infty}(\theta_i;z)\}_{int} \sim E^i_\theta f_1(h;z)\theta_i \; ; \text{ as } \theta_i \to 0 \, , \; 0 < z < \infty \qquad (D.1)$$

where,

$$f_1(h;z) = \left(\frac{-i4\pi}{k\eta} \right) \frac{ike^{ikz}}{4K_+(k)} \sum_{n=1}^{\infty} \frac{(\gamma_{0n} - ik)}{\gamma_{0n}(\gamma_{0n} + ik)} K_+(i\gamma_{0n}) e^{-\gamma_{0n} z} \qquad (D.2)$$

The internal current given in (D.1) is well behaved near $\theta_i = 0$ and goes to the physically anticipated limit of zero at $\theta_i = 0$. This may be attributed to the fact that the internal current expression in (43) upon

which (D.1) is based is an exact expression and must possess the correct physical behavior.

The external current on a semi-infinite $(0 \leq z \leq \infty)$ receiving antenna is given by the combination of the primary receiving current, $I^R_\infty(\theta_i;z)$ in (15), and the reflected current, $I^R_{refl}(\theta_i;z)$ in (25), i.e.,

$$I^R_{S\infty}(\theta_i;z) = E^i_\theta\{V(\theta_i;z) - V(\theta_i;0)R(\theta_i)U(\theta_i;z)\}\ ; \quad 0 < \theta_i < \pi\ , \quad 0 < z < \infty \qquad (D.3)$$

Using (9) for $U(\theta_i;z)$, (16) for $V(\theta_i;z)$ and (26) with (27) for $R(\theta_i)$, we find in the near-grazing situation,

$$I^R_{S\infty}(\theta_i;z) \sim -E^i_\theta \left(\frac{-i4\pi}{k\eta} \right) \frac{\pi^2}{3} \frac{e^{ikz}}{8} \left[\frac{1}{\theta_i \ell n^3 \theta_i} \right]\ ; \quad \text{as} \quad \theta_i \to 0\ , \quad 0 < z < \infty \qquad (D.4)$$

which "blows up" at $\theta_i = 0$. Because of the violation of the condition in (8), this behavior should not be unexpected. However, numerical data in this instance has shown that the misbehavior is limited to quite small values of $\theta_i \sim 10°$. Similarly, near the end of a semi-infinite receiving antenna we have from (D.3) with (9), (16), and (26) with (27),

$$I^R_{S\infty}(\theta_i;z) \sim E^i_\theta V(\theta_i;0) \left\{ F_1(\theta_i) - [1 - F_1(\theta_i)] \left[F_2(\theta_i) - i2kz \sin^2 \left(\frac{\theta_i}{2} \right) \frac{\ell n(2kz)}{2C_w + i\pi - 2\ \ell n(\sin\theta_i/2)} \right] \right\}$$

$$: \text{as} \quad z \to 0 \qquad (D.5)$$

where,

$$F_1(\theta_i) = \begin{cases} \dfrac{B_r(1-\cos\theta_i) - C(1-\cos^2\theta_i)}{1 - B_r\cos\theta_i + C\cos^2\theta_i} & ; \quad 0 \le \theta_i \le \pi/2 \\ \dfrac{B_r(1-\cos\theta_i) - C}{1 - B_r\cos\theta_i} & ; \quad \pi/2 \le \theta_i \le \pi \end{cases} \tag{D.6}$$

and,

$$F_2(\theta_i) = \sum_{n=1}^{\infty} \frac{(-1)^n}{2n+1} \left[\frac{\pi}{2C_w + i\pi - 2\,\ell n(\sin\theta_i/2)} \right]^{2n} \tag{D.7}$$

Under the assumption that the electrical radius, ka, is small compared to unity, the above quantities, $F_1(\theta_i)$ and $F_2(\theta_i)$, will also be quite small. Hence, the current in (D.5) will be at a relatively small level at $z = 0$.

Turning to the other form of $U(\theta_i;z)$ in (13), we have for the behavior of the external current in (D.3) using (16) and (26),

$$I^R_{S\infty}(\theta_i;z) \sim -E^i_\theta \left(\frac{-i4\pi}{k\eta} \right) \frac{e^{ikz}}{4} \left[-i3kz + \frac{B_r - 2C}{1 - B_r + C} \right] \left(\frac{\theta_i}{\ell n\ \theta_i} \right)$$

$$; \text{ as } \theta_i \to 0\,, \quad 0 < z < \infty \tag{D.8}$$

which goes to zero at $\theta_i = 0$. So even though the basic condition in (8) is violated here, the correct physically expected result is still obtained. Near the end of the semi-infinite cylinder, we have from (13) with (16) and (26) in (D.3),

$$I^R_{S\infty}(\theta_i;z) \sim E^i_\theta V(\theta_i;0) \left\{ F_1(\theta_i) - [1-F_1(\theta_i)] \left[-i2kz \sin^2 \frac{\theta_i}{2} \frac{\ell n(2kz)}{2C_w + i\pi - 2\,\ell n(\sin\theta_i/2)} \right] \right\}$$

; as $z \to 0$ (D.9)

where $F_1(\theta_i)$ is given in (D.6). At $z = 0$, the external current predicted by (D.9) is typically a very small value.

D.2. Semi-infinite transmitting antenna

The external current on a semi-infinite $(0 \leq z \leq \infty)$ cylindrical transmitting antenna with a delta function voltage source at $z = z_0$ is given by the combination of the primary current, $I^T_\infty(z_0;z)$ in (19), and the reflected current, $I^T_{refl}(Z_0;z)$ in (32), i.e.,

$$I^T_{S\infty}(z_0;z) = I^T_\infty(z_0;z) - I^T_\infty(z_0;0)R(\pi)U(\pi;z) \; ; \quad 0 < z < \infty \qquad (D.10)$$

The behaviors of the current near the end using both forms of $U(\pi;z)$ in (9) and (13) are found to be,

$$I^T(z_0;z) \sim I^T(z_0;0) \left\{ F_1(\pi) - [1-F_1(\pi)] \left[F_2(\pi) \frac{-i2kz\ \ell n(2kz)}{2C_w + i\pi} \right] \right\}$$

; as $z \to 0$ (D.11)

and,

$$I^T(z_0;z) \sim I^T(z_0;0) \left\{ F(\pi) - [1-F(\pi)] \left[\frac{-i2kz\ \ell n[2kz]}{2C_w + i\pi} \right] \right\}$$

; as $z \to 0$ (D.12)

respectively. At the end, $z = 0$, the currents predicted by (D.11) and (D.12) are small, the latter which employed (13) for $U(\pi;z)$ being smaller than the former which employed (9) for $U(\pi;z)$.

Although small values of current were obtained at the end in both the receiving and transmitting cases above using both forms of $U(\theta_i;z)$ in (9) and (13), none of these results agree with the negative of the internal penetrating current at the end, discussed in Section 6, which is a function of powers of ka. This is not an unexpected result, since our theory is based upon the condition that, $\Omega(z) = 2\,\ell n(2z/a) >> |\ell n[2kz\,\sin^2(\theta_i/2)|$, which is violated in these limits. Nevertheless, the above limiting forms are for the most part sufficiently well-behaved to permit useful data to be obtained in the finite length cylindrical antenna formulas (discussed in Section 5) over most of the antenna length and for a major portion of the possible angles of incidence.

D.3 Finite length receiving antenna

The internal current near the $z = -h$ end of a finite length $(-h \leq z \leq h)$ cylindrical receiving antenna predicted by (54) with (9) used for $U(\theta_i;z)$ in the near-grazing, $\theta_i \sim 0°$, situation behaves essentially as,

$$I^R_{int}(\theta_i;z) \sim E^i_\theta f_1(h;z) \left(\frac{1}{\theta_i \ell n^3 \theta_i} \right) ; \quad \text{as} \quad \theta_i \to 0\,, \; z \simeq -h \qquad (D.13)$$

where,

$$f_1(h;z) = \left(\frac{i4\pi}{k\eta} \right) \frac{\pi^2}{3} \frac{e^{ikh}}{8} \frac{R(\pi)U(\pi;2h)}{1 - [R(\pi)U(\pi;2h)]^2} \sum_{n=1}^{\infty} T_{0n}(\pi) e^{-\gamma_{0n}(h+z)} \qquad (D.14)$$

Hence, the internal current near the $z = -h$ end of a finite length receiving antenna predicted by (54) with (9) "blows up" at grazing, $\theta_i = 0$, incidence in much the same manner as the external current given in (D.4) in which (9) was also used for $U(\theta_i;z)$ in the grazing incidence limit. A similar functional behavior to that in (D.13) is obtained in the other near-grazing situation, $\theta_i \to \pi$, i.e.,

$$I^R_{int}(\theta_i;z) \sim E^i_\theta f_2(h;z) \left\{ \frac{1}{(\pi - \theta_i)\ell n^3(\pi - \theta_i)} \right\} ; \quad \text{as} \quad \theta_i \to \pi \quad , \; z \sim -h \qquad (D.15)$$

where,

$$f_2(h;z) = \left(\frac{i4\pi}{k\eta} \right) \frac{\pi^2}{3} \frac{e^{-ikh}}{8} \frac{1}{1 - [R(\pi)U(\pi;2h)]^2} \sum_{n=1}^{\infty} T_{0n}(\pi) e^{-\gamma_{0n}(h+z)} \qquad (D.16)$$

The behaviors of the internal current near the opposite end of the antenna, $z \to -h$, may be obtained from the above limits with appropriate re-interpretation of the incident angle of the uniform plane wave.

The limiting behavior of the external current distribution on a finite length receiving antenna given in (35) with (9) used for $U(\theta_i;z)$ as $\theta_i \to 0$ is given by,

$$I^R(\theta_i;z) \sim E^i_\theta f_3(h;z) \left\{ \frac{1}{\theta_i \ell n^3 \theta_i} \right\} ; \quad \text{as} \quad \theta_i \to 0 ; \quad -h < z < h \qquad (D.17)$$

where,

$$f_3(h;z) = \left(\frac{i4\pi}{k\eta} \right) \frac{\pi^2}{3} \frac{e^{ikh}}{8} \left\{ e^{-ik(h-z)} + \frac{R(\pi)U(\pi;2h)}{1 - [R(\pi)U(\pi;2h)]^2} R(\pi)U(\pi;h+z) \right.$$

$$\left. - \frac{1}{1 - [R(\pi)U(\pi;2h)]^2} R(\pi)U(\pi;h-z) \right\} \qquad (D.18)$$

The current distribution near-grazing stated above shares the same functional behavior with respect to θ_i as the semi-infinite cylindrical antenna limiting formula in (D.4), i.e., it "blows up" at $\theta_i = 0$. Although, the physically expected result is a zero current at grazing incidence, $\theta_i = 0$, the above misbehavior of the receiving current formula using (9) for $U(\theta_i;z)$ does not invalidate this formulation, but can be shown in most cases to limit the range of applicability to incident angles in the range, $10° \lesssim \theta_i \lesssim 170°$. Because of the symmetry of the receiving formula noted in (37), a similar behavior for the receiving current is obtained in the limit as $\theta_i \to \pi$.

Also to be considered is the limiting form for the finite length cylindrical antenna current at the ends. Again using (9) for $U(\theta_i;z)$ in (35) we obtain,

$$I^R(\theta_i;z) \sim E^i_\theta \left\{ V(\theta_i,-h) \left[F_1(\theta_i) \right.\right.$$

$$- [1 - F_1(\theta_i)] \left(F_2(\theta_i) - i2k(h+z) \sin^2 \frac{\theta_i}{2} \frac{\ell n[2k(h+z)]}{2C_w + i\pi - 2\,\ell n(\sin\theta_i/2)} \right.$$

$$+ C^R(\pi - \theta_i) \left[F_1(\pi) \right.$$

$$\left.\left.\left. - [1 - F_1(\pi)] \left(F_2(\pi) - i2k(h+z) \frac{\ell n[2k(h+z)]}{2C_w + i\pi} \right) \right] \right\}$$

$$; \text{ as } z \to -h, \quad 0 < \theta_i < \pi \qquad \text{(D.19)}$$

where $F_1(\theta_i)$ and $F_2(\theta_i)$ are given in (D.6) and (D.7) and are small for values of ka that are small compared to unity. The current at $z = -h$ predicted by (D.19) is typically a small value, although it will not correspond to the negative of the internal penetrating current at the end

discussed in Section 6. The behavior of the current near the opposite end, $z = +h$, may be obtained by means of the symmetry relationship in (37).

Repeating the limiting procedures for the receiving antenna current in (35) using (13) for $U(\theta_i;z)$, first of all for the internal current near the $z = -h$ end in the near-grazing situation, yields,

$$I^R_{int}(\theta_i,z) \sim E^i_\theta f_1(h;z)\theta_i + O\left\{\frac{\theta_i}{\ell n\ \theta_i}\right\} \quad ; \quad \text{as} \quad \theta_i \to 0\ ,\ z \approx -h \qquad (D.20)$$

where $f_1(h;z)$ is given in (D.2). Hence, the dominant behavior of the internal current near $z = -h$ on the finite antenna is essentially given by the behavior of the current near the end of a semi-infinite antenna near grazing as given in (D.1). A zero current is thus obtained at $\theta_i = 0$. The behavior of the internal current near $z = -h$ on a finite length receiving antenna from (35) with (13) as the incident angle, tends to the other grazing angle, $\theta_i \to \pi$, is given by,

$$I^R_{int}(\theta_i;z) \sim E^i_\theta f_5(h;z)\left(\frac{(\pi-\theta_i)}{\ell n(\pi-\theta_i)}\right) \quad ; \quad \text{as} \quad \theta_i \to \pi\ ,\ z \approx -h \qquad (D.21)$$

where,

$$f_5(h;z) = \left(\frac{-i4\pi}{k\eta}\right)\frac{e^{ikh}}{4}\left[1 + \frac{1}{2C_w+i\pi} + \frac{i2k}{\gamma_{0n}-ik} - \frac{B_r}{1+B_r} - \frac{\left[i6kh - \frac{B_r-2C}{1-B_r+C}\right]}{1-[R(\pi)U(\pi;2h)]^2}\right]$$
$$\sum_{n=1}^{\infty} T_{0n}(\pi)e^{-\gamma_{0n}(h+z)} \qquad (D.22)$$

The behavior of the external current on a finite length cylindrical receiving antenna predicted by (35) using (13) for $U(\theta_i;z)$ is given by,

$$I^R(\theta_i;z) \sim E^i_\theta f_6(h'z) \left(\frac{\theta_i}{\ell n\, \theta_i} \right) \; ; \quad \text{as} \quad \theta_i \to 0 \, , \; -h < z < h \qquad (D.23)$$

where,

$$f_6(h'z) = \frac{-i4\pi}{k\eta} \frac{1}{4} \left\{ e^{ikz} \left[i3k(h+z) - \frac{B_r - 2C}{1 - B_r + C} \right. \right.$$

$$+ e^{ikh} \left[i6kh - \frac{B_r - 2C}{1 - B_r + C} \right] \frac{R(\pi)U(\pi;2h)R(\pi)U(\pi;h+z)}{1 - [R(\pi)U(\pi;2h)]^2}$$

$$\left. - e^{ikh} \left[i6kh - \frac{B_r - 2C}{1 - B_r + C} \right] \frac{R(\pi)U(\pi;h-z)}{1 - [R(\pi)U(\pi;2h)]^2} \right. \qquad (D.24)$$

The functional behavior of the current in (D. 23) with respect to the incident angle, θ_i, is the same as the behavior noted in (D.8) which also employed (13) for $U(\theta_i;z)$. Consequently, the physically anticipated zero current is obtained in (D. 23) at grazing incidence, $\theta_i = 0$. This must be judged as a fortunate happenstance, since our theory is not expected to hold for very small incident angles. Also by means of the symmetry relationship in (37), a similar functional behavior can be observed as the opposite grazing incidence angle, $\theta_i = \pi$, is approached.

The external current near the end of a finite length cylindrical receiving antenna predicted by (35) with $U(\theta_i;z)$ given by (13) has the limiting form,

$$I^R(\theta_i;z) \sim E^i_\theta \left\{ V(\theta_i;-h) \left[F_1(\theta_i) \right. \right.$$

$$- [1 - F_1(\theta_i)] \left[-i2k(h+z)\sin^2 \left(\frac{\theta_i}{2} \right) \frac{\ell n[2k(h+z)]}{2C_w + i\pi - 2\, \ell n(\sin\theta_i/2)} \right] \Bigg]$$

$$\left. + C^R(\pi - \theta_i) \left[F_1(\pi) - [1 - F_1(\pi)] \left[-i2k(h+z) \frac{\ell n[2k(h+z)]}{2C_w + i\pi} \right] \right] \right\}$$

$$; \text{ as } \quad z \to -h \, , \; 0 < \theta_i < \pi \qquad (D.25)$$

where $F_1(\theta_i)$ is given in (D.6). (D.25) typically predicts a very small value at $z = -h$. Although it will not correspond to the negative of the internal penetrating current at the end discussed in Section 6. The functional behavior of the current near the opposite end at $z = +h$, can be shown to be similar to that in (D.25) via the symmetry relationship in (40).

Comparing the limiting forms of the currents in (D.13), (D.15), (D.17) and (D.19) with those in (D.20), (D.21), (D.23) and (D.25) corresponding to the use of (9) and (13), respectively, for $U(\theta_i;z)$ in the finite length receiving antenna formula in (35), the latter form of $U(\theta_i;z)$ must be judged the more attractive in the near grazing as well as the end vicinity situations. Not only is the correct zero current specified at grazing incidence when (13) is used for $U(\theta_i;z)$ in (35), but the current at the ends is smaller and thus more manageable. Both of these characteristics are particularly important in the case of the electrically short antenna discussed in Section 8.

D.4 Finite length transmitting antenna

Finally we consider the limiting forms of the external current at the ends of a finite length $(-h \leq z \leq h)$ cylindrical transmitting antenna. First using (9) for $U(\pi;z)$ in (38) we find,

$$I^T(z_0,z) \sim V_0[U_s(h+z_0) + C^T(h+z_0)]$$

$$\left\{ F_1(\pi) - [1 - F_1(\pi)] \left[F_2(\pi) - \frac{i2k(h+z)\ell n[2k(h+z)]}{2C_w + i\pi} \right] \right\}$$

$$; \text{ as } z \to -h \qquad (D.26)$$

where $F_1(\pi)$ and $F_2(\pi)$ are given in (D.6) and (D.7) and are normally small for values at ka sufficiently less than unity. And using (13) for $U(\pi;z)$ in (38) yields the behavior,

$$I^T(z_0;z) \sim V_0[U_s(h+z_0) + C^T(h+z_0)]$$

$$\left\{ F_1(\pi) - [1 - F_1(\pi)] \left[\frac{-i2k(h+z)\,\ell n[2k(h+z)]}{2C_w + i\pi} \right] \right\}$$

$$; \text{ as } \quad z \to -h \qquad \text{(D.27)}$$

Both of the above forms of the transmitting current at the end, $z = -h$, are typically small, the second one using (13) for $U(\pi;z)$ being the smaller. Although neither limit approaches the negative of the internally penetrating current at the end predicted by the relationships discussed in Section 6. A functional behavior similar to the above for the current near the opposite end of the antenna, $z = +h$, may be obtained via the symmetry relationship in (40).

Appendix E. Approximation for the summation in the expression for the current at the cylinder end

Consider the summation from (43) of the text with $z = 0$,

$$S = \sum_{n=1}^{\infty} \frac{ik(\gamma_{0n} - ik)}{\gamma_{0n}(\gamma_{0n} + ik\cos\theta_i)} K_+(i\gamma_{0n}) \tag{E1}$$

Numerical data reveals that the asymptotic form of $K_+(\alpha)$ in (46) may be used for $K_+(i\gamma_{01})$ with little error provided that $ka \lesssim 1$. Then (E1) may be rewritten as

$$S \approx ika \sum_{n=1}^{\infty} \frac{[a\gamma_{0n} - ika]^{\frac{1}{2}}}{a\gamma_{0n}(a\gamma_{0n} + ika\cos\theta_i)} \tag{E2}$$

Since we are considering $ka \lesssim 1$ and since $\rho_{0n} \geq 2.4048\ldots$, appropriate Taylor series expansions may be performed on the terms in (E2), leading to

$$\begin{aligned} S \approx \{ &(ika)\sum_{n=1}^{\infty} \rho_{0n}^{-3/2} - (ika)^2[\tfrac{1}{2} + \cos\theta_i]\sum_{n=1}^{\infty}\rho_{0n}^{-5/2} \\ &-(ika)^3[\tfrac{7}{8} - \tfrac{1}{2}\cos\theta_i - \cos^2\theta_i]\sum_{n=1}^{\infty}\rho_{0n}^{-7/2} \\ &-(ika)^4[-\tfrac{9}{16} - \tfrac{11}{8}\cos\theta_i + \tfrac{1}{2}\cos^2\theta_i + \cos^3\theta_i]\sum_{n=1}^{\infty}\rho_{0n}^{-9/2} + \cdots\} \end{aligned} \tag{E3}$$

The summations in (E3) involving the zeroes of the Bessel function, J_0, may be approximated by

$$\sum_{n=1}^{\infty} \rho_{0n}^{-m/2} \approx \sum_{n-1}^{20} \rho_{0n}^{-m/2} + \int_{20.5}^{\infty} [(x - 1/4)\pi]^{-m/2} dx \; ; \quad m = 3,5,7,\ldots \tag{E4}$$

The integral in (E4) approximates the original summation above n = 20 and utilizes the asymptotic form for the zeroes, $\rho_{0n} \sim (n - 1/4)\pi$. For values of ka less than unity, S is fairly well approximated by the first four summations shown explicitly in (E3). Performing these summations in the approximate manner of (E4) allows us to write S in the approximate form,

$$S = \sum_{m=1}^{4} A_m(\theta_i)(ika)^m \tag{E5}$$

where

$$A_1(\theta_i) = 0.5831 \tag{E6}$$

$$A_2(\theta_i) = -0.1364[\tfrac{1}{2} + \cos(\theta_i)] \tag{E7}$$

$$A_3(\theta_i) = -0.0498[\tfrac{7}{8} - \tfrac{1}{2}\cos\theta_i - \cos^2\theta_i] \tag{E8}$$

and

$$A_4(\theta_i) = -0.0198[-\tfrac{9}{16} - \tfrac{11}{8}\cos\theta_i + \tfrac{1}{2}\cos^2\theta_i + \cos^3\theta_i] \tag{E9}$$

Appendix F. The end conductance of a finite length cylindrical antenna

An interesting quantity worth mentioning is the conductance seen by a TM_{ON} mode inside and near one of the ends of a cylindrical antenna. Employing the Wiener-Hopf technique, the reflected current due to an internal current, which is of the form, $e^{\gamma_{ON} z}$, incident upon the end of a semi-infinite $(0 \leq z \leq \infty)$ cylinder is approximately given by, [31],

$$I_{refl}^{s\infty}(z) \approx \frac{1}{2}\left(\frac{k + i\gamma_{ON}}{\rho_{ON}}\right)^2 K_+(i\gamma_{ON}) \sum_{n=1}^{\infty} \rho_{0n}^2 \frac{K_+(i\gamma_{0n})}{\gamma_{0n}(\gamma_{ON} + \gamma_{0n})} e^{-\gamma_{0n} z}$$

$$- R(\theta_{ON}) U(\theta_{ON}; z) \; ; \quad 0 \leq z \leq \infty \qquad \text{(F1)}$$

where $K_+(\alpha)$ is discussed in Appendix C, $i\gamma_{ON}$ is the propagation constant of the TM_{ON} circular waveguide mode given in (45), ρ_{ON} is the N^{th} ordered zero of the Bessel function, J_0, and finally $R(\theta_{ON})$ and $U(\theta_{ON}; z)$ are the reflection coefficient and canonical integral evaluated at $\theta_{ON} = \cos^{-1}(-i\gamma_{ON}/k)$ given in (26) and (3), respectively. The first term in (F1) corresponds to internally reflected TM_{0n} circular waveguide modes, while the second term corresponds to the externally transmitted current which in this form is valid under the condition in (8). From (F1) the TM_{ON} mode current reflection coefficient at the point, $z = \ell$, inside the cylinder is simply,

$$\Gamma_{ON}^{s\infty}(\ell) = \left[\left(\frac{k + i\gamma_{ON}}{2\gamma_{ON}}\right) K_+(i\gamma_{ON})\right]^2 e^{-2\gamma_{ON}\ell} \qquad \text{(F2)}$$

Through a transmission line analogy [25], we may write the end admittance of the TM_{ON} mode at $z = \ell$ as,

$$Y_e^{s\infty}(\ell) = \left| \frac{1 + \Gamma_{ON}^{s}(\ell)}{1 - \Gamma_{ON}^{s}(\ell)} \right| Y_{ON} \tag{F3}$$

where,

$$Y_{ON} = \frac{4\pi k}{i\gamma_{ON}\eta} \; ; \quad \eta = 120\,\pi \tag{F4}$$

is the analogous transmission line characteristic admittance for the TM_{ON} circular waveguide mode.

By instituting the multiple reflection concept utilized in this report (see Section 5), we may formulate an expression for the external current on a finite length $(-h \leq z \leq h)$ cylinder from the initial externally transmitted current in (F1). This first component of the external current as well as all of the higher order reflections propagate approximately as e^{ikz}, so that the corresponding wave incidence is $\theta_i = \pi$. The constructed external current distribution on a finite length cylinder due to an incident internal TM_{ON} mode current, $e^{\gamma_{ON}(h+z)}$, is given by,

$$\begin{aligned} I^{ext}(z) = & -R(\theta_{ON})U(\theta_{ON}\,;h+z) \\ & + \frac{R(\theta_{ON})U(\theta_{ON};2h)}{1-[R(\pi)U(\pi;2h)]^2}\,R(\pi)U(\pi\,;h-z) \\ & - \frac{R(\theta_{ON})U(\theta_{ON};2h)R(\pi)U(\pi;2h)}{1-[R(\pi)U(\pi;2h)]^2}\,R(\pi)U(\pi\,;h+z)\;; \\ & \qquad\qquad -h \leq z \leq h \end{aligned} \tag{F5}$$

With the knowledge of the external current incident upon the end, $z = -h$, from (F5), the penetrating current near this end may be formulated from the transmission characterization in Section 6 and is given by,

$$I^{ext\to int}(z) = \frac{R(\theta_{ON})U(\theta_{ON};2h)R(\pi)U(\pi;2h)}{1-[R(\pi)U(\pi;2h)]^2} \sum_{n=1}^{\infty} T_{0n}(\pi)e^{-\gamma_{0n}(h+z)}; \quad z \gtrsim -h \qquad (F6)$$

where $T_{0n}(\theta_i)$ and $i\gamma_{0n}$ are given in (44) and (45) of the text. The combination of the penetrating TM_{ON} mode current in (F6) and the original internally reflected TM_{ON} mode current from (F1) with respect to the incident current, $e^{\gamma_{ON}(h+z)}$, yields the TM_{ON} mode current reflection coefficient, a distance, ℓ, from the end, $z = -h$, given by,

$$\Gamma_{ON}(\ell) = \Gamma_{ON}^{s\infty}(\ell) + \frac{i2\pi}{\eta}\frac{k}{\gamma_{ON}}\frac{R(\theta_{ON})U(\theta_{ON};2h)R(\pi)U(\pi;2h)}{1-[R(\pi)U(\pi;2h)]^2}R(\theta_{ON})e^{-2\gamma_{ON}\ell} \qquad (F7)$$

The equivalent transmission line analogous end admittance corresponding to the TM_{ON} mode reflection coefficient in (F7) for the finite length cylinder is,

$$Y_e(\ell) = \left[\frac{1+\Gamma_{ON}(\ell)}{1-\Gamma_{ON}(\ell)}\right]Y_{ON} \qquad (F8)$$

where Y_{ON} is given in (F4). Figure F1 shows the TM_{01} mode end conductance at $z = 2a - h$, i.e., $\ell=2a$, for a finite-length $(-h \le z \le h)$ cylindrical antenna where $\Omega(h) = 2\ell n(2h/a) = 10$ as a function of the electrical length between $kh = 0.05$ and $kh = 3.5$. Also shown is the end conductance of a semi-infinite cylinder for the corresponding electrical radii between $ka = 0.00067$ and $ka = 0.0472$. Note that the end susceptance at this depth with the semi-infinite as well as the finite length cylinder is nominally given by $-Im\{Y_{01}\}$ from (F4). As could be expected the end conductance in both situations is quite small and the

Figure F1. End conductance for the TM_{01} circular waveguide mode at a depth equal to one diameter, i.e., 2a, inside the end of a tubular cylinder.

———— Effective aperture end conductance from eq. (F9) using (54) with (13).

— — — — Direct (Wiener-Hopf) end conductance from eq. (F8) with (13) used for $U(\theta_i;z)$.

. . . . . Semi-infinite cylinder (electrical radius, shown in top scale, corresponds to the electrical radius of the finite length cylinder for $\Omega(h) = 10$) end conductance *from the effective aperture relation in* eq. (F9) using (43) or the direct (Wiender-Hopf) relation in eq. (F3), both formulations yielding similar results.

Note: the exact value of the term, $K_+(i\gamma_{01})$, calculated using the formula given by Mittra and Lee [15, Sec. 5-2,(3)] has been used in all of the above formulations. Otherwise, eq. (27) has been used to calculate $K_+(\alpha)$ for $-k \leq \alpha \leq k$.

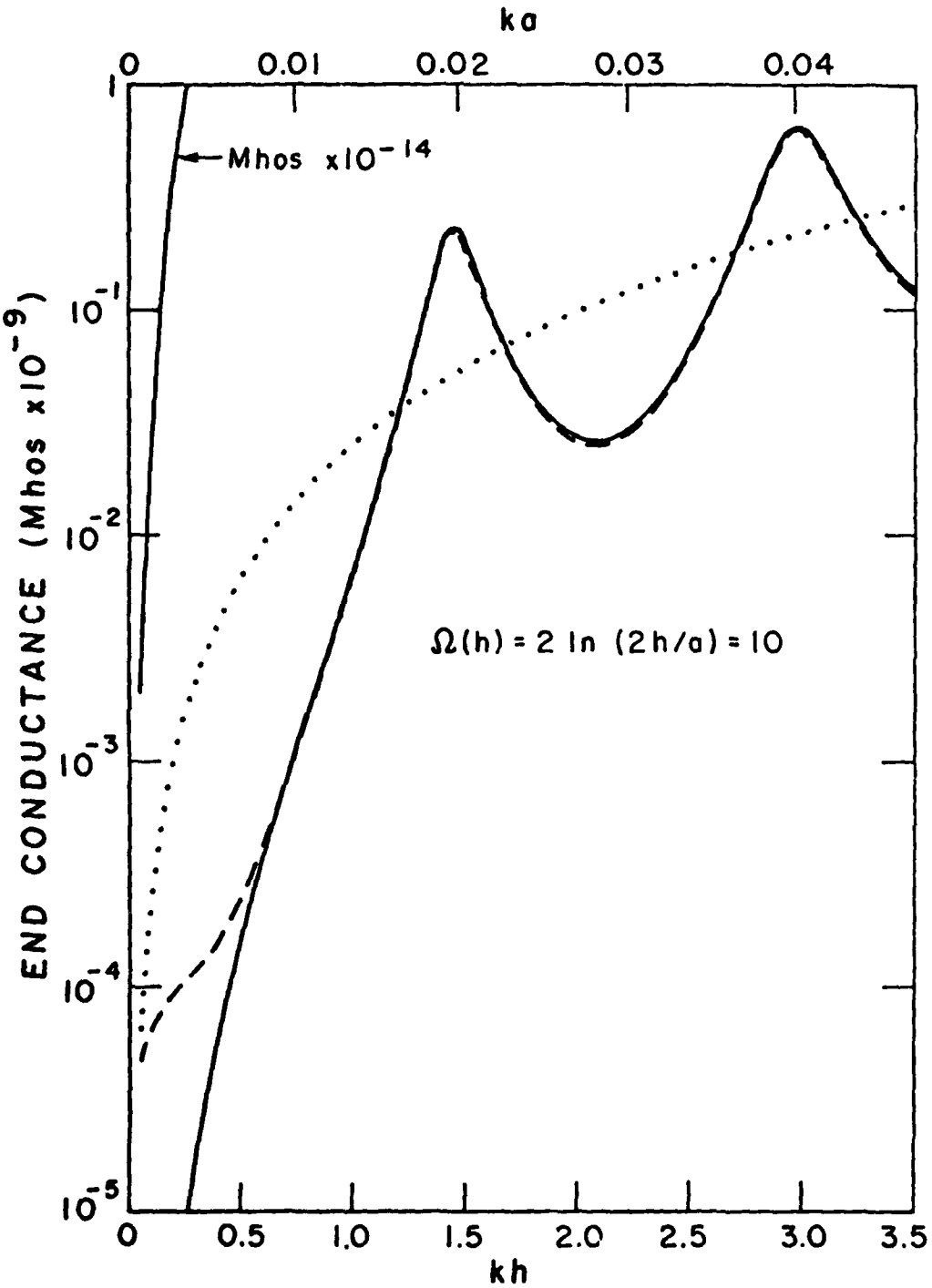
ka
0
0.01
0.02
0.03
0.04
Mhos x10⁻¹⁴
END CONDUCTANCE (Mhos x10⁻⁹)
1
10⁻¹
10⁻²
10⁻³
10⁻⁴
10⁻⁵
Ω(h) = 2 ln (2h/a) = 10
0
0.5
1.0
1.5
2.0
2.5
3.0
3.5
kh

finite length end conductance oscillates above and below the semi-infinite end conductance beyond the first resonant length, $kh \approx \pi/2$. At the smaller values of kh , the finite length end conductance takes an interesting although unlikely diversion from the expected smoothly decreasing behavior. The end conductance may also be calculated from the formula of Chang and Rispin [30] which is based upon the effective aperture of the antenna and in the present situation may be written as,

$$G_e = \frac{k^2\eta}{8\pi} \int_0^{\pi} |I_{01}^{sc}(\theta_i;\ell)/E_0^i|^2 \sin\theta_i \, d\theta_i \qquad (F9)$$

$|I_{01}^{sc}(\theta_i;\ell)/E_\theta^i|$ is the magnitude of the short circuit TM_{01} mode current at ℓ and is equal (if we neglect the multiple reflections in the region, $-h \leq z \leq -h+\ell$) to twice the magnitude of the internally penetrating TM_{01} mode current given in (43) for the semi-infinite cylinder and in (54) for the finite length cylinder. In order to neglect the perturbation of the external current and the multiple reflections of the TM_{01} mode within the end of the cylinder due to the short circuit at $z = \ell - h$ it is necessary to require that $\ell \gtrsim 2a$ in this conductance formulation. The semi-infinite and finite length end conductances obtained from (F9) for an antenna where $\Omega(h) = 2\ell n(2h/a) = 10$ is also included in Figure F1. The semi-infinite cylinder end conductances from both the direct and effective aperture methods in (F3) and (F9) with (54), respectively, are for all practical purposes, the same. And the agreement between the two finite length end conductances in Figure F1 at the larger values of kh is very good. However, at the smaller values of kh , the effective aperture end conductance from (F9) with (54) continues to decrease smoothly for shorter electrical lengths as opposed to the odd

behavior of the directly formulated end conductance in (F8). We accept the validity of the effective aperture result on the grounds that it depends only upon the magnitude of the associated current which is assumed to be fairly accurate, since the magnitude of the receiving current on the electrically short cylindrical antenna predicted by our formulas compared very well with an accepted existing theory in Section 8. On the other hand, the direct formulation in (F8) depends on the phase of the reflected current, which we know is not accurately determined by our formulas applied to the electrically short cylindrical antenna.

Appendix G. Electrically thick antennas on the order of a few wavelengths in length

The application of our theory to the electrically thick (up to $ka \approx 1$) cylindrical antenna whose length is on the order of a few free space wavelengths is based upon observations in Section 4 which imply that the basic condition in (8) may be relaxed for the larger values of ka to the point where $\Omega(z) = 2\,\ell n(2z/a)$ need only be somewhat larger than $|\ell n[2kz\,\sin^2(\theta_i/2)]|$ to achieve reasonably accurate results for the primary and secondary currents on the antenna. Although the application of our theory (using (13) for $U(\theta_i;z)$) has already been demonstrated for the electrically thick antenna in Section 7, we shall present results in this appendix for similar and even shorter antennas, based upon our formulas using (9) for $U(\theta_i;z)$. And again we note, that for all of the antennas to which our theory is applicable, the total (external and internal) current distribution is, for all practical purposes, given by the external current distribution alone, except in the near vicinity of the ends.

G.1 Electrically thick receiving antenna

The current distribution on an electrically thick, $ka = 1$, finite length, $kh = 3\pi$, cylindrical antenna as calculated from (35) using (9) for $U(\theta_i;z)$ is shown in Figure G1 for the incident angles (of the uniform plane wave) of $\theta_i = \pi/6$, $\pi/3$, and $\pi/2$. Normal incidence data given by Wu, et al. [35] based upon the theory of Kao [18] for the azimuthally uniform z-directed current is also shown in this figure for comparison. And the resulting agreement between the two sets of normal incidence ($\theta_i = \pi/2$) data is excellent (except, of course, near

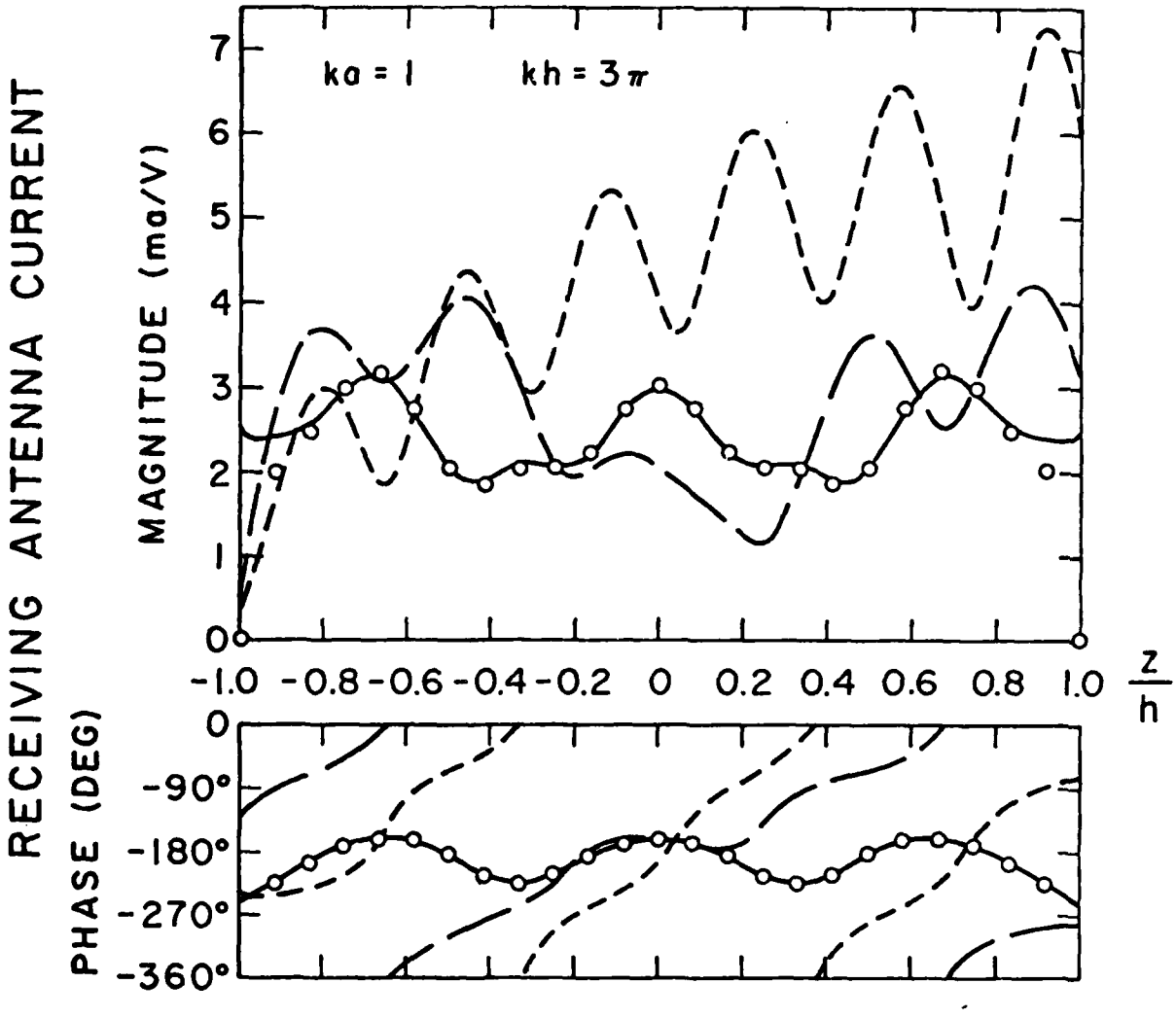

Figure G1. Current distributions on a three wavelengths long, electrically thick, cylindrical receiving antenna normalized to the incident electric field and the wavelength, i.e. $I^R(\theta_i;z)/\lambda E^i$.

——— $\theta_i = \pi/2$
— — $= \pi/3$
– – – – $= \pi/6$

} from eq. (35) with (9) used for $U(\theta_i;z)$

o $\theta_i = \pi/2$ Numerically evaluated data from Wu, et al. [35].

the ends) and better than the agreement which was previously obtained and shown in Figure 21 in which the other approximate form of $U(\theta_i;z)$ in (13) was used in the receiving current expression given in (35). And even further, Figure G2 shows the receiving current distribution, as calculated from (35) using (9) for $U(\theta_i;z)$, on an electrically thick, $ka = 1$, antenna whose electrical length is one half that of the antenna in the previous figure, i.e., $kh = 3\pi/2$. The agreement between our normal incidence ($\theta_i = \pi/2$) result and the numerically obtained normal incidence data of Kao [18] is again excellent. An attempt to apply our theory to this antenna, ($ka = 1$ and $kh = 3\pi/2$), using the other approximate formula for $U(\theta_i;z)$, which is given by (13), met with much less success. However, of all the many examples studied in the preparation of this report, it was only for these electrically thick antennas did the use of (9) for $U(\theta_i;z)$ show a decided advantage over the use of (13) for $U(\theta_i;z)$ in our finite length antenna formulas. Hence, our theory involving the use of (13) for $U(\theta_i;z)$ was featured in the text of this report. And although a near-grazing incidence, $\theta_i = \pi/36$, distribution was included in the receiving antenna examples in the text, no near grazing results have been shown in Figures G1 and G2, due to the misbehavior of our receiving current formula for small incident angles (see Appendix D) when (9) is used for $U(\theta_i;z)$.

G.2 Electrically thick transmitting antenna

A recalculation of the input conductance for the tubular antennas considered in Figure 29 (which used (13) for $U(\pi;z)$ in (41) for the calculation), this time using (9) for $U(\pi;z)$ in (41) results in the curves shown in Figure G3. Data from the numerical approach of Chang [27] and [28] and the experimental method of Hartig [29] which were used for

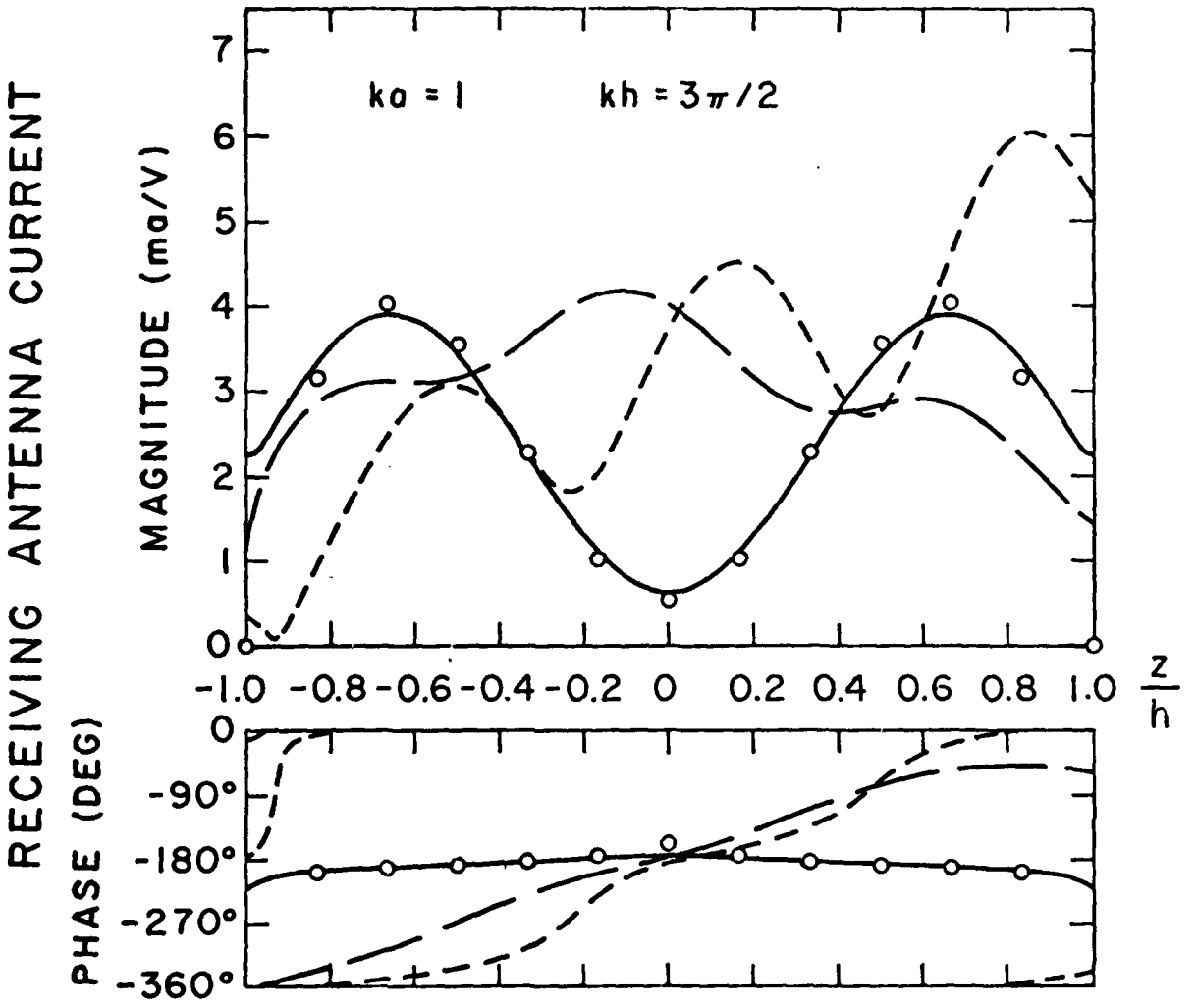

Figure G2. Current distributions on a three-halves wavelength long, electrically thick, cylindrical receiving antenna normalized to the incident electric field and the wavelength, i.e., $I^R(\theta_i;z)/\lambda E^i_\theta$.

——— $\theta_i = \pi/2$
— — — $= \pi/3$
– – – – $= \pi/6$

} from eq. (35) with (9) used for $U(\theta_i;z)$

o $\theta_i = \pi/2$ Numerically evaluated data from Kao [18].

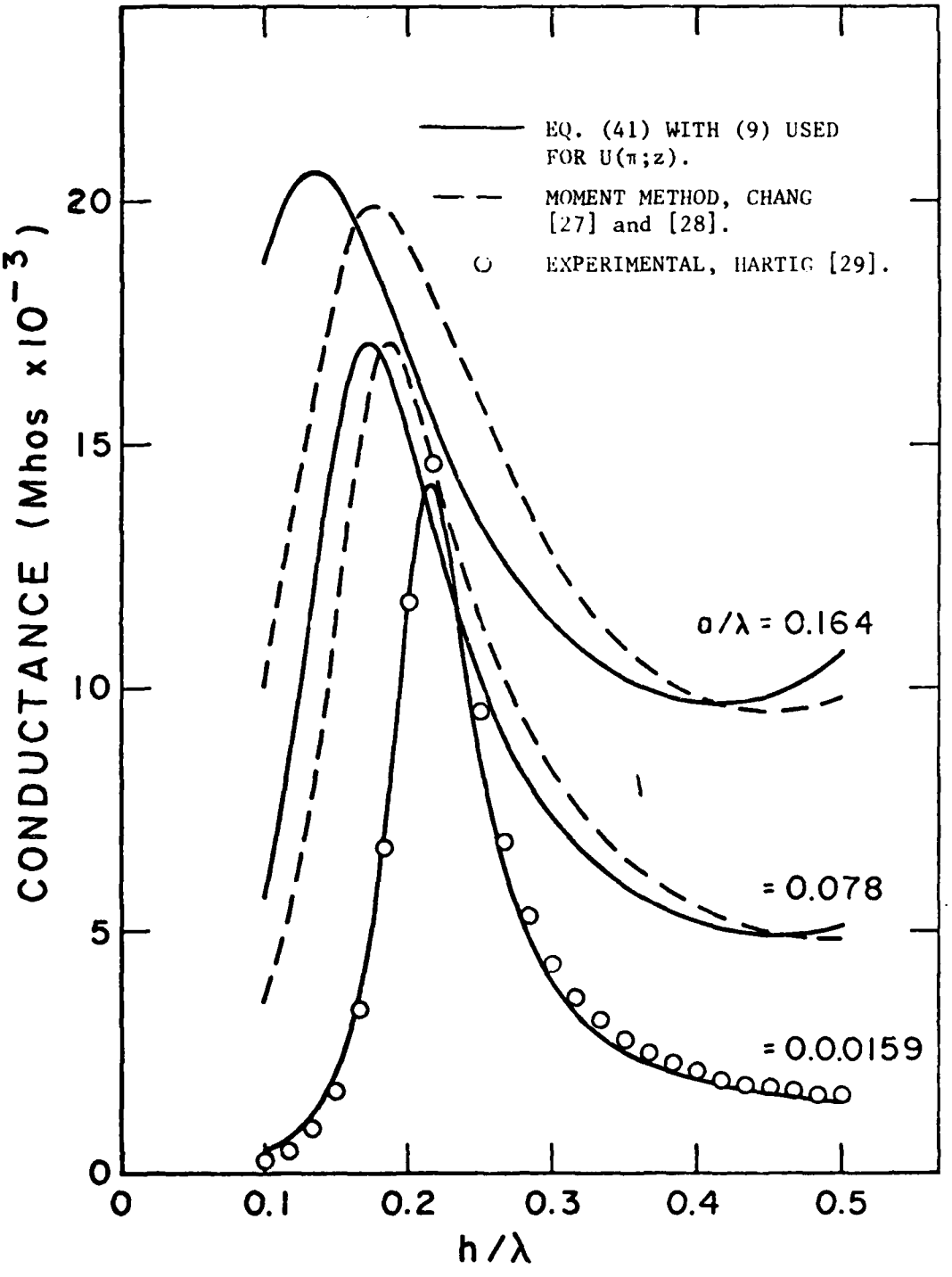

Figure G3. Input conductance of three electrically thick, center fed, cylindrical antennas as a function of the normalized half-length, h/λ .

comparison in Figure 29 is also included in Figure G3. A close inspection and comparison of Figures 29 and G3 reveals about the same level of agreement between our theory and the others in the latter figure where (9) was used for $U(\pi;z)$. However, as explained in the previous sub-section, (13) was used for $U(\pi;z)$ in the text examples, since it had shown a wider range of applicability.

Further, in Figure G4 we have repeated the conductance data from Figure 30 for a center-fed tubular antenna where $h/a = 10$ and included results obtained from (41) in which (9) has been used for $U(\pi;z)$. We note that in this figure the two forms of $U(\pi;z)$ (given by (9) and (13)) when used in the admittance formula given in (41) yield slightly different results, although both conductance curves are consistent with the numerical data of Harrington and Mautz [26]. Figure G5 is identical with Figure 31 which showed the input conductance for an off-center fed, $z_0 = \pm h/2$, tubular antenna where $h/a = 10$, except for the additional conductance data obtained from (41) this time using (9) for $U(\pi;z)$. And again all three sets of data are consistent.

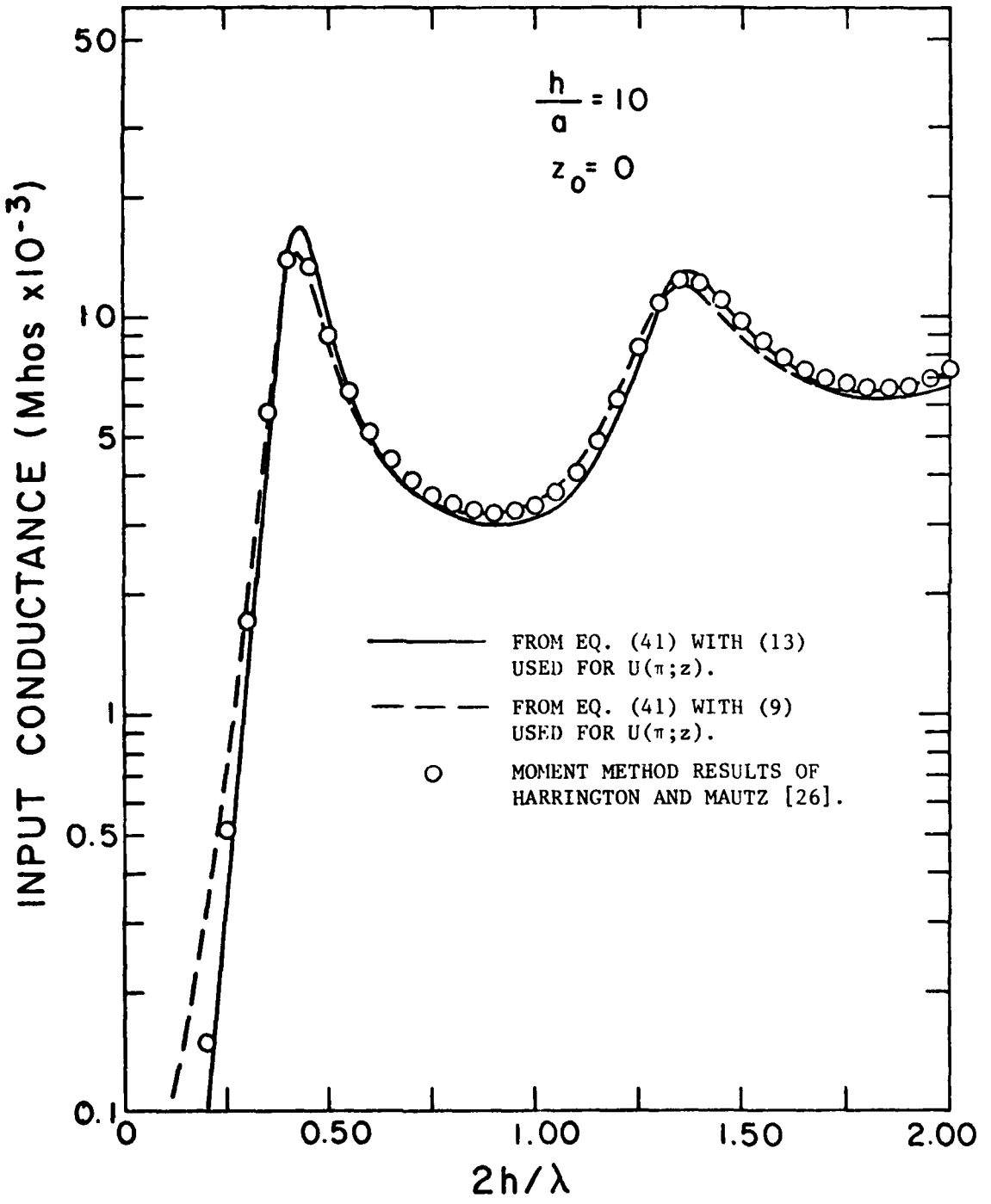

Figure G4. Input conductance of a center fed cylindrical antenna as a function of the normalized length, $2h/\lambda$.

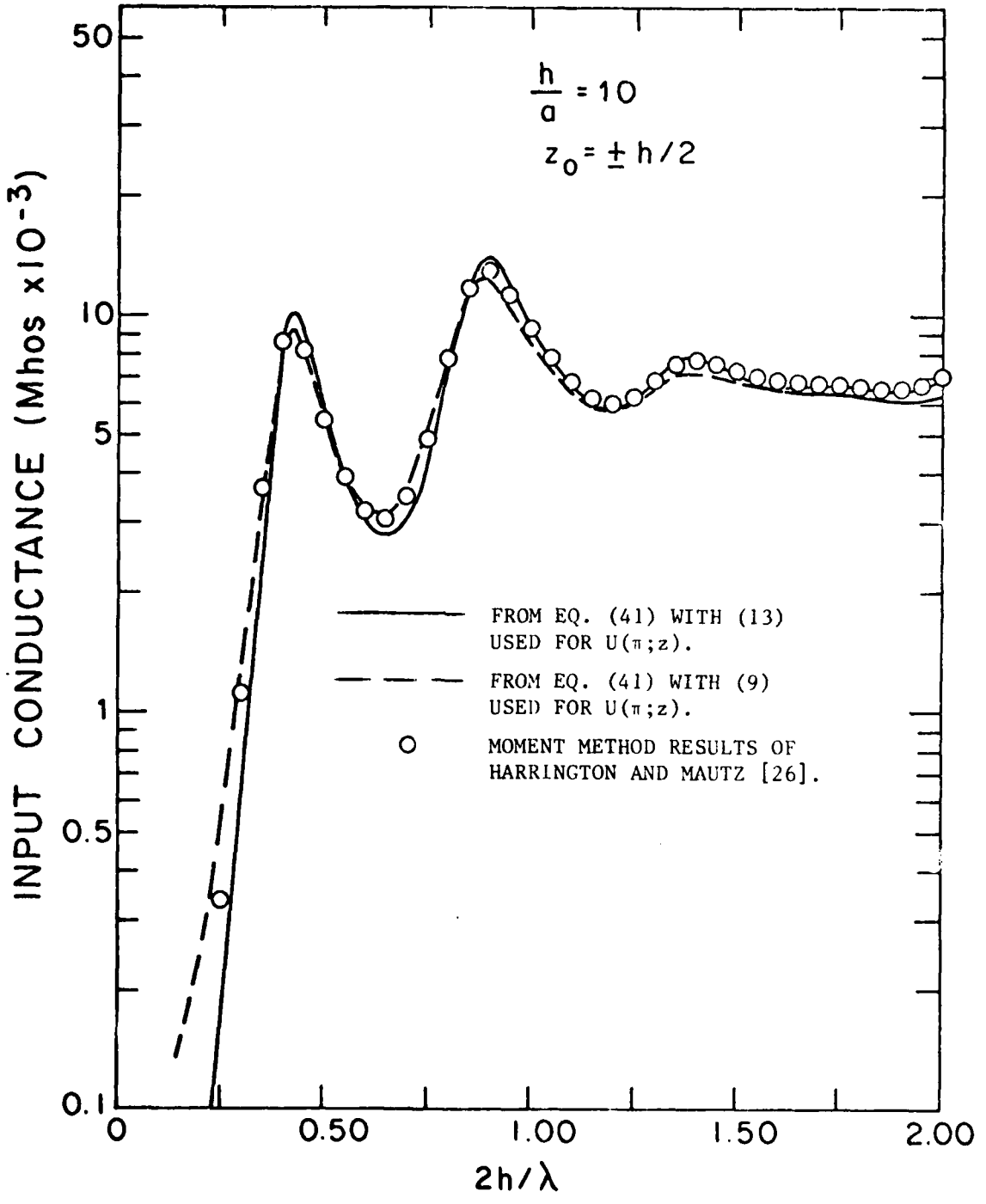

Figure G5. Input conductance of an off-center fed cylindrical antenna as a function of the normalized length, $2h/\lambda$.

Appendix H. Far field radiation from a cylindrical transmitting antenna

The far-field radiation pattern of a finite length, $-h \leq z \leq h$, cylindrical antenna having a delta function source of strength, V_0 volts, at $z = z_0$ (similar to the antenna shown in Figure 16c) can be written in terms of [33, Sec. 2-10],

$$E_\theta(r,\theta,\phi) = \frac{-ik\eta}{4\pi} \sin\theta \frac{e^{ikr}}{r} \int_{-h}^{h} \int_{-\pi}^{\pi} J_z^T(a,\phi',z') e^{-ikz'\cos\theta} e^{-ika\sin\theta\cos\phi'} a\,d\phi'\,dz'; \quad kr >> 1 \qquad (H.1)$$

where $J_z^T(a,\phi,z)$ is the z-directed component of current density on the cylinder. $E_\theta(r,\theta,\phi)$ is the θ-directed (θ is measured from the positive z axis in Figure 16c) electric field at the far field point (r,θ,ϕ) in a spherical coordinate system coincident with the implied cylindrical coordinate system of Figure 16c. Since $J_z^T(a,\phi,z)$ is uniform about the cylinder, we take the total current as $I^T(z_0;z) = 2\pi a J_z^T(a,\phi,z)$ and performing the ϕ' integration, we get,

$$E_\theta(r,\theta,\phi) = \frac{-ik\eta}{4\pi} \sin\theta\, J_0(ka\sin\theta) \frac{e^{ikr}}{r} \int_{-h}^{h} I^T(z_0;z') e^{-ikz'\cos\theta} dz', \quad kr >> 1 \qquad (H.2)$$

where J_0 is the Bessel function of the first kind. Although our approximate expression for $I^T(z_0;z)$ in (38) may be used in (H.2) to determine the far field, the integration of some of the terms requires further approximations and leads to a more complicated result than is actually necessary.

The far field expression in (H.2) may be stated in a more convenient manner if we first consider a similar receiving antenna. The current distribution on an antenna used as a receiving element can be found by

integrating the response of the antenna to a unit voltage impulse, i.e., $I^T(z';z)/V_0$, with the differential voltage,

$$E^i_\theta(a,\theta,z')dz' = \sin\theta\, J_0(ka\sin\theta)E^i_\theta e^{ikz'\cos(\pi-\theta)}\, dz' \qquad (H.3)$$

over the range, $-h \leq z \leq h$. Here $E^i_\theta(a,\theta,z')dz'$ corresponds to the azimuthally uniform differential component of voltage applied to the antenna when illuminated by a uniform plane wave having a θ-directed component of electric field, E^i_θ, and incident at an angle, $\pi - \theta$, with respect to the positive z-axis. Noting that the exact form of $I^T(z';z)$ would satisfy the reciprocal relationship, $I^T(z';z) = I^T(z;z')$, [34, Sec. 9-10], the receiving current distribution can be written as,

$$I^R(\pi-\theta\,;z) = -\sin\theta\, J_0(ka\sin\theta)\,\frac{E^i_\theta}{V_0}\int_{-h}^{h} I^T(z;z')e^{-ikz'\cos\theta}\, dz' \qquad (H.4)$$

Using (H.4) with $z = z_0$ in (H.2) allows the far field to be written as,

$$E_\theta(r,\theta,\phi) = \frac{ik\eta}{4\pi}\frac{e^{ikr}}{r}V_0\,\frac{I^R(\pi-\theta\,,z_0)}{E^i_\theta}\;;\quad kr >> 1 \qquad (H.5)$$

Acknowledgements

The authors wish to express their thanks to Dr. Edward F. Kuester for the many helpful discussions and comments he offered. And special thanks to Ann Ponder, Janice Wilson and Marie Kindgren for their patience and the high-quality technical typing they provided in the preparation of this report. This research was supported by the U.S. Office of Naval Research under contract number N00014-76-C-0318.

PRECEDING PAGE BLANK-NOT FILMED


DAT
FILM